1-1-2012

Cellular plasticity in white adipose tissue: in vivo identification of bipotent adipocyte progenitors in adult white adipose tissue

Yun-hee Lee
Wayne State University,

CELLULAR PLASTICITY IN WHITE ADIPOSE TISSUE: *IN VIVO* IDENTIFICATION OF BIPOTENT ADIPOCYTE PROGENITORS IN ADULT WHITE ADIPOSE TISSUE

by

YUN-HEE LEE

DISSERTATION

Submitted to the Graduate School

of Wayne State University,

Detroit, Michigan

in partial fulfillment of the requirements

for the degree of

DOCTOR OF PHILOSOPHY

2012

MAJOR: PATHOLOGY

Approved by:

_____

Advisor Date

_____

_____

_____

_____

DEDICATION

This dissertation is dedicated to my family, without whose support, this process would not have been possible. My parents, Yang-Bae Lee and Mi-Soo Cho, support throughout my life, and have given me the opportunity of an advanced degree. Thank you very much for always being there for me. I would also like to thank my brother, Jane Lee, and sister, Seung-Hee Lee, who are sharing joy with me and brightening my days. I thank my parent-in-laws, Min-Chae Jung and Pil-Soon Kim, for their support and love.

Most especially, to thank my husband, Young-Suk Jung, and lovely children, Seoyun and Seunghun, who have always stood by me, dealt with all of my absence and reminded me to love life. There is no way to say thank you enough. I also thank my church friends for their help during my hardest time.

ACKNOWLEDGMENTS

It gives me great pleasure in acknowledging the support and guidance of many people during the course of my dissertation work:

Most especially to my mentor, Dr. James Granneman for constant mentorship, guidance and encouragement throughout my PhD work. He was so passionate about science. He made every experience fun and exciting, and helped me to realize my dream to grow as an independent scientist. To my co-mentor and graduate officer, Dr. Todd Leff, his discerning nature has been precious during various obstacles in my research and graduate program. Thank you to my committee members, Dr. Robert G. MacKenzie, Dr. Hyeong-Reh Kim and Dr. Shijie Sheng, for your direction, suggestions and advice. Thanks to Eric Van Buren in the Karmanos Cancer Institute core facilities for your help with flow cytometric analysis. Thank you to all members of the Granneman lab for their aid and camaraderie over the years. A special thank you, to Emilio Motillio,and Anelia Petkova. Emilio, his constant help and input to my project enable me to continue study. Your friendship is especially dear to me. Anelia worked together to solve the problems during research and was always willing to provide excellent technical supports for preparing histologic samples. I really appreciate and am grateful to all of you: Jannifer Tyrrell, Olga Astapova, Vickie Kimler, Li Zhou, Ljiljana Mladenovic, and Heidi Zhang.

TABLE OF CONTENTS

LIST OF TABLES

LIST OF FIGURES

Chapter 1. Introduction

1.1 Obesity and adipose tissue

Obesity is a multidimensional metabolic disorder linked to an increased risk of several common and severe diseases, including insulin resistance, type 2 diabetes, cardiovascular diseases, and certain types of cancer (1). Recent epidemiologic studies have estimated that obesity is the leading contributor to the overall disease burden in the US (2, 3), emphasizing its life-threatening complications. Obesity is characterized by increased lipid storage and adipose tissue mass (4). However, the impact of obesity varies widely among individuals, even with a similar degree of body mass index (BMI) (5). Increasing data suggest that dysfunction of adipose tissue, rather than the level of total adiposity, is a key indicator of metabolic disorders (6, 7).

Adipose tissue has evolved to store excess energy by hyperplastic and/or hypertrophic growth; however, under obesogenic conditions, such as chronic nutritional oversupply, adipose tissue is often unable to meet the demand for additional lipid storage. In many cases, limited lipid storage capacity and expandability of adipose tissue cause ectopic accumulation of lipid and its by-products in major metabolic organs (liver, muscle, pancreatic β-cells) and subsequently lead lipotoxic side effects, including activation of inflammatory pathways, cellular

dysfunction and disturbed systemic metabolism (8). Within this context, lipotoxicity resulting from dysfunctional adipose tissue is thought to be one of the key events that underlie the development of obesity-induced insulin resistance and metabolic disease (9, 10).

In general, two therapeutic strategies have been applied to reverse from lipotoxicity: first, to optimize the anabolic function of adipose tissue, thereby rerouting lipid from lipid-intolerant organs to fat tissue; or second, to increase the catabolic function of adipose tissue to reduce fat mass. For example, the thiazolidinedione (TZD) class of anti-diabetic drugs has been clinically used to restore adipose tissue insulin sensitivity, in part by enhancing fat deposition (11). In addition, TZDs normalize secretion of multiple adipokines to reduce inflammatory signaling and improve metabolic profiles (9, 11). Another attractive approach is to augment energy expenditure by promoting oxidative metabolism in adipose tissue (12). The increased metabolism would function to regulate body weight and temperature (13-15). β3-adrenergic receptor (ADRB3) agonists have been reported to stimulate thermogenesis, increase metabolic rate, and have anti-obesity and anti-diabetic effects in rodent models (3, 16-20).

In theory, it may be possible to improve the metabolic character of adipose tissue by activating progenitors to generate new adipocytes that ultimately have improved catabolic or anabolic characteristics. (21). At the present time, identity of the adipocyte progenitors and the mechanisms that control the progenitor fate and behaviors were poorly characterized. Therefore,

improved knowledge on adipocyte progenitors is required to address the current epidemic of obesity and its related diseases. Specifically, recruitment of beneficial adipocytes by controlling progenitor dynamics would be one of the strategies to prevent or treat obesity and its associated diseases.

1.2 White and brown adipose tissue

Adipose tissue has been classically defined into two functional and histological types: white and brown, which differ in several important properties (22). White adipose tissue (WAT) stores excess calories as triglycerides and releases energy sources as fatty acids and glycerol for systemic use by other organs (23). WAT can be subcategorized into subcutaneous and visceral depots. Visceral depots are more strongly associated with metabolic complications, while subcutaneous beds appear protective against these metabolic syndromes (23). In contrast, brown adipose tissue (BAT) is primarily a thermoregulatory organ (22). It contains an ample number of mitochondria and is characterized by a dense vascular network and nerve supply (22). Since BAT provides heat to the body in response to adrenergic input via the blood stream, these structural features are important for this organ to exert its function to protect the organism from a cold environment (24). The thermogenesis of BAT is critically related to uncoupling protein 1 (UCP1), which uncouples proton gradients from ATP synthesis (22). UCP1 is

specifically expressed in BAT, and is considered to be a prototype BAT marker.

The ability of BAT to burn calories may enable it to be manipulated for novel anti-obesity strategies (3, 12, 15, 18). To support this view, it has been estimated that, if fully activated, 50 g of brown adipocytes would be sufficient to burn 20% of the daily energy intake (15). This potential power has been substantiated by the demonstration of major roles of BAT in TG clearance and glucose disposal and consequent improvement of metabolic profiles in rodent models (16, 19). Increasing evidence from clinical studies suggests that BAT mass and activity inversely correlate with BMI and adipose tissue mass (25-27). The potential role of this organ in human metabolism suggests that activation of BAT might be a therapeutic tool with multiple implications in metabolic disease (18, 28, 29).

1.3 Cellular plasticity of adipose tissue.

WAT possesses exceptional plasticity, enabling dynamic modulation of its metabolic and cellular characteristics in response to various stimuli. For example, WAT can increase adipocyte mass and number dramatically under high fat feeding (30, 31), and it can regenerate in the setting of injury (32) or surgical partial removal (33). PPARγ agonists are known to expand WAT by recruiting progenitors and promoting adipogenesis of preadipocytes (34, 35). In addition,

WAT has a capacity to transition between white and brown, manifesting significant changes in metabolic activity and functional phenotype. There are multiple reports demonstrating that traditional white fat depots can adopt brown fat-like characteristics under certain physiological and pharmacological conditions, such as cold exposure and β-adrenergic stimulation (14, 24, 36-43). Since β3-adrenergic receptors (ADRB3) are mainly expressed in adipose tissues, selective ADRB3 agonists, such as CL316.243 (CL), have been utilized to study β-adrenergic control of WAT. The WAT of chronically CL-treated mice becomes darker in color and undergoes a metabolic switch to a more brown-like phenotype. This remodeling includes catabolic gene transcription, mitochondrial biogenesis and elevation of metabolic rate, (**Figure 1**).(44).

One of the most prominent events of catabolic remodeling is the appearance of UCP1 expressing multilocular brown adipocytes as clusters diffused within WAT (14). It remains unclear, however, which cellular components give rise to these inducible brown adipocytes (iBA). Current views on cellular plasticity suggest that alterations in cellular identity might occur through genetic reprogramming of adult somatic cells: by conversion from one mature cell type to another, called transdifferentiation; or reversion to a stem cell-like or a less-differentiated state with subsequent alternative differentiation, called dedifferentiation (45). Evidence from detailed morphological analysis on iBA at ultrastructural levels suggest that conversion from mature WA

to BA during cold acclimatization and β-adrenergic stimulation is achieved by transdifferentiation processes (44, 46).

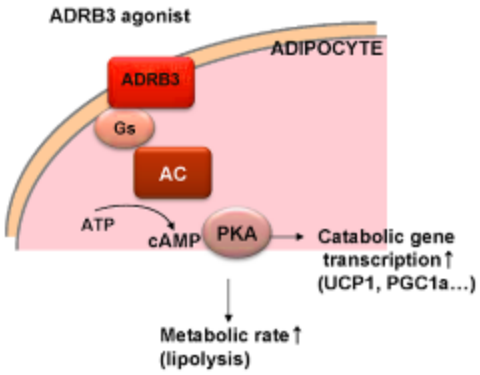

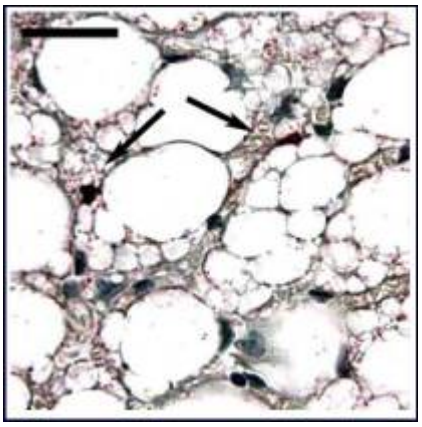

Figure 1. WAT remodeling during ADRB3 activation.

(A) Molecular mechanisms that mediate catabolic remodeling of adipose tissue druing ADRB3 stimulation. Downstream signals mediated by PKA activation upregulate genes involved in mitochondrial biogenesis, and fatty acid oxidation. PKA can directly increase HSL (hormone sensitive lipase) activity. (B) Multilocular adipocytes that appear in eWAT during CL treatment come from proliferating cells. BrdU immunohistochemistry showing numerous multilocular adipocytes containing BrdU-positive nuclei (arrows). Nuclei of BrdU-positive adipocytes were defined by surrounding internal lipid droplets. Paraffin sections were counter-stained with hematoxylin. Bar = 25 μm (43).

Although mature WA can undergo transdifferentiation to generate iBA, this mechanism cannot explain newly-born iBA from proliferating cells, because WA are post-mitotic. As shown in **Figure 1**, when CL-treated mice were co-infused with BrdU for 7 days to label proliferating cells, 20% of brown-like adipocytes in WAT were positive for BrdU, indicating that proliferating progenitors give rise to iBA by ADRB3 stimulation (43); however, the identity and biology of iBA

progenitors are unknown.

1.4 Developmental origin of brown and white adipose tissue

Recently, several elegant lineage tracing studies enabled breakthrough findings on developmental origin of BAT, and discovered common progenitors for muscle and BAT (47, 48). *In vivo* fate-mapping has shown that progenitors derived from the central dermomyotome (paraxial mesoderm) give rise to the interscapular BAT (48), suggesting that the interscapular brown fat and skeletal muscle may share a common developmental ancestry. In support of this notion, lineage-tracing studies have established that early myogenic factor (MYF5)-expressing progenitors can give rise to both skeletal muscle and BAT in the interscapular and perirenal depots (47). Moreover, the iBA emerging in WAT in response to ADRB3 stimulation never expresses MYF5, suggesting that classical BA that reside in interscapular BAT and iBA in WAT originate from distinct lineages (47).

In a study conducted by Graff's group, the direct precursors of WA in developing mouse WAT were identified as a population that express PPARγ and reside on the periphery of blood vessels in WAT (49). These cells differentiate into adipocytes *in vitro* and proliferate and give rise to adipocytes after transplantation. This population expresses preadipocyte markers (Pref1, GATA3). These cells were further defined as being in the mural compartment of vasculature, based on their pericyte marker expressions (PDGFRβ, NG2). A recent study done by this group

also demonstrated that dynamic and molecular phenotype of PPARγ+ pericyte-like progenitors were regulated by thiazolidinedione (TZD) treatment (50). However, it is not known whether these committed precursors of WA serve as adult adipose stem cells in response to other adipogenic conditions or ADRB3 stimulation.

1.5 Adipocyte progenitors in adult adipose tissue

Adipocytes form during the perinatal period as well as during homeostatic turnover in adult WAT throughout life. In addition to the normal growth, adipocytes are highly dynamic, expanding in response to various stimuli (51). These cellular responses enable adipose tissues to expand to accommodate increased energy intake and to serve as a crucial player in a complex network balancing energy homeostasis. The adult fat growth pattern is due to both changes in the number and size of adipocytes (23) . The hyperplasic feature of adipose tissue highlights the potential presence of a stem compartment, since in cases where the differentiated cells, such as adipocytes, are postmitotic, tissue regeneration and turnover depends entirely on stem cell differentiation (52). Therefore, to explain the mechanism of adipose tissue turnover and hyperplasia, it has been hypothesized that renewal occurs via an adult stem cell residing in the stromal vascular fraction (SVF) of adipose tissue.

With the demonstration of the presence of mesenchymal stem cells (MSC) in SVF from adult adipose tissue including human and mouse tissue (53, 54), SVF of adipose tissue has been extensively studied as potential progenitor pool. MSC are known to be common progenitors for bone, cartilage and adipose tissue during development (55). These MSC found in multiple types of adult tissues have been proposed to function as tissue specific stem cells, However, this assumption still lacks good experimental proofs *in vivo* setting, partly due to lack of MSC specific markers that enable *in vivo* lineage tracing (54, 55). Therefore, how the putative MSC contribute to the maintenance or remodeling/ repair of adult tissues has not been defined.

In the search of adipocyte progenitor markers, a recent study on adult adipose stem cells performed by Friedman's group shed light on the molecular signature of white adipose stem cells/progenitors in adult mice (56). Friedman's group used FACS to isolate a Lin-CD29+CD34+Sca-1+CD24+ population of cells with an increased capacity for differentiation into adipocytes over heterogeneous stromal vascular fraction, claiming that these populations are adult adipose stem cells (56). When transplanted into a lipodystropic mouse, these cells reconstitute the epidydimal fat pad, improve the metabolic profile and correct lipodystrophy-related symptoms.

In addition to WAT pads, WA can be formed in numerous tissues, including muscles. A recent work has addressed the question of whether ectopic adipocytes in skeletal muscle arise

from a population developmentally distinct from myogenic progenitors (57, 58). These investigators identified a new population, PDGFRα+ cells present in skeletal muscle, as the origin of intramuscular adipocytes. While PDGFRα+ cells differentiated into adipocytes in degenerative muscle *in vivo*, they fail to turn into adipocytes in regenerative muscle, implying that different microenvironments affect their fate.

While WA progenitors which reside in WAT and muscle have been found as mentioned above, there are no studies that identify progenitors that give rise to nascent brown-like adipocytes in WAT upon ADRB3 stimulation.

Table 1 Summary of distinct characteristics of adipocyte progenitors (AP)

Phenotype	***Developmental WAP***	***AP in adult WAT***	***Ectopic AP in Muscle (PDGFRA+ cells)***
Cell surface marker			
CD24	ND	+	-
CD34	+	+	+
Sca1	+	+	+
PDGFRα	ND	ND	+
PDGFRβ	+	ND	-
Anatomical location	Mural compartment	ND	Interstitial space
Number of cells	50%	0.8%	

1.6 PDGFRα in developmental biology

The PDGF family consists of two receptor genes, PDGFRα and PDGFRβ and four ligand genes, PDGFA, B, C and D (59). These four PDGF chains act as disulphide-linked dimers, and five different dimeric isoforms have been described so far; PDGF-AA, PDGFAB, PDGF-BB, PDGF-CC and PDGF-DD (60). PDGF-AA and PDGF-CC exclusively act through PDGFRα, while PDGF-DD activates PDGFRβ. PDGF-BB can bind and activate either receptor homodimer (PDGFRαα or PDGFRββ) and heterodimer (PDGFRαβ) (61). The PDGF ligands exert their function by causing dimerization and auto-phosphorylation of the PDGF receptors (59). This, in turn, results in activation of a multitude of intracellular signaling cascades. The outcomes of these signaling events are diverse and include proliferation, migration, and survival (59, 61).

PDGFRα+ cells exist throughout the body at various developmental stages. During early development, PDGFRα and PDGFA are involved in broad spectrum of development, including embryogenesis, neural crest formation, central nerves system and several organogenesis (61). In adult beings, PDGFRα expression seems more confined in specific progenitor populations. For instance, PDGFRα+ cells in brain are known as oligodendrocyte progenitor cells (62-64). As mentioned above, muscle-derived PDGFRα+ cells have shown their adipogenic potential and identified a progenitor population that is responsible for ectopic adipocyte formation in muscle

(57, 58, 65). In addition, PDGFRα expression in mesenchymal stem cells has been reported *in vitro* culture system (55). Although no studies investigate the involvement of PDGFRα signaling in adipose tissue development and remodeling, PDGFRα activation has been shown to stimulate proliferation and inhibit adipogenic differentiation in cultured preadipocytes (66, 67).

1.7 Progenitor niches

A stem cell niche, a concept introduced by Scholfield (68), is an organized structural unit specialized to facilitate cell-fate decisions in a proper spatio-temporal manner (69). Recent studies have elucidated the important role of niche in adult stem cell biology, including hematopoietic, intestinal crypt, hair follicle and neural stem cells (70). Cell-cell contacts and interactions in stem cell niches also involve chemokine signaling and alterations in extracellular matrix (ECM). It is likely that signals from adipose stromal vascular units surrounding progenitors mediate cell fate decisions. Supporting this idea, in our preliminary findings, adipose cellular components change dramatically in number and cell type during the course of β-adrenergic remodeling. Especially, macrophages are recruited in CL-treated WAT and are present in vicinity of proliferating progenitors. Therefore, we are proposing that macrophages are a major contributor of niche environment that regulate progenitor behaviors.

1.8 Adipose tissue macrophages

Macrophages are highly heterogeneous hematopoietic cells found in almost every tissue throughout the body (71). Macrophages monitor tissue environment for early sign of infection or tissue damage, responsible for innate immune system and can adapt and respond to a large variety of microenvironmental signals. Recent publications have shown that macrophages are recruited to adipose tissue, displaying tremendous heterogeneity in their activities and functions (72-74).

Macrophage can be activated by two distinct programs, classical and alternative activation (75). Classical activation is initiated by the products from bacterial infection, including lipopolysaccharide (LPS) and interferon-γ, generating highly pro-inflammatory macrophages (M1) (76). On the other hand, alternative activation is triggered by products from parasitic infection, such as IL-4 and IL-13, producing anti-inflammatory macrophages (M2) (77). These anti-inflammatory macrophages are usually associated with tissue repair and regeneration/ remodeling phenomenon (78). A large number of differentially regulated markers (**Table 2**) has been identified and the most distinguishable parameter is the expression of key enzymes that regulate arginine metabolism (79). Macrophages in the classical activation utilize arginine to generate nitric oxide (NO) via inducible nitic oxide synthases (iNOS). Alternatively activated macrophages upregulate argniase 1 and metabolize it into precursors for DNA and collagen

synthesis required for tissue remodeling (79)..

While pro-inflammatory classically activated macrophages (M1) are found in obese/insulin resistance states, resident macrophages, such as those present in the adipose tissue of lean mice, display the alternatively activated phenotype (M2) (80). Infiltration of M1 macrophages into expanding AT with obesity become primary source of inflammatory cytokines that promote insulin resistance (79). On the contrary, protective effects of M2 macrophages have been reported in several metabolic disease models. For instance, M2 macrophages enhance insulin sensitivity and macrophage polarization toward alternative state is mediated by PPARγ dependent mechanisms (79, 81), Surprisingly, a recent study demonstrated that M2 macrophage in adipose tissue secret catecholamine to increase catabolism and sustain thermoregulatory function during cold exposure (82). Several *in vitro* cultures studies showed that macrophage-conditioned medium inhibit preadipocyte apoptosis and promote survival in a PDGF-dependent manner (83, 84). However, effects of M2 macrophages on *in vivo* adipocyte progenitors are not well understood.

Table 2. Macrophage heterogeneity

	M1 (proinflamatory)	*M2 (anti-inflamatory)*
Activator	Classical activation by IFN-γ and LPS	Alternative activation by IL-4 or IL-13
Phenotype	Increased production of pro-inflammatory cytokines, iNOS and ROS; increased expression of MHC class II molecules and ; increased antigen presentation; and increased microbicidal activity	Increased endocytic activity; increased expression of mannose receptor, dectin-1 and arginase; increased cell growth; increased tissue repair; and increased parasite killing
Molecular marker	Pro-inflmammtory cytokines (IL-12IL-6, TNF-a) CD86	Ariginase1, IL-10, YM1, FIZZ1
Physiologic function	Promotion of Th1 response Killing of intraceluar pathogens	Promotion of Th2 response Encapsulation and clearance of parasites Tissue remodeling and immunoregulation

1.9 Hypothesis and aims of the project

The organizing hypothesis of this research is that WAT contains brown adipocyte progenitors which contribute to β-adrenergic remodeling. Our preliminary findings together with published data lead to the following specific hypotheses: 1) ADRB3 stimulation induces the proliferation of iBA progenitors within WAT. 2) The ADRB3 stimulation recruits macrophages and create adipogenic niches that provide developmental cues for the fate determination of the progenitors toward brown adipocytes. 3) PDGFRα+ progenitors in WAT possess stem cell

characteristics, including clonogenicity, self-renewal and multipotent differentiation. 4) PDGFRα+ cells become WA in response to white adipogenic stimuli.

The goal of this PhD project is to fully characterize iBA progenitors and their niches in mouse adipose tissues, and to identify molecular mechanisms by which β-adrenergic stimulation promotes proliferation and brown adipogenesis within WAT. This hypothesis will be tested by three specific aims: (1) To characterize the molecular phenotype, behaviors and fates of iBA progenitors (PDGFRα+ cells) following ADRB3 stimulation in WAT. (2) To determine the role of adipose tissue macrophages (ATM) on the progenitor activity. (3) To examine stemness and differentiation potentials of FACS-isolated PDGFRα+ cells. (4) To investigate their contribution to WA formation during normal growth and HFD feeding.

This is an initial step in a broader research objective to determine if there are iBA progenitors in human white adipose tissue, and to determine if enhancement of BAT development via pharmacological intervention or cell therapy is feasible and beneficial in a clinical setting. Data generated from these experiments will improve our understanding of adipocyte biology, providing valuable information on adipocyte progenitor lineage specification and mechanisms that control adipocyte progenitors. Finally, data obtained from these studies may contribute to the development of new anti-obesity therapies that target adipose progenitor pools to recruit beneficial adipocytes.

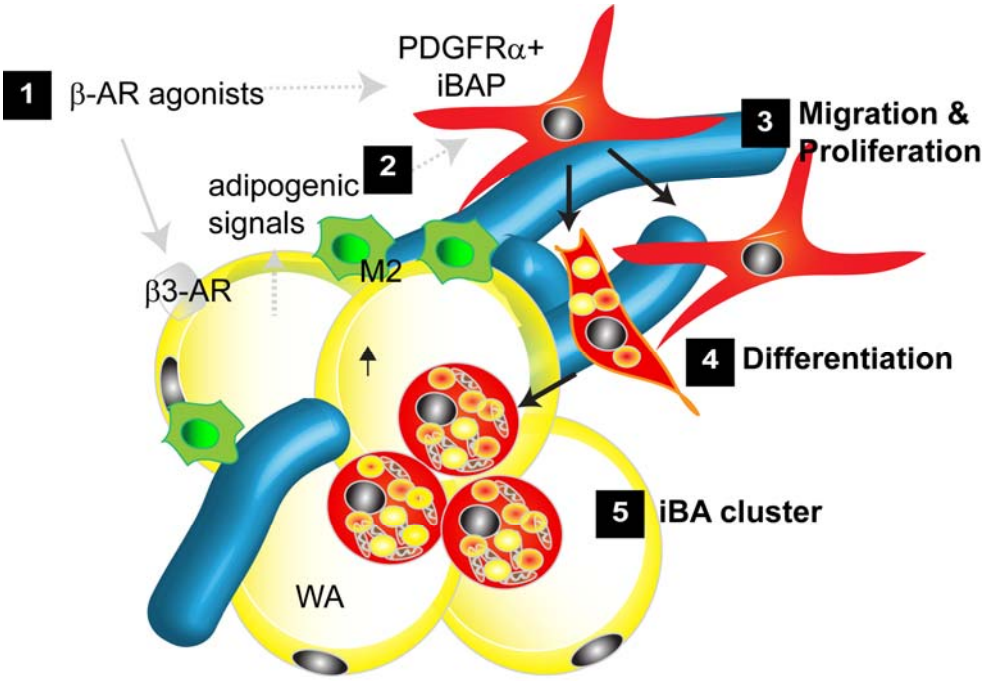

Figure 2. Cellular plasticity in remodeling of adipose tissue by ADRB3 stimulation. (1) In response to continuous ADRB3 stimulation, (2) WA liberated FFA and FFA-derived signals and recruit immune cells. (3) iBAP that reside in close apposition with vasculature start to proliferate and migrate. Immune cells may secrete mitogenic signals to induce proliferation and migration of the iBAP. (4) Interaction with other niche components may direct progenitors to differentiation in BA. (5) The progenitors undergo multiple divisions, generation iBA clusters.

Chapter 2. Methods and Materials

2.1. Mice

129S1/SvImJ (129S1; stock no. 002448), C57BL/6J (C57B/6; stock no. 000664), B6.129S4-Pdgfra_tm11(EGFP)Sor/J (Pdgfra-H2BeGFP; stock no. 007669), C57BL/6-Tg(CAG-EGFP)1Osb/J (GFP; stock no. 003291), and B6.Cg-Gt(ROSA)26Sor_tm9(CAG-tdTomato)Hze/J (85) (R26-LSL-tdTomato; stock no. 007909) were purchased from the Jackson Laboratory. Pdgfra-CreER^{T2} mice (64) were obtained from William Richardson (University College London). All animal protocols were approved by the Institutional Animal Care and Use Committee at Wayne State University.

For continuous β-adrenergic stimulation, mice were infused with CL (0.75 nmol/h) by mini-osmotic pumps (ALZET) for up to 7 days. For BrdU cumulative labeling, BrdU (Sigma, 20 μg/h) were infused with CL for 7 days by mini-osmotic pump. For EdU flash-labeling, mice were injected with EdU (Invitrogen, 2 nmol/mouse, I.P.) at indicated time described in the text. For dual pulse labeling, mice were injected first with EdU and then BrdU (2 mg/mouse) with 24 h interval. BrdU was detected by immunostaining, as described below. EdU was detected according to the instructions of the manufacturer (Invitrogen). Intestines from each individual mouse were used as positive controls for EdU or BrdU detection.

Cre recombination in double transgenic mice (Pdgfra-CreERT2/R26-LSL-tdTomato) was induced by administering tamoxifen dissolved in sunflower oil (Sigma, 300 mg/kg, P.O.) on each of 5 consecutive days. CL treatment or HFD were started 1 week after the first dose of tamoxifen. We included no tamoxifen controls to confirm that tdTomato expression is undetectable in the double transgenic mice gavaged with vehicle (oil only).

For high fat diet experiment, 60% fat diet was introduced at 5-6 weeks of age and continued for 8 weeks. Body weight was registered regularly. Body composition was analyzed by quantitative nuclear magnetic resonance (NMR) using an EcoMRI apparatus (Echo Medical Systems, Houston, TX).

For tyrosine kinase inhibitor experiment, 129S1 mice were treated with sunitinib (50mg/kg/day) or vehicle (1% methylcellulose solution) alone by gavage for 7 days. Two hours after the first sunitinib treatment, CL-loaded miniosmotic pumps were inserted, and mice with sham-surgery were used as control. One week after CL infusion and sunitinib treatment, the animals were sacrificed by cervical dislocation. Adipose tissue and intestine were collected, and processed for mRNA, protein, and histology analysis.

2.2. Tissue processing and immunostaining

Tissues were fixed with 10% formalin overnight at 4 °C, paraffin embedded and 5 μm

thick sectioned. For whole mounts, fixed tissues were minced into ≤2mm^3 small pieces. Immunostaining was performed in either paraffin sections or whole mount tissue. Samples were pre-incubated with permeabilization buffer (0.5% TritonX 100 in PBS) and blocking buffer (5% normal donkey serum in PBS) for 30 min at room temperature, and then incubated sequentially with primary antibody and secondary antibody, all in blocking buffer. For BrdU detection, paraffin sections were incubated in 2 N HCl for 45 min at 37 °C before permeabilization. After washing with TPBS (0.1% Tween 20), samples were counterstained with DAPI. Slides were coverslipped in mounting medium (Dako) and examined by fluorescence microscopy. Species matched IgG were used as nonspecific controls. Primary antibodies used for immunostaining were: PDGFRα (goat, R&D, 2.5 μg/mL), PPARγ (rabbit, Cell Signaling 1:200), PLIN1 (rabbit (86), 1:500; goat, Everest, 1:250), UCP-1 (rabbit, Alpha Diagnostic International, 2.5 μg/mL; goat, Santa Cruz, 1:100), PDGFRβ (rat, eBioscience, 1:100), CD34 (rat, eBioscience, 1:100), SMA (mouse, Sigma, 1:200), GFP (goat, GeneTex, 1:300) and tdTomato (rabbit, Clontech, 1:100). Following secondary antibodies were used: Alexa Fluor 488– or 594– conjugated donkey antibody to goat IgG, goat or donkey antibody to rabbit IgG, goat antibody to rat IgG (Invitrogen, 1:1,000), and Cy5-conjugated goat antibody to rabbit IgG (Jackson Labs, 1:200).

2.3. Adipocyte sizing and counting

Total adipocyte numbers in eWAT of mice from the HFD study were calculated as previously described (87). Briefly, eWAT adipocyte cell sizes (>300/mouse) were determined from phase-contrast images of fixed whole mounts using IPlab software, and mean triglyceride (TG) mass/adipocyte calculated as = $0.4790/10^6 \cdot [3.\sigma^2 \cdot \text{diameter} + (\text{diameter})^3]$. Tissue adipocyte cellularity determined by dividing tissue TG content by mean fat cell TG mass. Total tdTomato+ adipocytes were estimated by extrapolation from the number of cells counted in 10 mg samples.

2.4. WAT SVC and adipocyte fractionation

Adipose tissues were washed with PBS, minced and digested with type II collagenase (2 mg/mL) in KRBB containing 10mM HEPES (pH 7.4), and 3% BSA for 1 h at 37 °C. Preparations were passed through a 300 μm mesh, and centrifuged at 500g for 5 minutes. Floating adipocytes were collected by aspiration. Pellets containing the stromal vascular (SV) fraction were incubated in red blood cell lysis buffer for 5 min at room temperature, passed through a 40 μm mesh and then collected by centrifugation at 500 g for 5 min. The resultant cell preparations were subjected to immunostaining or flow cytometry.

2.5. Flow cytometry

For FACS analysis, SV fractions from mouse WAT were resuspended in PBS plus 2% FBS, and 0.5mM EDTA. Cells were incubated with anti-PDGFRα (CD140a) -PE, and other cell surface marker antibodies for 30 min on ice. Antibodies used were anti-CD34-FITC, anti-Sca1-FITC, anti-CD24-FITC, and IB4-FITC. For PDGFRβ staining, SV fractions from Pdgfra-H2BeGFP mice were incubated with anti-PDGFRβ (CD140b) -PE. This strategy was adopted because the signals for APC-conjugated anti-PDGFRα antibodies were too low to permit quantification with available anti-PDGFRα antibodies. Species matched IgG were used as nonspecific controls. For cell sorting, SV cells from GFP mice were labeled with anti-PDGFRα (biotynylated, R&D system) and streptavidin-PE sequentially. SV fractions from Pdgfra-reporter mouse WAT (Pdgfra-H2BeGFP or Pdgfra-CreER^{T2}/R26-tdTomato) were sorted based on native fluorescence (GFP or tdTomato, respectively).

Antibodies used for flow cytometry were: PDGFRα (-PE, Biolegend, 1:200), CD34 (-FITC, Biolegend, 1:100), Sca1 (-FITC, eBioscience, 1:200), IB4 (-FITC, molecular probe, 1:50), CD24 (-FITC, Biolegend, 1:1000), PDGFRβ (-PE, Biolegend, 1:100).

2.6. Cell culture of FACS-isolated cells

SVCs of adipose tissue from Pdgfra-H2BeGFP mice were FACS-sorted by GFP

fluorescence. Single cell sortings were performed on a Matrigel coated 96-well plate. Proliferating clones were maintained for 2 weeks in growth medium (DMEM supplemented with 20% FBS and 2.5 ng/ml bFGF), and adipogenic differentiation was induced by adipogenic induction medium (DMEM with 20% FBS, 1μg/ml Insulin, 0.25μM dexamethasone, and 0.5 mM 1-methyl-3-isobutylmethyl-xanthine (IBMX). Three days later, clones were place in DMEM with 20% FBS and 1 μg/ml insulin for 4 days. A minimum of 39 colonies derived from the PDGFRα+ single cells in each depot was analyzed for the adipogenic differentiation. Colonies were stained for Lipid (LipidTox) to identify adipocytes and UCP1 to identify BA.

In a separate experiment, FACS-purified GFP+ and GFP- cells were collected by centrifugation at 500 g for 5 min, seeded at density of 2.5 x 10^4/well in 48-well plates, and expanded in growth medium. For adipogenic differentiation, confluent cells were exposed for 7 days to insulin (1 μg/ml) in DMEM supplemented with 10% FBS. For the acute β-adrenergic stimulation, cells were treated with isoproterenol (10 μM) for 4 h.

2.7. Transplantation of FACS-isolated cells

FACS-purified PDGFRα$^+$ and PDGFRα$^-$ cells from GFP mice were collected by centrifugation at 500 g for 5 min. For each fraction, 10^5 cells were immediately mixed with Matrigel (150 μl) and injected subcutaneously into the hind limbs of syngenic recipient mice

(C57B/6) that were anesthetized using Avertin. Entire transplants were collected after 4 weeks, and stained for PPARγ, PLIN1, or lipid (nile red). Donor cell-derived adipogenesis in transplants was calculated by the number of GFP^+ adipocytes ($PPAR\gamma^+$ nile red^+) divided by the number of total adipocytes.

2.8. Macrophage depletion

Mice were injected with 300ul (approximately 110 mg/kg of clodronate) liposomes i.p. or equal volume of PBS liposomes. The injection was repeated every second days to maintain depletion. CL-loaded pumps were inserted after the second injection and macrophage depletion was confirmed by immunostaining and qPCR to detect macrophage specific marker expression.

2.9. Explant cultures: Organotypic culture

Epididymal WAT was dissected from tamoxifen-treated Pdgfra-$CreER^{T2}$/R26-LSL-tdTomato mice, washed with PBS, and individual pieces of tissues were transferred to standard 24-well plates or 35 mm dishes with poly-l-lysine-coated glass bottoms for imaging. Tissues were incubated for 5 min at 37 °C without medium to promote adherence, and then tissues were cultured in DMEM supplemented with 10% FBS. After reaching full confluence, cultures were exposed to insulin (1 μg/ml) in growth medium for 4 days, and then exposed to EdU (10 μM) 2 h

before fixation. Fixed cultures were stained for EdU, UCP1 and PLIN1 to assess proliferation and differentiation.

2.10. Migration assay

To examine the effect of PDGF, OPN on chemotactic migration of PDGFRA+ cells, transwell assays were performed using cell culture inserts (8-mm pore size, BD Bioscience). Stromavascular fraction of eWAT from h2BeGFP mice were suspended at 2X10^5 cells/ml in DMEM with 0.1% BSA, and 0.2 ml of the suspensions were placed on the upper surfaces of the inserts ($4X10^4$/ well of 24-well plate). The medium (0.6 ml, 0.1% BSA DMEM) containing PDGF-AA (Invitrogen, 50 ng/ml) or OPN (R&D system, 200 ng/ml) as a chemoattractant was added in the lower well (Falcon 24-well plate, BD Falcon). The cells were allowed to migrate to the lower surface of the membrane for 6 h and 16 h at 37°C. The unmigrated cells on the upper surfaces were wiped off using cotton swabs, and the inserts were washed with PBS twice, fixed with 4% paraformaldehyde for 15min at RT, permeabilized with 0.5% TritonX in PBS and stained with DAPI for 10 min. Membranes were subsequently mounted onto a microscope slide using mounting medium (Dako). The migratory activity was denoted as the average number of migrated GFP+ cells and GFP- cells. Each cell fraction was counted manually in 5 random 10X fields for each condition with triplicate repeated measure. No serum (0.1% BSA) and 10% FBS

serum containing medium were used for negative and positive controls.

2.11. Microscopy

Fluorescence and bright-field microscopy was performed using an Olympus IX-81 microscope equipped with a spinning disc confocal unit, and 40X (0.9NA) and 60X (1.2NA) water immersion objectives, using standard excitation and emission filters (Semrock) for visualizing DAPI, FITC (Alexa Fluor 488), Cy3 (Alexa Fluor 555, 594, Nile Red) and Cy5 (Alexa Fluor 647, LipidTox), as described (88). Confocal z-stacks were captured for whole mount tissue by imaging up to 12 optical sections at 0.4-1 μm increments. Raw data of single optical sections (paraffin sections) or confocal z-stacks (whole mount tissues) were processed using IPlabs software (Scanalytics, BD Biosciences) and Adobe Photoshop.

2.12. Western blot

Protein was extracted using RIPA lysis buffer (25 mM Tris, pH 7.5, 150 mM NaCl, 1% Triton X-100, 0.5% Na deoxycholate, 1% NP-40, 0.5% sodium dodecyl sulfate, and 1 mM EDTA) containing protease inhibitors (Roche). Western blot was performed as described (89).

Protein concentrations were measured using the standard BCA protein assay method (Pierce). Equal amounts of protein (40μg) were loaded in each lane. Proteins were separated by

gele electrophoresis using precast 4-20% gel (Pierce). The gel was run at 140 V for 45-60 min. Proteins were transferred onto polyvinylidenedifluoride (PVDF) membranes at 0.4 A for 1h using Tris-glycine buffer (containing 20% methanol) in a Bio-Rad transfer system. PVDF membranes were then blocked in 5% milk in Tris-buffered saline with 0.05% Tween 20 (TBS-T) for 30 min at RT. The primary antibody was prepared in 5% milk in TBS-T. PVDF membranes were incubated in the primary antibody solution at 4℃ overnight. PVDF membranes were washed three times with TBS-T and then incubated in the secondary antibody solution in 5% milk TBS-T for 1h at RT. ECL Western Blotting Substrate (Pierce) was used for chemiluminescence detection.

Antibodies used for western blot were UCP1 (rabbit, Alpha Diagnostic International, 1:1000), OPN (goat, 1:2000), PDGFA (rabbit, Santa Cruz, 1:1000), PDGFB (rabbit, Milipore, 1:2000), PDGFC (goat, R&D system. 1:1000), PDGFD (rabbit, 1:2000), Actin (goat, Santa Cruz, 1:500) and GAPDH (mouse, Chemicon, 1:1000).

2.13. Gene expression analysis

Total RNA was extracted using Trizol (Invitrogen) and mRNA was reverse-transcribed using Superscript III (Invitrogen) and oligo dT primers (Fermentas). 50 ng of cDNA was analyzed in a 20 µl quantitative PCR reaction (ABsolute Blue QPCR SYBR, ThermoScientific) with 70 nM of primers. Expression data were normalized to the house keeping gene peptidyl-

prolyl cis-trans isomerase A (PPIA) using the delta-delta CT method (2-ΔΔCT), as described (90). Specific primer sequences used for PCR are listed in Table S1, and all other primers have been described previously (90, 91)

Table 3 Primer sequences used

Gene	Forward (5'-3')	Reverse (5'-3')
Cd24	TGCTCCTACCCACGCAGATT	GCGTTACTTGGATTTGGGGAAGCA
Cd29	GGACCTTTTGGGTTGAGCTTATT	AAAAAGTCTAACCCCCATATTGGA
Cd34	GACTTCCCCCTTCCTCTGAC	AATCAGGACCCCTGTTCTCC
Cidea	CTAGCACCAAAGGCTGGTTC	CACGCAGTTCCCACACACTC
Dio2	CCAGCACCGGAAAGAGGAAA	TCCTTGCACCATGACCCAAA
Elovl3	GAGAAAGGATGCCACACAAC	GAGGCTCCATCTTTCTTTCC
Fabp4	TGGGGATTTGGTCACCATCCGGT	GGGCCCCGCCATCTAGGGTT
Lpl	CGACTCCTACTTCAGCTGGC	ACACTGCTGAGTCCTTTCCC
Pdgfra	AGCAGGCAGGGCTTCAACGG	ACACAGTCTGGCGTGCGTCC
Pdgfrb	CATCATGAGGGACTCAAACT	GATGGCATTGTAGAACTGGT
Plin1	GAGTCAGCGACAGCTTCTTC	CTTGACGAGAAGCGACCTT
Sca1	GTTTGCTGATTCTTCTTGTGGCCC	ACTGCTGCCTCCTGAGTAACAC

2.14. Statistical analysis

Statistical analyses were performed with GraphPad Prism 5. Data are presented as mean ± SEM. Statistical significance between two groups was determined by unpaired t-test or Mann-Whitney test, as appropriate. Comparison among groups was performed using one-way ANOVA or two-way ANOVA, with Bonferroni posttests to determine the relevant p values. Fisher's exact test was used to evaluate differences in cell distributions.

Chapter 3. Identification of iBA progenitors

3.1 iBA in eWAT come from proliferating cells during ADRB3 stimulation.

Previous experiments demonstrated that a significant fraction of BA induced in WAT by ADRB3 stimulation can be derived *de novo* from proliferating progenitors (43). In the present experiments, we investigated the contribution of proliferation to BA induction using a low dose of the ADRB3 agonist CL316,243 (CL) that resulted in greater levels of proliferation without signs of lipolysis-induced inflammation (43, 89, 90). Control and CL-treated mice were coinfused with 5-bromo-2'-deoxyuridine (BrdU) to cumulatively label proliferating cells (**Figure 3**), and the mitotic index and the proportion of BrdU labeling in $UCP1^+$ adipocytes were determined in epididymal (eWAT), inguinal (iWAT) and interscapular (BAT) fat pads.

ADRB3 activation induced expression of UCP1 in iWAT within 3 days of treatment, whereas pronounced expression of UCP1 (i.e, detected by immunoblot) was observed in eWAT only after 7 days(Figure 3B). Under control conditions, virtually no $UCP1^+$ cells were detected in WAT, and < 0.4% of nucleated cells incorporated BrdU over 7 days in WAT or BAT (Figure 3C). CL treatment increased the mitotic index of cells in both eWAT and iWAT; however, the mitogenic effect of CL was far greater in eWAT (**Figures 3F**). The vast majority of $UCP1^+$ cells observed in eWAT were positive for BrdU (82.2 ± 3.6% of total $UCP1^+$ cells, (**Figures 3D and**

3E), indicating most inducible BA (iBA) in eWAT came from newly-born cells. In contrast, only 5.8 ± 3.0% of $UCP1^+$ cells in iWAT were $BrdU^+$ (**Figure 3E and 3G**). These results indicate that most UCP1+ cells in eWAT are derived from the induction of brown adipogenesis from progenitors, whereas the upregulation of UCP1+ expression in iWAT involves the conversion or 'transdifferentiation' of existing WA into a BA phenotype. Cellular expression levels of UCP1 were similar among UCP+ multilocular cells in IBAT, iWAT and eWAT (**Figures 3D, 3E and 3H**). CL had no effect on cell proliferation in BAT, further supporting differences in the origin of constitutive and inducible BA.

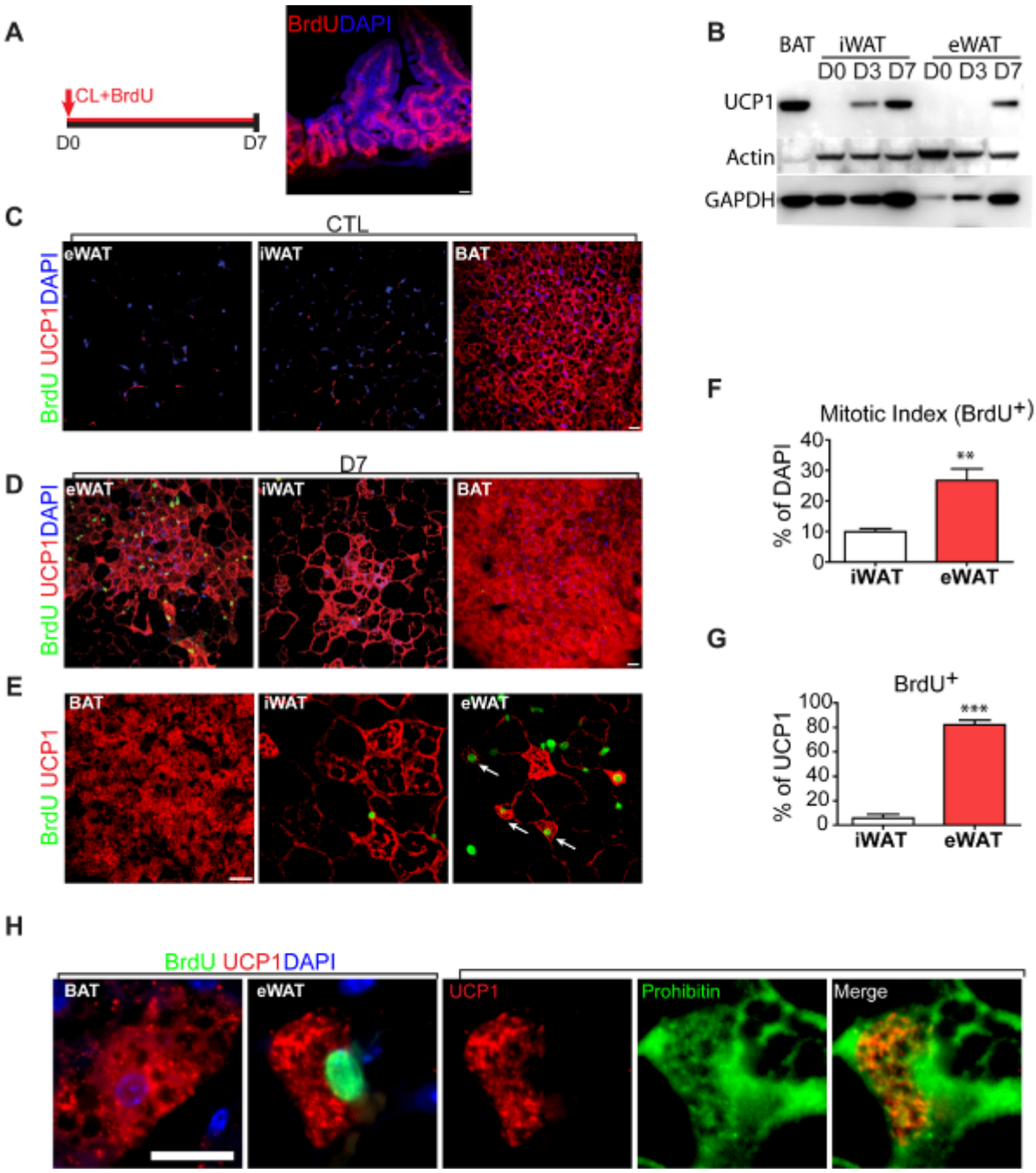

Figure 3. iBA in eWAT are derived from proliferating cells during β3-adrenergic stimulation

(A) Cumulative BrdU labeling during continuous CL316,243 (CL) treatment. A representative image of intestine paraffin sections stained for BrdU (red) from mice infused with BrdU for 7 days. BrdU continuously labeled proliferated cells from crypts through villi. (B) Immunoblot analysis of WAT from 129S1 mice treated with CL. Equal amounts of proteins were run, and blots sequentially probed for UCP1, and loading controls. (C, D) Low magnification fields of adipose tissue paraffin sections from CTL (BrdU only) and D7 (CL + BrdU) mice double-stained for BrdU (green) and UCP1 (red). $BrdU^+$ cells were rarely detected in WAT without CL treatment. (E) Higher magnification of BA in BAT and iBA (double-labeled for

BrdU and UCP1. (F) CL induced greater proliferation in eWAT versus iWAT (n = 4 per group, p=0.006). (G) Proliferation of iBA in iWAT and eWAT. Values are the percentage of BrdU+,UCP1+ to total UCP1+ cells. (mean ± SEM, n = 4 per group, p<0.0001). (H) in eWAT, showing comparable levels of UCP1 expression and subcellular localization. The merged image (right, green: prohibitin, red: UCP1) demonstrates mitochondrial targeting of UCP1 protein in iBA. Nuclei were counterstained with DAPI (Blue). Bars = 20 μm.

3.2. Tracking of proliferation identifies PDGFRα+ cells as potential iBA progenitors.

We next sought to characterize the phenotype of cells that were flash-labeled with EdU after 1, 2, and 3 days of CL treatment (**Figure 4A**). Flash labeling (2 hr) demonstrated that CL treatment produced pronounced proliferation that peaked after 3 days of treatment (**Figures 4B**). As detailed below, proliferating cells did not express detectible PDGFRβ, α-smooth muscle actin (SMA), or CD24, which are found in WA progenitors (49, 56). The recent report identifying PDGFRα as a marker of ectopic adipocyte progenitors in skeletal muscle (57, 58) prompted us to examine PDGFRα expression. PDGFRα$^+$ cells constituted 16.5 ± 0.7% of total cells in control WAT. We found nearly 80% of actively dividing cells expressed PDGFRα after the first day of CL treatment (**Figure 4C and 4D**). Unexpectedly, a terminal adipocyte differentiation marker, Perilipin1 (PLIN1), was also expressed in numerous EdU flash-labeled (i.e., 2 hr exposure) cells, especially after 3 days of CL treatment. EdU$^+$ adipocytes were small (< 10 μm) and contained small lipid droplets, indicating that newly-differentiating adipocytes can divide (92). (We have not observed cell division in mature, unilocular adipocytes.) Interestingly, > 90% of EdU$^+$ cells

expressed PDGFRα or PLIN1 (**Figure 4C – 4E**), but none expressed both markers at the same time (**Figure 4C**, compare upper and lower panels). Importantly, the frequency of PDGFRα expression in EdU^+ cells declined as PLIN1 expression increased, suggesting that $PDGFR\alpha^+$ progenitors might become $PLIN1^+$ iBA over the course of CL treatment. Because the population of $PDGFR\alpha^+$ cells did not change during CL treatment, it appears that some newly-divided cells replenish the progenitor pool while others down-regulated PDGFRα and differentiated into BA.

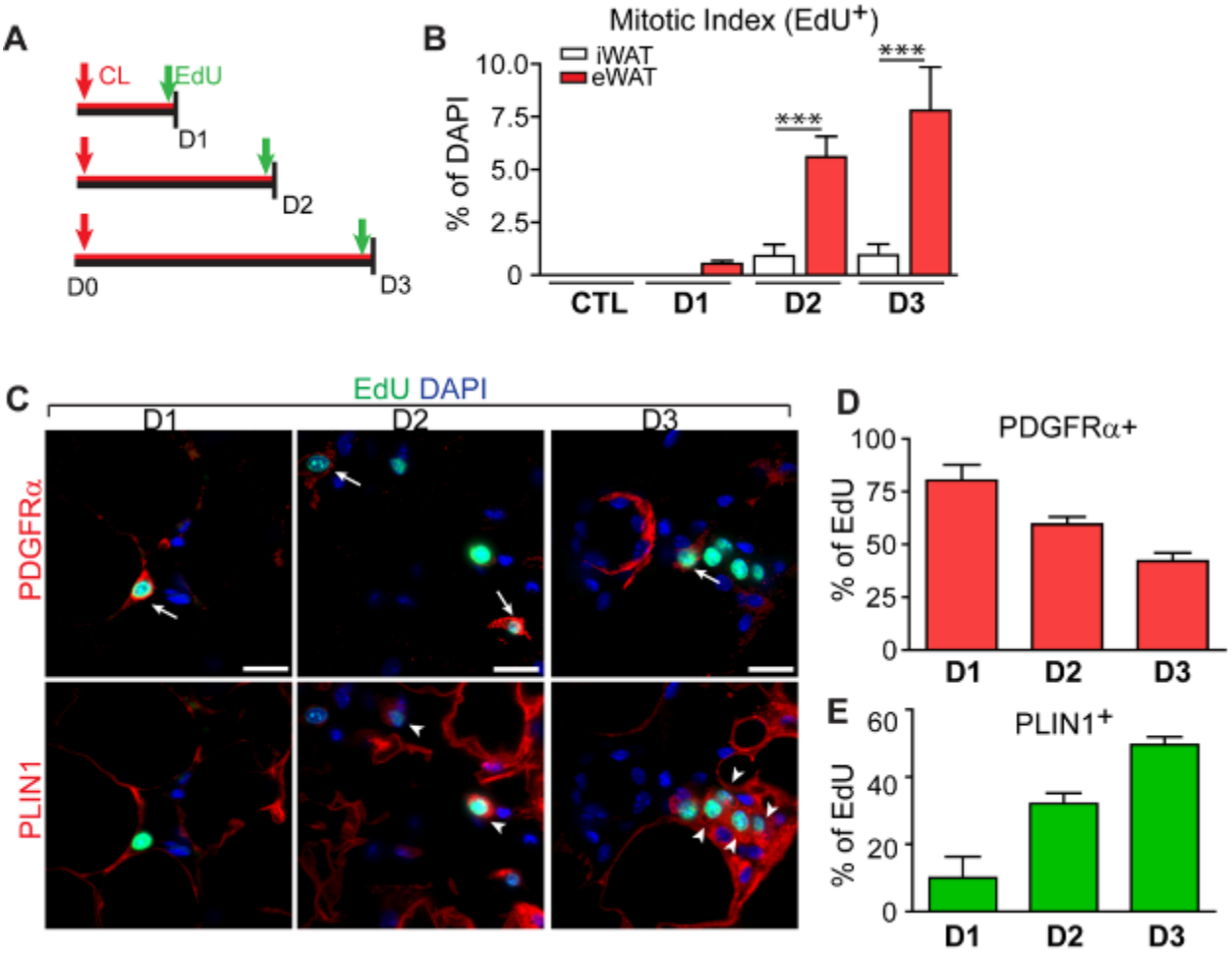

Figure 4 Proliferation cells express either PDGFRA or PLIN1. (A) EdU flash-labeling. 129S1 mice were infused with CL up to 3 days and injected with EdU 2 h before analysis. (B) CL significantly increased mitotic indices of both eWAT and iWAT ($p<0.0001$), and the effect was significantly greater in eWAT versus iWAT (ANOVA interaction $p=0.0033$, post-test ***$p<0.001$) (mean ± SEM, n = 3-4 per group). (C) Representative images of eWAT paraffin sections triple-stained for PDGFRα, PLIN1 and EdU on D1, D2, or D3 of CL treatment. Note that images of a given day are the same microscopic field. Top row shows merge of PDGFRα (red) and EdU (green), while bottom row is merge of PLIN1 (red) and EdU (green). Arrows mark PDGFRα+ EdU+ cells. Arrow heads mark PLIN1+ EdU+ cells. Nuclei were counterstained with DAPI (Blue). Triply stained images demonstrate that PLIN1 and PDGFRα expression are mutually exclusive. Bars = 20 μm. (D, E) Quantification of PDGFRα+ EdU+ cells, or PLIN1+ EdU+ cells in eWAT paraffin sections (mean ± SEM, n = 3-4 per group). Nearly all proliferating cells in eWAT express either PDGFRα or PLIN1. The percentage of PLIN1+, EdU+ cells increased over time (G, $p=0.0004$) as the percentage of PDGFRα+, Edu+ cells declined (F, $p=0.002$).

To trace the fates of proliferating cells in eWAT, mice were given single injections of EdU on the third day of CL infusion, when proliferation is maximal, and the phenotypic characteristics of EdU-labeled cells were evaluated over time (**Figure 5A**). Over the 24 h period after flash-labeling, the number of EdU^+ cells expressing PDGFRα progressively decreased as the number of EdU^+ cells expressing PLIN1 increased (**Figure 5C-5E**), indicating that proliferating cells lose PDGFRα expression as they become fat cells. By 24 h after EdU injection, most proliferating cells were multilocular and expressed PLIN1 (88.1 ± 4.3%) and UCP1 (85.4 ± 3.8%) (**Figure 5F**).

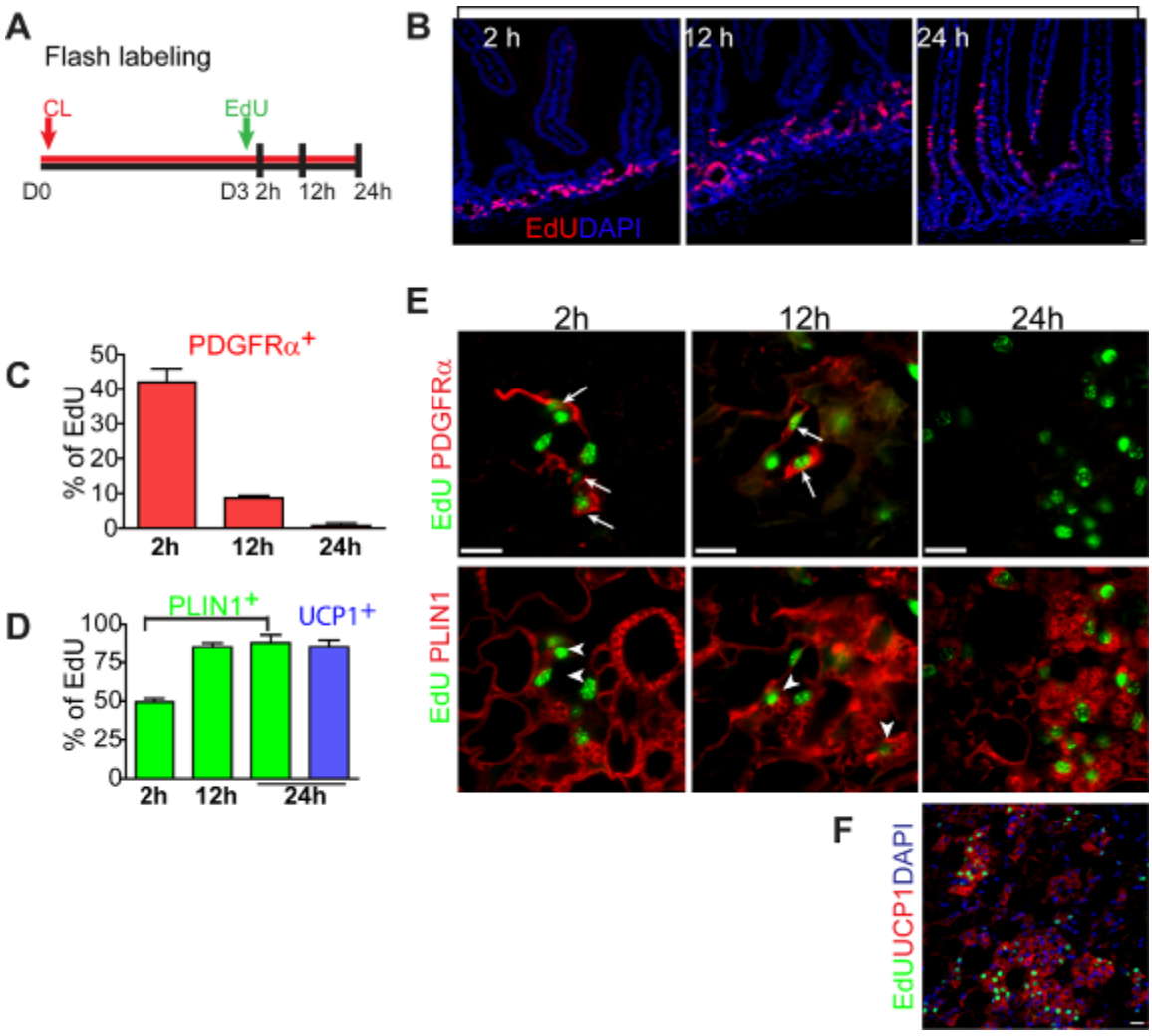

Figure 5. Tracing of proliferating cells identifies PDGFRα+ cells as potential iBA progenitors. (A) Fate tracing of cells labeled with EdU on the third day of CL treatment. 129S1 mice were infused with CL, injected with EdU on D3, and analyzed at indicated time points. B) Representative images of intestine paraffin sections stained for EdU (red) at indicated time points after EdU injection. EdU+ (red) intestinal stem cells that actively proliferated were detected in crypts 2h after EdU injection while EdU+ cells progressively differentiated over time and were detected in villi at 24h after EdU injection. ((C, D) Proportion of each cell type is expressed as percentage of the total EdU+ cells (mean ± SEM, n = 3-4 per group). PDGFRα expression declined (p=0.0002) as PLIN1 expression appeared (p=0.0001) in EdU-labeled cells. By 24 h, 85% of EdU+ cells expressed UCP1. (E) Representative images of eWAT paraffin sections triple-stained for PDGFRα, PLIN1 and EdU at 2 h, 12 h, and 24 h after EdU injection. Top row shows merge of PDGFRα (red) and EdU (green), while bottom row is merge of PLIN1 (red) and EdU (green) of the same field. Arrows mark PDGFRα+ EdU+ cells. Arrow heads mark PLIN1+ EdU+ cells. (F) Low magnification fields of eWAT paraffin sections double-stained for EdU (green) and UCP1 (red) at 24h after EdU injection. Bars = 20 μm.

We performed an additional experiment to trace a relatively pure population of PDGFRα$^+$ cells by labeling cells with EdU on day 1 (**Figure 6**). As expected, 88.8±1.8% of EdU$^+$ cells expressed PDGFRα, and two days later most EdU$^+$ cells tagged became multilocular brown adipocytes that expressed PPARα, PLIN1 and UCP1. Interestingly, 16.0 ± 1.6% of EdU$^+$ cells labeled on day 1 retained PDGFRα expression two days later (**Figure 6**), indicating that PDGFRα$^+$ cells undergo self-renewal as well as adipogenic differentiation. To test whether undifferentiated (PDGFRα$^+$, PLIN1$^-$) and newly-differentiated (PDGFRα$^-$, PLIN1$^+$) cells can undergo multiple divisions. CL-treated mice were injected with EdU on the first day of CL treatment and again with BrdU one day later (**Figure 7**). Data from this dual pulse labeling indicated that 48.0 ± 11.3% of EdU$^+$ PLIN1$^+$ cells (that divided on day 1) were marked by BrdU on day 2, demonstrating that a significant number of iBA progenitors divided more than once.

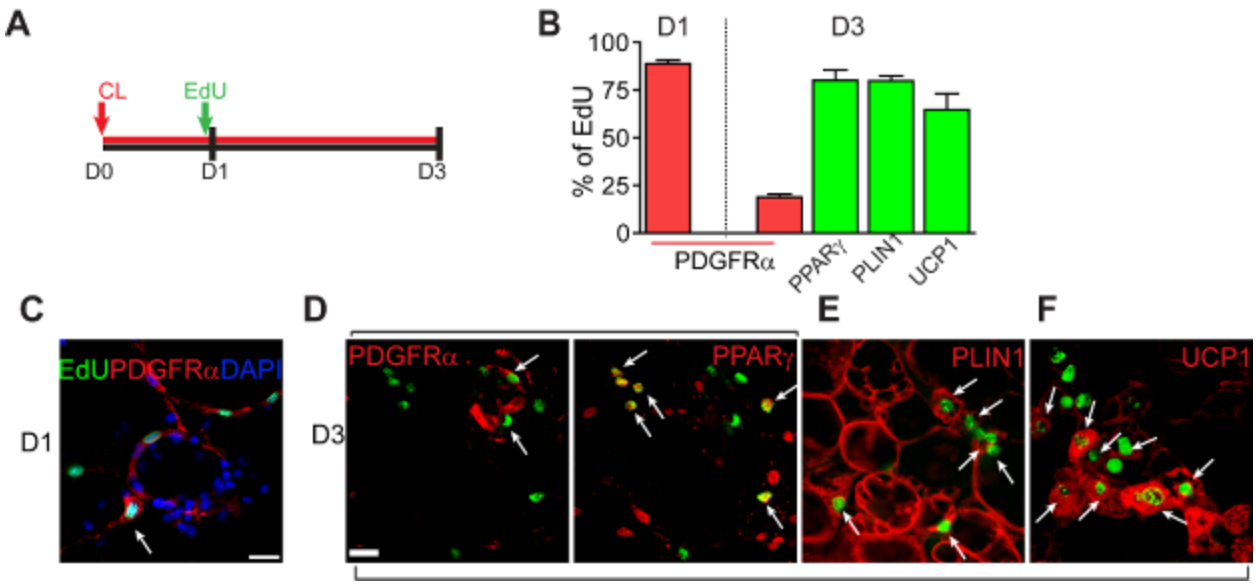

Figure 6. Tracing of proliferation identifies PDGFRα+ cells as potential iBA progenitors. (A) Fate tracing of cells labeled with EdU on the first day of CL treatment. 129S1 mice were infused with CL injected with EdU on D1 and analyzed 2 h (D1) or 48 h (D3) after EdU injection. (B) Distribution of markers in EdU+ cells (mean ± SEM, n = 3-4 per group). The pattern of PDGFRα and PPARγ expression in EdU+ cells changed significantly between D1 and D3 (Fisher's exact test, $p<0.0001$). (C) Representative images of eWAT whole mounts double-stained for PDGFRα (red) and EdU (green) on D1. Mitotic figures of EdU+ PDGFRα+ cells (arrows). (D-F) Representative images of eWAT whole mounts or paraffin sections on D3. (G) Triple staining for PDGFRα PPARγ and EdU. (Left) Merge of PDGFRα (red) and EdU (green). (Right) Merge of PPARγ (red) and EdU (green). (H) Double staining for PLIN1 (red) and EdU (green). (I) Double staining for UCP1 (red) and EdU (green). Double positive cells are marked by arrows. Bars = 20 μm.

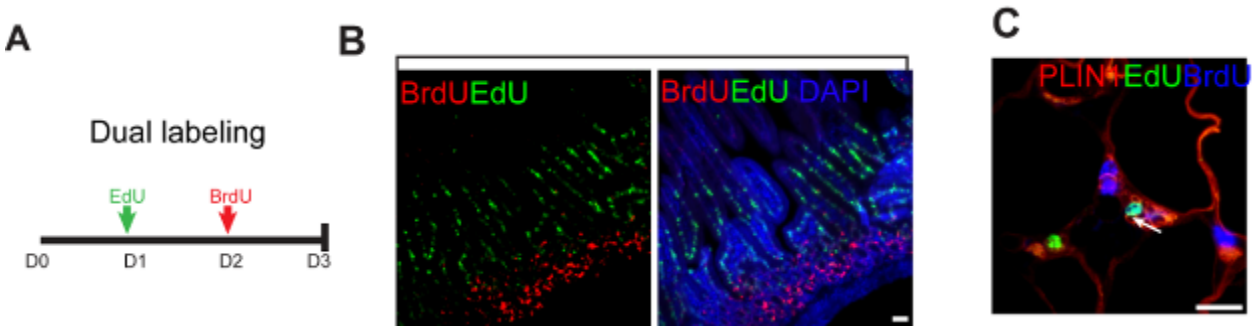

Figure 7. iBAP undergo multiple divisions during brown adipogenic differentiation. (A, B) Double staining of intestine paraffin section shows that each thymidine analog labeled discrete cell populations in intestine: EdU-labeled cells (green) were detected in migrating populations, while BrdU-tagged cells (red) were located near crypts. No double-positive (EdU^+ $BrdU^+$) cells were detected. (C) Triple staining for PLIN EdU and BrdU. Triple positive cells are marked by arrows. Bars = 20 μm.

3. 3. Phenotypic and morphological characteristics of PDGFRα+ progenitors

Confocal imaging of whole mount adipose tissue revealed the unique morphology of $PDGFR\alpha^+$ cells. These cells extended multiple thin cytoplasmic processes (~50μm in length) that were in close proximity to stromal cells, adipocytes and capillaries (**Figure 8**). Although sometimes coursing along capillaries, the processes of $PDGFR\alpha^+$ cells extended into the interstitial space **(Figure 8 arrows).** $PDGFR\alpha^+$ cells were also observed on large diameter blood vessels, however, these cells were not labeled by thymidine analogs, and thus do not contribute directly to brown adipogenesis induced by CL. As mentioned earlier, WA progenitors have been identified as $PPAR\gamma^+$ pericyte-like cells that express SMA and PDGFRα (49). In

contrast, adipose tissue PDGFRα$^+$ cells labeled immunochemically or genetically (below) were negative for SMA, PPARγ (**Figure 8A**). Furthermore, unlike pericytes/adipocyte progenitors, stromal PDGFRα$^+$ cells were larger and did not share a collagen IV basement membrane with endothelial cells as do PDGFRα$^+$ pericytes (**Figure 9**). Analysis of eWAT stromal cells by FACS demonstrated that PDGFRα$^+$ cells are a subpopulation of cells expressing the stem cell markers CD34 and Sca1 (Figure 8B); however, FACS analysis failed to detect significant coexpression with WA progenitor markers CD24 and PDGFRα or the endothelial cell marker isolectin IB4.

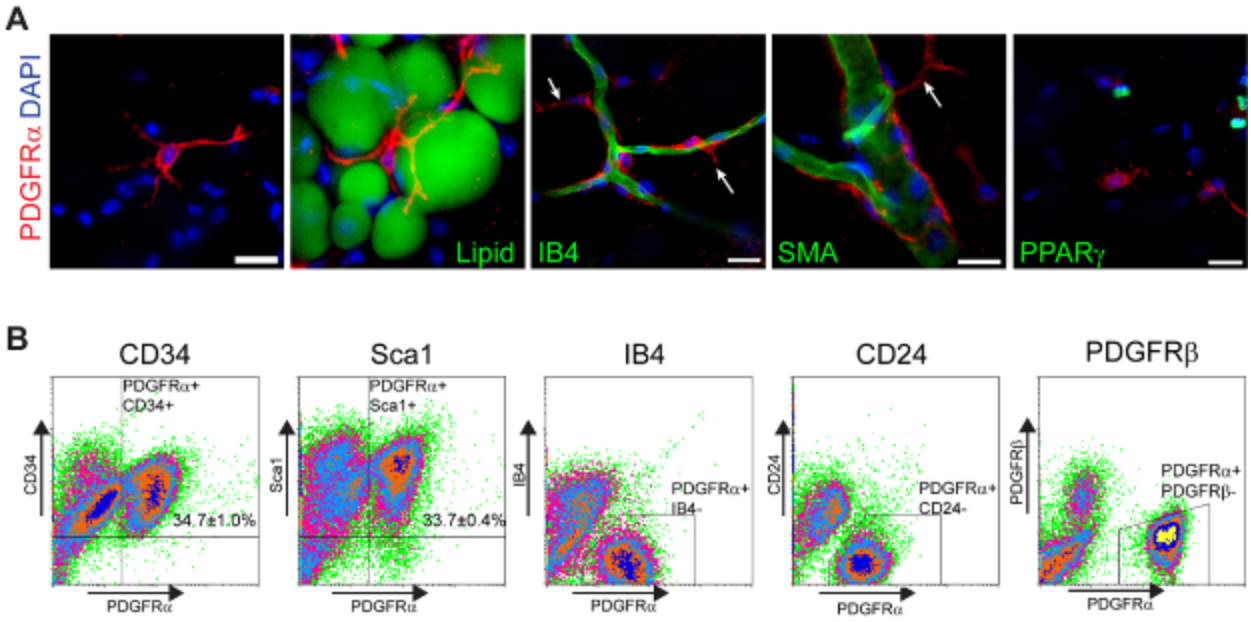

Figure 8. Phenotypic and morphological characteristics of PDGFRα$^+$ cells. (A) Immunostaining of PDGFRα+ cells in eWAT whole mount from control 129S1 mice. (A) Stellate morphology of PDGFRα+ cells (red). Each cell had multiple processes, some up to 50 μm long, and contacted multiple cells, including adipocytes (Lipid+). PDGFRα+ cells were often in close apposition to IB4+ vasculature (green), but did not constitute the mural compartment, indicated by extended processes (arrows). PDGFRα+ cells were negative for SMA and PPARγ. Nuclei were counterstained with DAPI. Bars = 20 μm. (B) FACS analysis on cell surface marker expression of PDGFRα+ cells. PDGFRα+ cells were uniformly positive for CD34 and Sca1, but negative for IB4, CD24, and PDGFRβ. The percentage of double positive cells are indicated on the flow profile (mean ± SEM, n = 3 independent analyses).

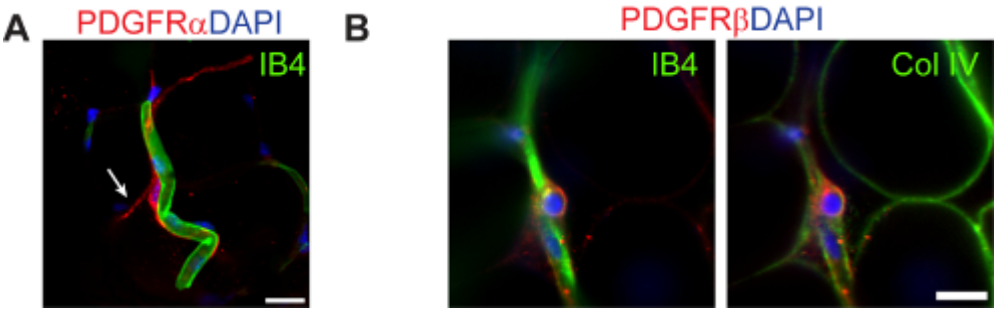

Figure 9. Morphological characteristics of PDGFRα+ progenitors. (A) Double staining of whole mount eWAT from control 129S1 mice. Stellate–like PDGFRα^{+} cells were often in close apposition to IB4^{+} capillaries (green), but did not constitute the mural compartment, indicated by processes (arrow) extending into the interstitial space. (B). Triple staining for PDGFRβ, IB4, and collagen IV. (Left) Merge of PDGFRβ (red) and IB4 (green) fluorescence. (Right) Merge of PDGFRβ (red) and collagen IV (green) florescence. PDGFRβ^{+} cells were enclosed by basement membrane (collagen IV^{+}). Nuclei were counterstained with DAPI. Bars = 20 μm.

3.4 PDGFRα + progenitors become BA during ADRB3 stimulation.

3.4.1 Lineage tracing using inducible reporter system.

To provide conclusive information on the fate of the PDGFRα expressing progenitors, we performed *in vivo* lineage tracing with two different PDGFRα reporter lines. In one series of experiments, we crossed Cre-responsive (stop codon floxed) reporter mice (85) with mice expressing tamoxifen-inducible CreER^{T2} under the control of PDGFRα promoter (64) (**Figure 11A**). In this system, treatment of mice with tamoxifen induces expression of tdTomato in

PDGFRα^+ cells via Cre-mediated recombination. Because the induction is permanent, reporter expression remains in all the cells descending from the originally marked cells.

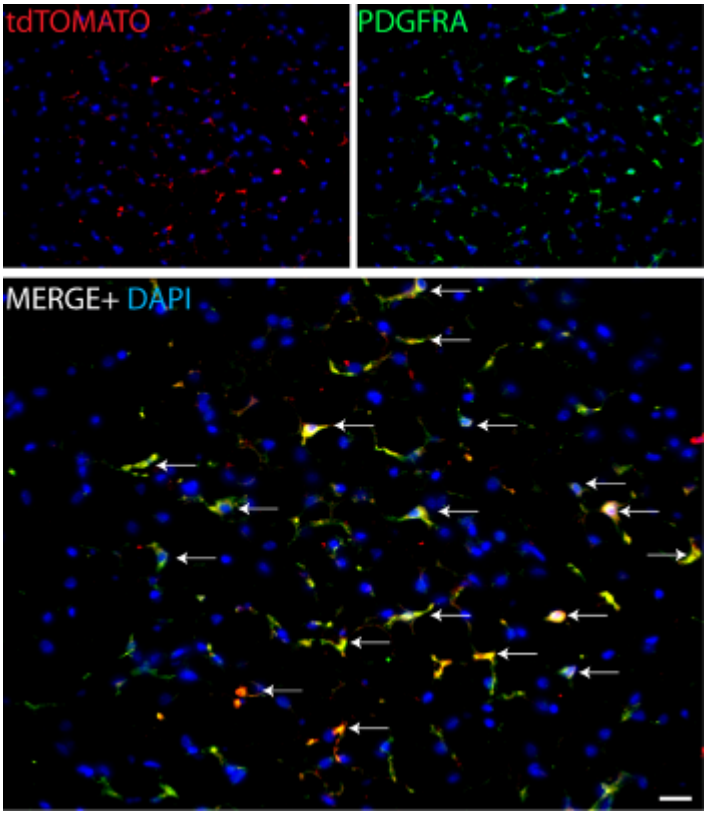

Figure 10. High efficiency and specificity of Pdgfra-Cre/ R26-LSL-tdTomato reporter system. A low magnification image of double staining of eWAT paraffin section from control Pdgfra-Cre/ R26-LSL tdTomato mice treated with tamoxifen for 5 days. Analysis was done 7 days after tamoxifen first dose. Red is tdTomato staining and green is PDGFRA staining. Merged image shows high efficiency and fidelity of tdTomato expression in PDGFRA expressing cells (PDGFRα^+ tdTomato$^+$/ PDGFRα^+ = 57.5 ± 5% in iWAT, 50.4 ± 3% in eWAT. n=3) Bars = 20 μm.

tdTomato was not observed in the absence of tamoxifen treatment. Tamoxifen induced strong tdTomato fluorescence with high efficiency in adipose tissues **(Figure 10:** PDGFRα^+ tdTomato$^+$/ PDGFRα^+ = 57.5 ± 5% in iWAT, 50.4 ± 3% in eWAT). Strong native fluorescence (tdTomato) was uniformly distributed throughout the cells and allowed 3D visualization of their fine structures in whole mount tissues. Consistent with immunostaining analysis, tdTomato-

labeled cells were often located in the perivascular region and displayed long thin processes that contacted adjacent adipocytes and vasculature (**Figure 11C**). Prior to CL treatment, all tdTomato$^+$ cells were positive for PDGFRα and CD34 (**Figure 11D**); however, tdTomato$^+$ cells did not express the developmental WA progenitor markers PPARγ, PDGFRβ, or SMA (**Figure 11C**).

After 7 days of CL treatment, nearly half of the tdTomato expressing cells had multilocular morphology and expressed BA markers PPARG, PLIN1, and UCP1 (**Figures 11E – 11H**). PPARG and PLIN1 are early markers of BA differentiation that were often observed in actively dividing cells. In contrast, UCP1 expression was only seen in cells that were more differentiated, which accounts for differences in the relative abundance of the early and late BA markers (also, see below). While half of tdTomato$^+$ cells were BrdU$^+$ (**Figure 11H**), over 90% of tdTomato$^+$ multilocular adipocytes were BrdU$^+$, indicating nearly all BA were derived from proliferating cells. As expected from EdU tagging experiments, multilocular tdTomato+ cells lacked expression of PDGFRα (**Figure 11E**, arrow heads), whereas stellate progenitors remained PDGFRα^+ (**Figure 11E,** arrows). Furthermore, the percentage of tdTomato$^+$ cells that became PLIN1$^+$ adipocytes was 3-fold higher in eWAT compared to iWAT (not shown). Finally, we isolated tdTomato$^+$ cells from control mice and mice treated with CL for 7 days by FACS and examined adipogenic gene expression (**Figure 11I**). Consistent with immunochemical analyses, CL treatment dramatically

upregulated expression of brown adipocyte markers Ucp1, Elovl3, Dio2 and Cidea. It should be noted that this analysis likely underestimates the effect of CL since floating adipocytes were not recovered.

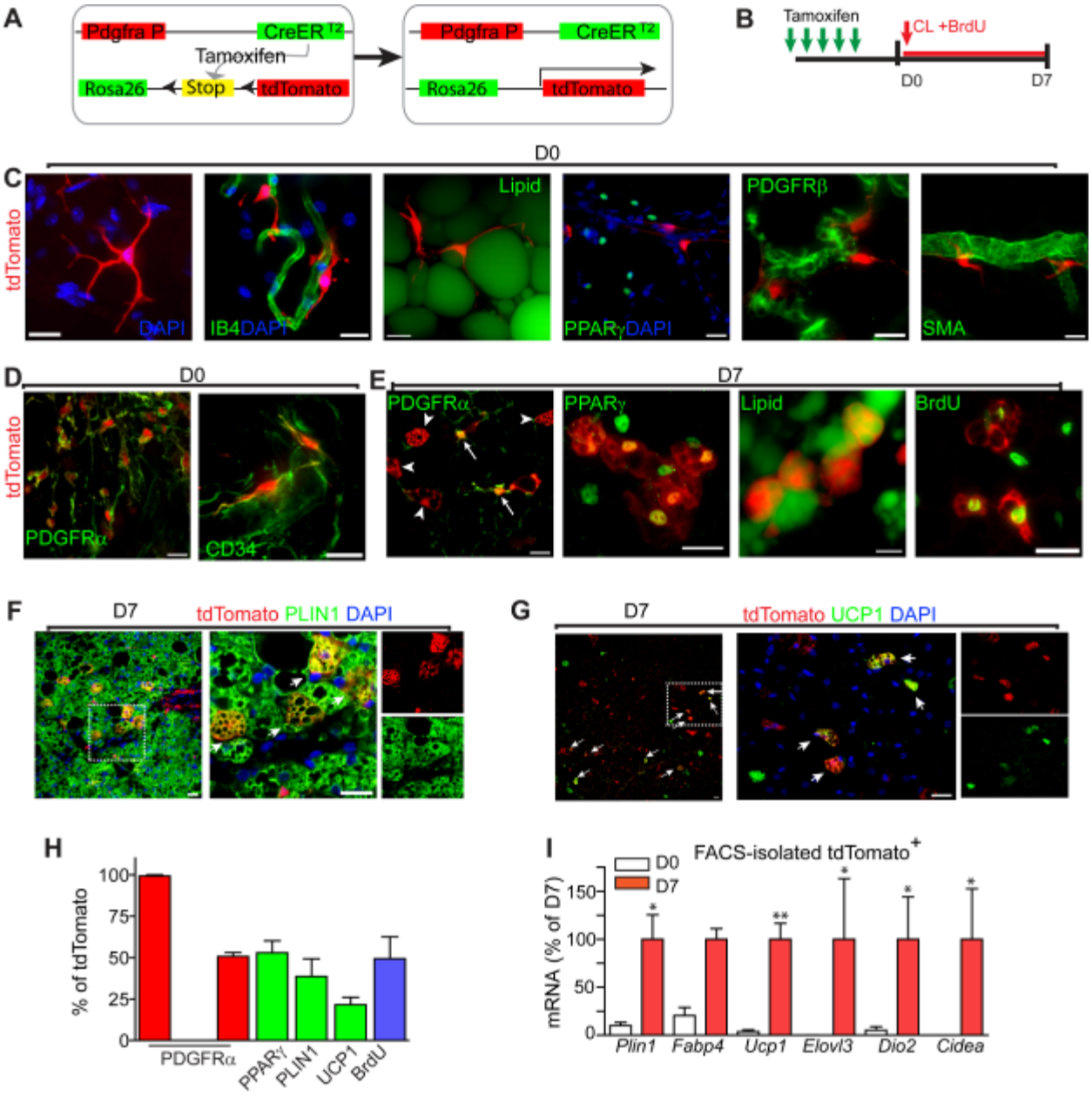

Figure 11. PDGFRα expressing progenitors become BA during β3-adrenergic stimulation: Pdgfra-CreER^{T2}/R26-LSL-tdTomato mouse study.

(A) Schematic diagram of the inducible Pdgfra-CreERT2/R26-LSL-tdTomato reporter system. (B)

Procedure of reporter induction and lineage tracing of tdTomato-labeled cells. Efficiency and specificity of reporter induction were analyzed 7 days after the first tamoxifen dose. Adipose tissue was analyzed before (D0) or 7 days (D7) after CL and BrdU infusion. (C,D) Characterization of reporter+ cells prior to CL treatment. Labeled cells were often found near blood vessels (IB4+) and had long processes that appeared to contact stromal cells and adipocytes (LipidTox+). tdTomato+ cells were negative for PPARγ, PDGFRβ, and SMA, but uniformly positive for PDGFRα and CD34. (E-G) Characterization of reporter+ cells following 7 days of CL treatment. tdTomato+ multilocular adipocytes (arrow heads) lacked expression of PDGFRα, whereas stellate-like progenitors (arrows) remained PDGFRα^{+}. tdTomato+ multilocular cells coexpressed PPARγ, UCP1, and contained PLIN1^{+} lipid droplets. Incorporation of BrdU of tdTomato+ multilocular adipocytes indicates that iBA came from proliferating cells. (F, G) Low magnification images of eWAT paraffin sections double stained for tdTomato and PLIIN1 (F), or UCP1 (G). Arrows mark double positive cells. Right is a magnified view of the boxed region from left. Bars = 20 μm. (H) Distribution of markers in tdTomato+ cells (mean ± SEM, n = 3 per group). All tdTomato+ cells expressed PDGFRα and none expressed PPARγ on day 0. By day 7, 47.3 ± 1.5% of tdTomato+ cells retained expression of PDGFRα while 52.9 ± 7.2 % of tdTomato+ cells expressed PPARγ (Fisher's exact test, $p<0.0001$). In addition, PLIN1 (38.7 ± 10.6%) and UCP1 (21.5 ± 4.4%) expression and BrdU incorporation (49.3 ± 13.2) were detected in tdTomato+ cells. (I) qPCR analysis of BA marker expression in Pdgfra-tdTomato tagged cells isolated by FACS, expressed relative mRNA levels of D7. BA markers were significantly upregulated in tdTomato+ cells after 7 days of CL treatment. (mean ± SEM, n = 4-5, *Plin1*: p=0.016, fatty acid bind protein 4 *(Fabp4)*: p=0.057, *UCP1*: p=0.008, and *Elovl3*: p=0.029, *Dio2*: p=0.033, *Cidea*: p=0.011)

3.4.2 Lineage tracing using constitutive reporter system.

In a second series of experiments, chromatin-targeted H2BeGFP that was transgenically expressed from the PDGFRα locus (**Figure 12A**) was used to trace the fate of PDGFRα^{+} cells in the absence of ongoing PDGFRα expression. Immunohistochemical analysis confirmed that prior to CL treatment, all GFP^{+} cells expressed PDGFRα, but not previously-established WA

progenitor markers (**Figures 12B and 12C**). As expected, nearly 80% of cells induced to divide after 1 day of CL were GFP^+, and few of these cells expressed $PPAR\gamma^+$ (**Figures 12E**). However, by day 3, 55.3 ± 6.3% of EdU^+ cells that divided on day 1 expressed both GFP and PPARγ (**Figures 12E and 12F**). Multilocular GFP^+ cells expressed PLIN1 and UCP1 that were targeted to lipid droplets and mitochondria, respectively (**Figures 12F and 12G**). It is important to note that these cells were negative for PDGFRα protein and the presence of GFP reflected prior, not current, expression of PDGFRα. Collectively, lineage tracing with two independent genetic marking systems clearly demonstrates that $PDGFR\alpha^+$ cells are BA progenitors within WAT.

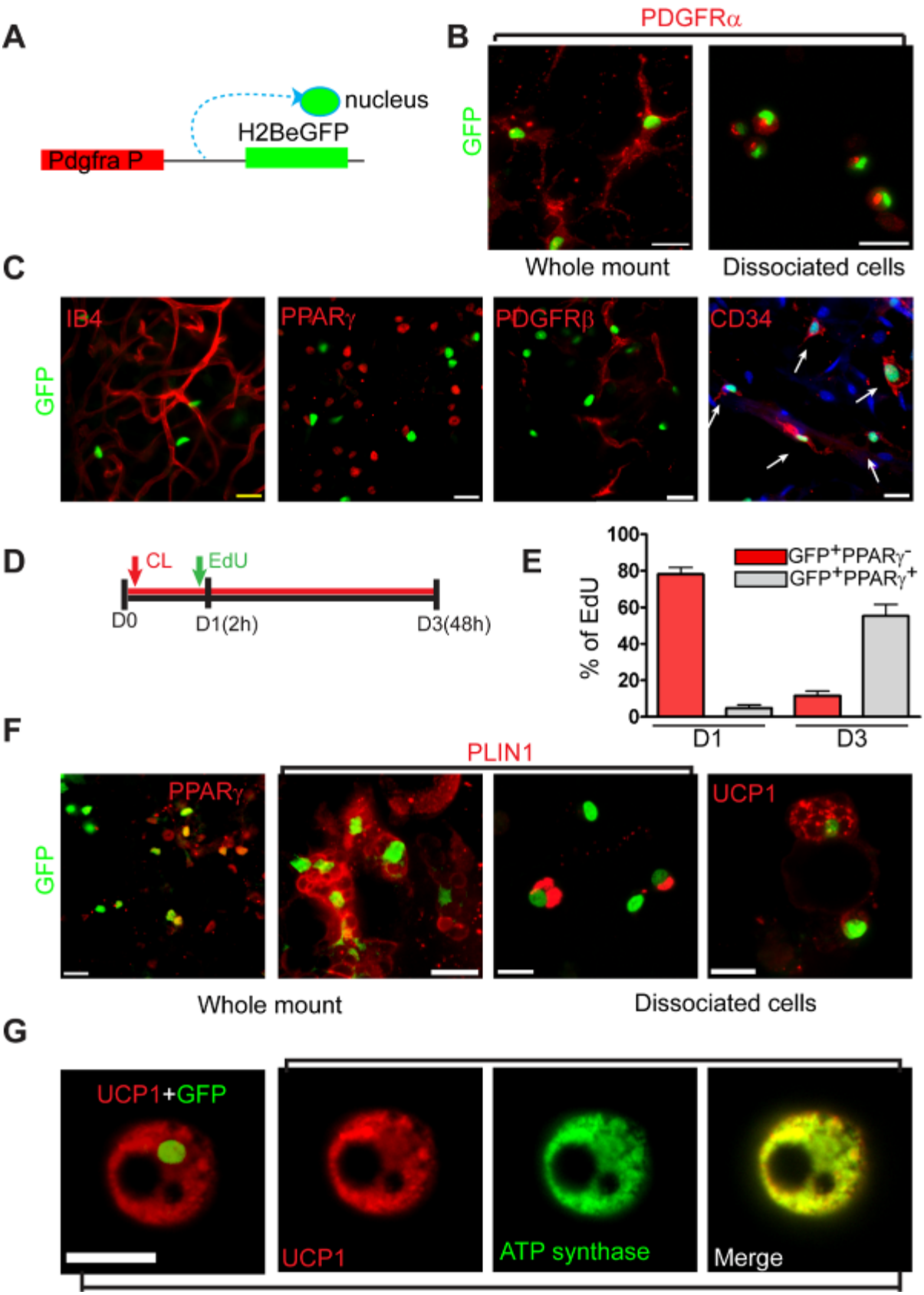

Figure 12. PDGFRα expressing progenitors become BA during β3-adrenergic stimulation: Pdgfra-

H2beGFP mouse study.

(A) Schematic diagram of Pdgfra-H2BeGFP reporter mouse. (B, C) Representative images of H2BeGFP expressing cells in eWAT stained for several markers before CL treatment (D0). (B) All GFP^+ (green) cells expressed PDGFRα (red) and *vice versa*. (C) GFP^+ cells were usually located near vasculature ($IB4^+$). GFP^+ cells were negative for PPARγ and PDGFRβ. All GFP^+ cells were positive for CD34, indicated by arrows. (D) Fate tracing of H2BeGFP expressing cells labeled with EdU on the first day of CL treatment. Pdgfra-H2BeGFP mice were infused with CL, injected with EdU on D1, and tissue examined 2 h (D1) or 48 h (D3) later. (E) Distribution of markers in EdU^+ cells (mean ± SEM, n = 4 per group). After the first day of CL treatment, 80.9% of EdU^+ cells expressed GFP and were negative for PPARγ. After the third day of CL treatment, 55.3% of EdU^+ cells on D3 expressed GFP and PPARγ (Fisher's exact test, $p< 0.0001$). (F, G) Representative images of whole mount or dissociated single cells from eWAT of Pdgfra-H2BGFP mice infused with CL for 3 days, showing BA marker expression in Pdgfra-GFP tagged cells (red) on D3. (G) Representative images of Pdgfra-H2BeGFP tagged iBA double-stained for UCP1 and ATP synthase. The merged image (green: ATP synthase, red: UCP1) demonstrates mitochondrial targeting of UCP1 protein in iBA. Bars = 20 μm.

3.5 iBA become convertible WA that can re-express UCP1 by ADRB3 stimulation.

To determine the fate of PDGFRα+ cell derived iBA after cessation of ADRB3 stimulation, we tagged PDGFRα+ cells with tdTomato using inducible Cre recombination, induced brown adipogenesis with CL treatment for 1 week, then withdrew ADRB3 stimulation for 3 weeks (**Figure 13A**). Following withdrawal of CL, tdTomato reporter tagged PLIN1+ cells exhibited a unilocular phenotype and lacked detectible expression of UCP1, indicating that these cells revert to WA phenotype (**Figure 13B,** Top low). Interestingly, brief treatment of mice with CL triggered these cells to express UCP1 and to revert to a multilocular phenotype (**Figure 13B,** Bottom low). These BA did not incorporate BrdU (i.e., were not generated *de novo*), and could

be readily distinguished from surrounding untagged WA that remained unilocular and lacked UCP1 expression. Overall, the frequency of UCP1 induction was nearly identical to iWAT, in which UCP1 expression is triggered in convertible adipocytes in the absence of proliferation (**Figure 13**). These data indicate that PDGFRα+ progenitors are convertible adipocytes whose brown adipogenic phenotype depends on the level of ongoing adrenergic activation.

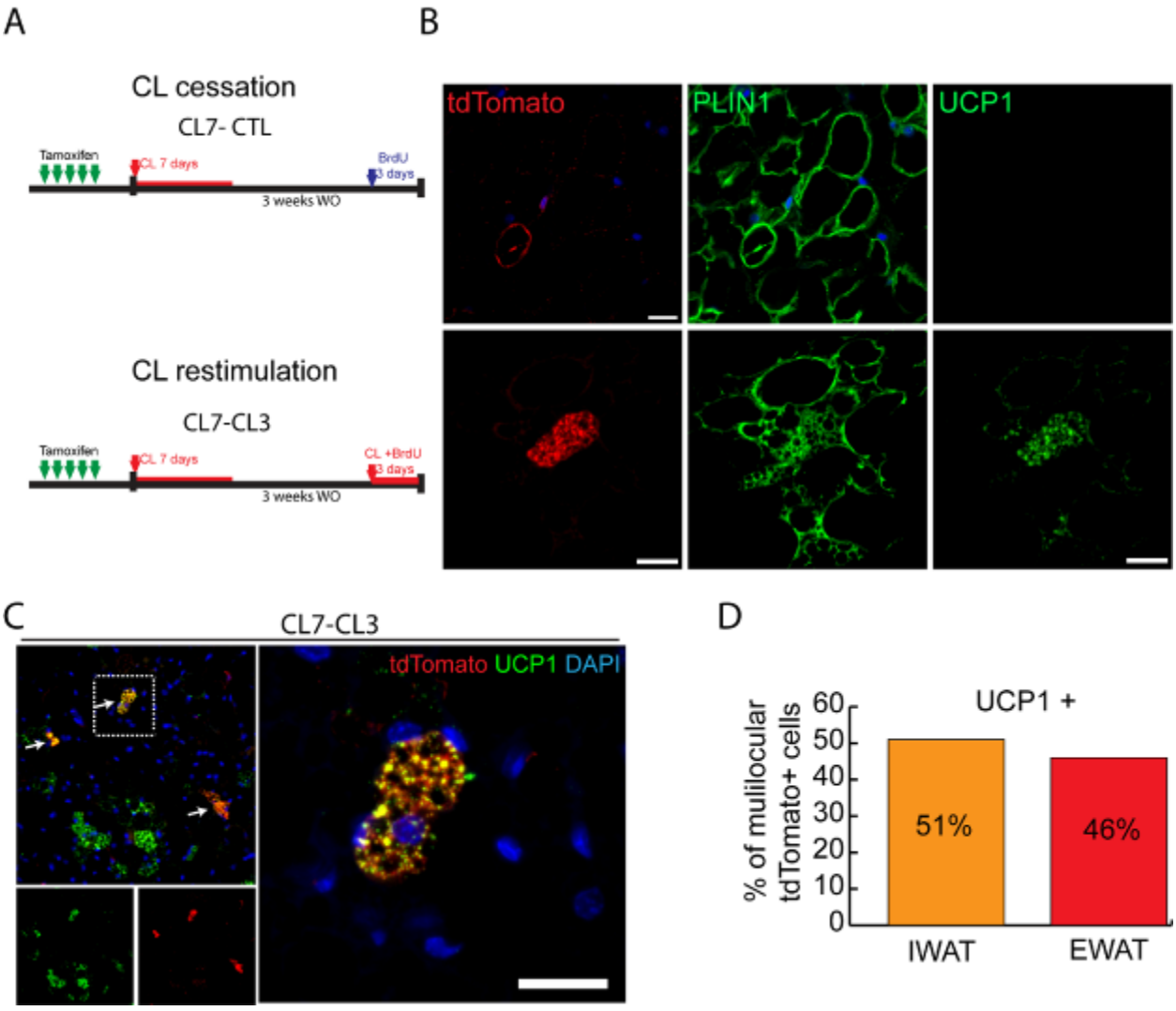

Figure 13. iBA become convertible WA that can re-express UCP1 by β-adrenergic stimulation.
(A) Schematic diagram of reporter induction and CL treatment procedures. (B) Representative images of tdTomato tagged cells in eWAT stained for PLIN1 and UCP1 (B, top row) after 3 weeks of CL washout period tdTomato converted into WA with no detectible level of UCP1 expression. (B, bottom row) After 3 days of CL treatment, tdTOmato tagged adipocyte become UCP1 expressing BA, indicating that they are convertible. (C) Low mag and High magnification image of paraffin section from CL restimulated group. (D) quantification of UCP1 expression in multilocular tdTomato+ adipocytes.

Chapter 4. Identification of adipocyte progenitor niches

4.1 Identification of cellular components in brown adipogenic niches

4.1.1. ADRB3-mediated proliferation in WAT correlates with CLS formation.

Our lineage tracing studies in combination with immunohistochemical analysis have shown that BA arise from proliferating progenitors that expressed PDGFRα, Sca1 and CD34 in WAT (**Chapter 3**). The extent of nascent BA generation from the progenitors is higher in eWAT compared to iWAT, even though eWAT and iWAT contained similar numbers of PDGFRα+ progenitors. These observations raise the possibility that differences in the response of iBA progenitors from abdominal and subcutaneous WAT might involve depot-specific differences in microenvironment triggered by adrenergic activation.

Defining progenitor niche components is essential to understand the progenitor biology since stem/progenitor cell niches in tissues regulate stem/progenitor cell behaviors through local signaling (93). Adipose tissue macrophages have been known to be involved in tissue remodeling and affect metabolic phenotype of adipose tissue (72, 79, 81, 91, 94). Therefore, to explore the possibility that macrophages may involve in progenitor activation/proliferation, we examined recruitment of macrophages and their correlation with proliferation of PDGFRα+ progenitor during CL treatment. 129S1 mice were infused with CL for 3 days and injected with

EdU 2hr before analysis. Macrophage recruitment in eWAT and iWAT from control and CL-treated mice were determined by immunohistochemistry and mRNA expression analysis (**Figure 14**). The number of F4/80+ macrophages was significantly increased in eWAT by CL treatment, and this recruitment was observed exclusively in eWAT (**Figure 14A-14C**). Consistently, expression of Emr1, the gene encoding F4/80, was significantly upregulated in eWAT, compared to control conditions and iWAT from CL-treated mice (**Figure 14D**). Triple staining for F4/80, PLIN1 and EdU demonstrated that macrophages formed crown-like structure (CLS), surrounding PLIN1 negative adipocytes and EdU+ proliferating cells were closely associated with CLS. CLS have been definedas cluster of macrophages that surround dead adipocytes to remove lipid debris from dying adipocyte. 59 ± 4.4% of EdU+ cells were found in close proximity with CLS (≤ 20μm), showing possible interaction between proliferating progenitors and macrophages (**Figure 14B**). Interestingly, newly differentiating EdU+ PLIN1+ adipocytes no longer contacted CLS, supporting the idea that macrophage trigger initial activation of progenitors (**Figure 15**). In addition, the number of CLS was higher in eWAT and positively correlated with levels of proliferation (**Figure 14E and 14F**). Together, analysis on adipose tissue macrophages during CL treatment suggested that CLS may contribute to form progenitor activation niches that promote proliferation of BA progenitors.

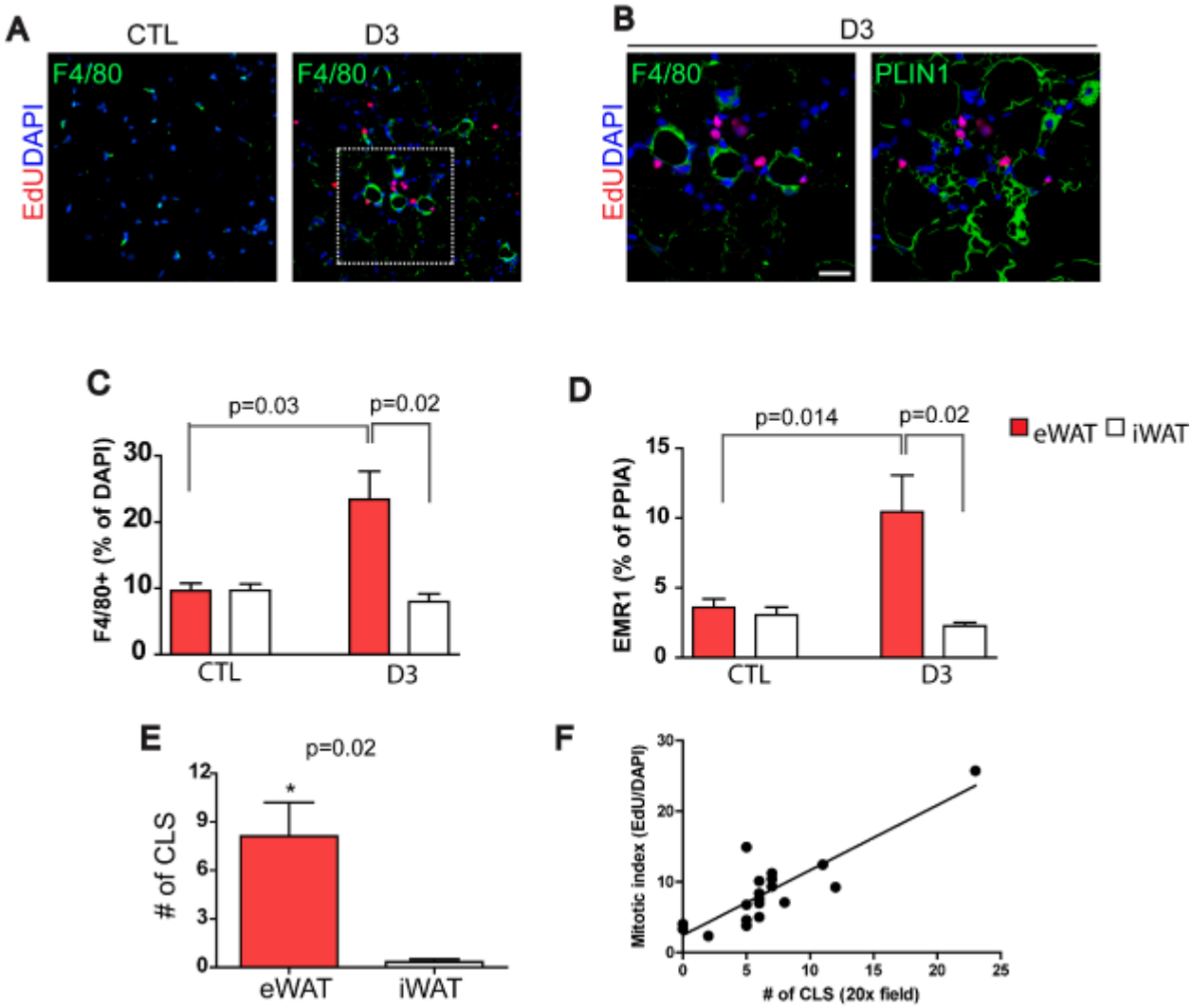

Figure 14. ADRB3-mediated proliferation correlates with CLS formation.

(A) Representative images of WAT paraffin sections from control or CL treated S1 mice stained for F4/80 and EdU on D3 of CL treatment. Images demonstrated close association of EdU+ proliferating cells with CLS. Nuclei counter-stained with DAPI. (B) Higher magnification of eWAT paraffin sections from CL treated S1 mice, triple-stained for F4/80 (left, green), PLIN1 (right: green) and EdU (red). Left is a magnified view of boxed region from (A), and right is the merge with PLIN and EdU in the same field, showing macrophages surround PLIN- adipocytes. (C) Quantification of F4/80+ cells during CL treatment, showing recruitment of F4/80+ cells in eWAT (n=3, CTL VS D3 P=0.020, eWAT vs iWAT p=0.004) (D) qPCR analysis for Emr1 expression, showing significant upregulation of a macrophage specific marker in eWAT on day 3 (n = 4 - 6 ,CTL vs. D3: p=0.0207 , eWAT vs. iWAT: p=0.0145) (E) Quantification of the number of CLS in WAT paraffin section from CL-treated mice (D3). (F) A positive correlation between the number of CLS and mitotic index (EdU+/DAPI+). >5 of 20X field images of paraffin sections from 3 of CL D3 mice were quantified, and individual numbers were plotted (r square= 0.7419, p<0.0001)

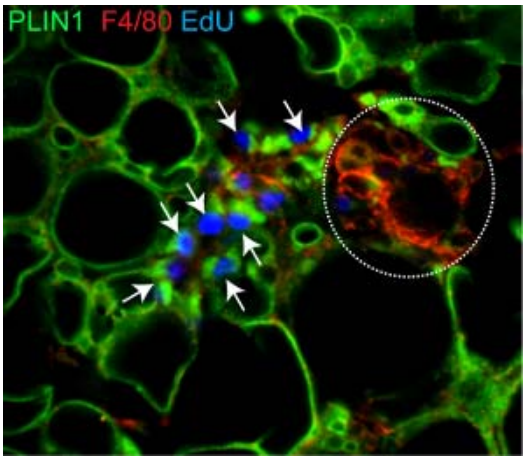

Figure 15. Newly-differentiated adipocytes from proliferating cells no longer associated with CLS. A Representative image of eWAT paraffin sections from CL treated S1 mice stained for F4/80, PLIN1 and EdU after three days of CL treatment. Arrows indicate newly-differentiate adipocytes. A circled region with dashed line indicates CLS.

4.1.2. ADRB3 recruit alternatively-activated macrophages.

To understand how macrophage recruitment affects the inflammatory phenotype of eWAT during CL, we examined proinflammatory (M1) and antiinflammatoty (M2) marker expression by qPCR. Data indicated that expression levels of M2 macrophage markers (arginase 1 and IL10) were upregulated, whereas expression levels of pro-inflammatory cytokines (PAI1, Ccl2, IL6) were unaffected by CL treatment (**Figure 16A**). Triple-staining for MGL1 (M2 marker), PLIN1 and Lipid in eWAT whole mount confirmed that M2 macrophages formed CLS and surrounded lipid droplets devoid of PLIN1 (i.e. dead adipocyte lipid core) (**Figure 16B**). CLS have been characterized in hypertrophied adipose tissue with advanced obesity (95). It has been proposed that M1 macrophages surround necrotic (PLIN negative) adipocytes to clear inert lipid droplets

generated from adipocyte death, becoming a major source of proinflammtory signals (73, 96). However, in the case of CLS found in CL-treated WAT, macrophages expressed the M2 phenotype and were negative for CD11c, implying specialized functions of M2 macrophages in catabolic tissue remodeling.

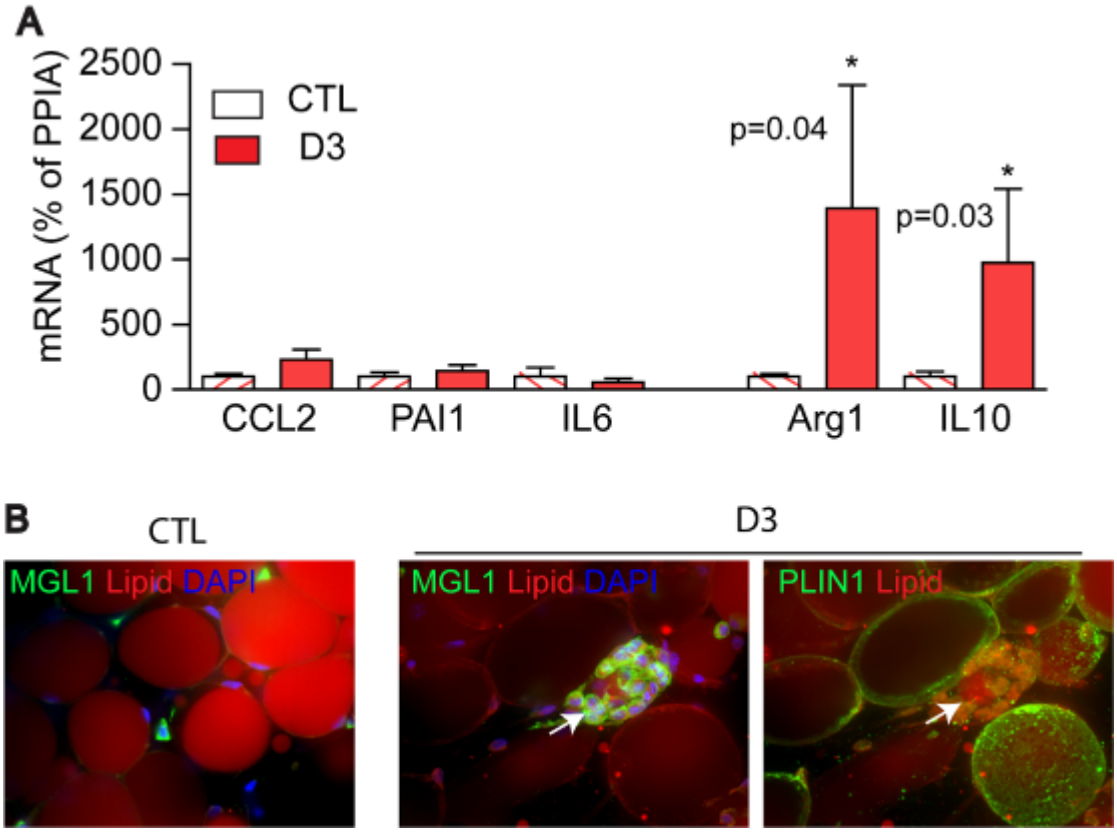

Figure 16. Alternatively activate macrophages form CLS in eWAT during ADRB3 stimulation.
(A) qPCR analysis for macrophage marker expression. CL increased expression levels of anti-inflammatory (M2) markers. CL had no effect on pro-inflammatory cytokine expression levels. (n= 4-6) (B) Representative images of whole mount eWAT stained for MGL1, Lipid and PLIN1 from control or D3 CL treated mice. MGL1 positive Macrophages (M2) formed CLS surrounding LipidTox positive lipid drolet (arrow) that avoid PLIN1 expression.

4.1.3 Proliferating PDGFRα+ cells actively recruited to CLS during ADRB3 stimulation.

We have established that iBA are generated from proliferation of PDGFRα progenitors (**chapter 3**). CLS formation is correlated with the number of proliferating cells, and actively proliferating cells that do not express PLIN1 are closely associated with CLS (**4.1.1**). Since we observed that the majority of proliferating cells expressed PDGFRα, we examined colocalization of PDGFRα+ cells within CLS. As expected, PDGFRα+ cells were closely associated with M2 macrophage aggregates as part of CLS (**Figure 17**). Quantification of proliferating EdU+ PDGFRα+ cells that were associated with F4/80+ cells (<5um distance) demonstrated that 84% (27 out of 32) of EdU+PDGFRα+ cells were located in close proximity with macrophages (**Figure 17B and 17C**). In control conditions, PDGFRα+ cells were found randomly scattered with only 15% (35 out of 225) in close association with macropahges. These data suggest that PDGFRα+ cells were actively recruited to CLS becoming part of CLS.

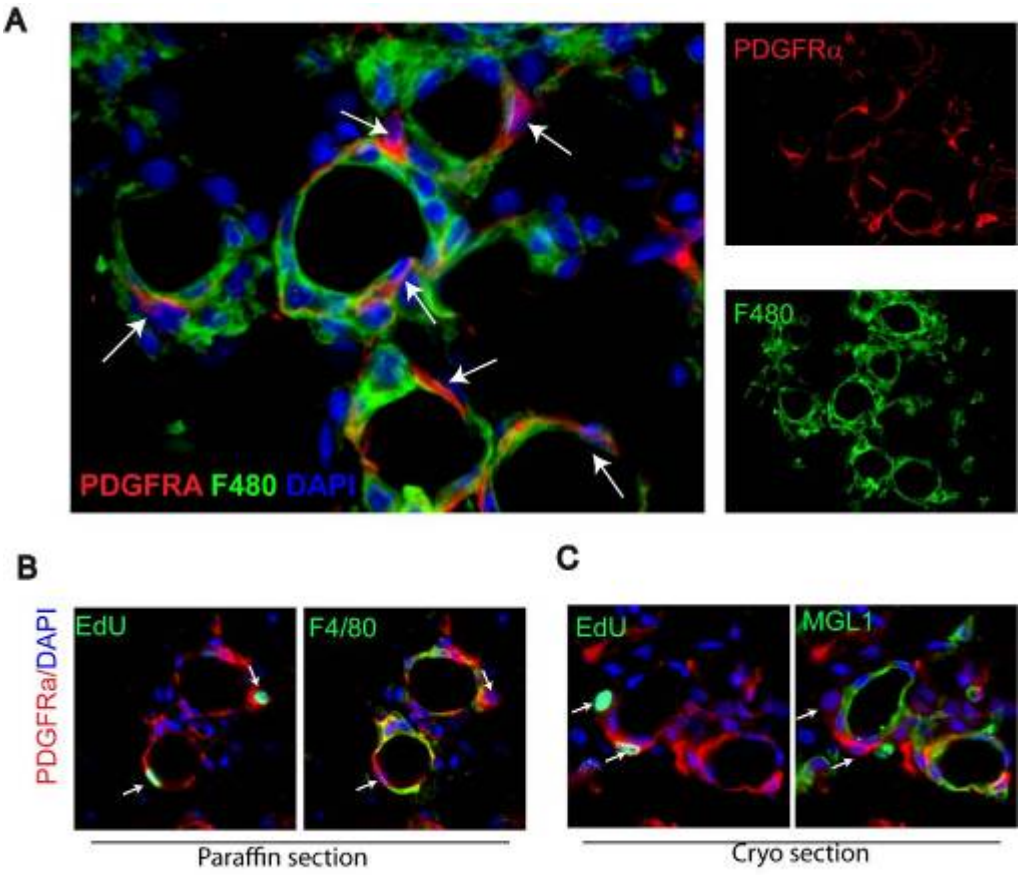

Figure 17. Close association between proliferating PDGFRα+ cells and M2 macrophages.
(A) Representative images of eWAT paraffin sections from 129S1 mice treated with CL for 3 days stained for F4/80 and PDGFRA. Arrows indicate PDGFRA+ cells within CLS. (B) Representative images of eWAT paraffin sections from 129S1 mice treated with CL for 3 days triply stained for F4/80, PDGFRA and EdU. Left is the merge of EdU (Green) and PDGFRA (red), and right is the merge of F480 (Green) and PDGFRA (red). EdU,PDGFRA double positive cells (proliferating progenitors) were closely associated with F480+ macrophages forming CLS. (C). Representative images of eWAT cryosections triply stained for MGL1, PDGFRA and EdU. Left is the merge of EdU (Green) and PDGFRA (red), and right is the merge of MGL1 (green) and PDGFRA (red).

4.1.4 Depletion of macrophages suppresses proliferation of BA progenitors.

To determine whether macrophages have a critical role in providing mitogenic signals to

the adipogenic niche, we examined if depletion of macrophages resulted in suppression of progenitor proliferation. Selective depletion of macrophages was achieved by injection of clodronate-containing liposomes. Liposomes are readily taken up by phagocytic cells, and consequently induce apoptosis of macrophages (97). Clodronate (CD) suspension (300μl/mouse) was administered (I.P) every second day to maintain macrophage depletion (**Figure 18A**). Control mice were injected with an equivalent volume of PBS-loaded liposomes. Mice received 3 days of CL infusion (0.75nmol/hr), were injected with EdU 2hr before sacrifice, and progenitor proliferation in each condition was analyzed. We confirmed depletion of macrophages by quantitative PCR analysis and showed decreased levels of macrophage specific marker expression in CD-treated versus control mice (**Figure 18B**). Macrophage depletion led to a significant reduction in the proliferation level in CL-treated eWAT (**Figure 18C and 18D**). Together these results indicate that macrophages critically provide the adipogenic niche with mitogenic signals and that macrophage-mediated activation of progenitors is at least in part responsible for the brown adipogenesis in CL treated eWAT.

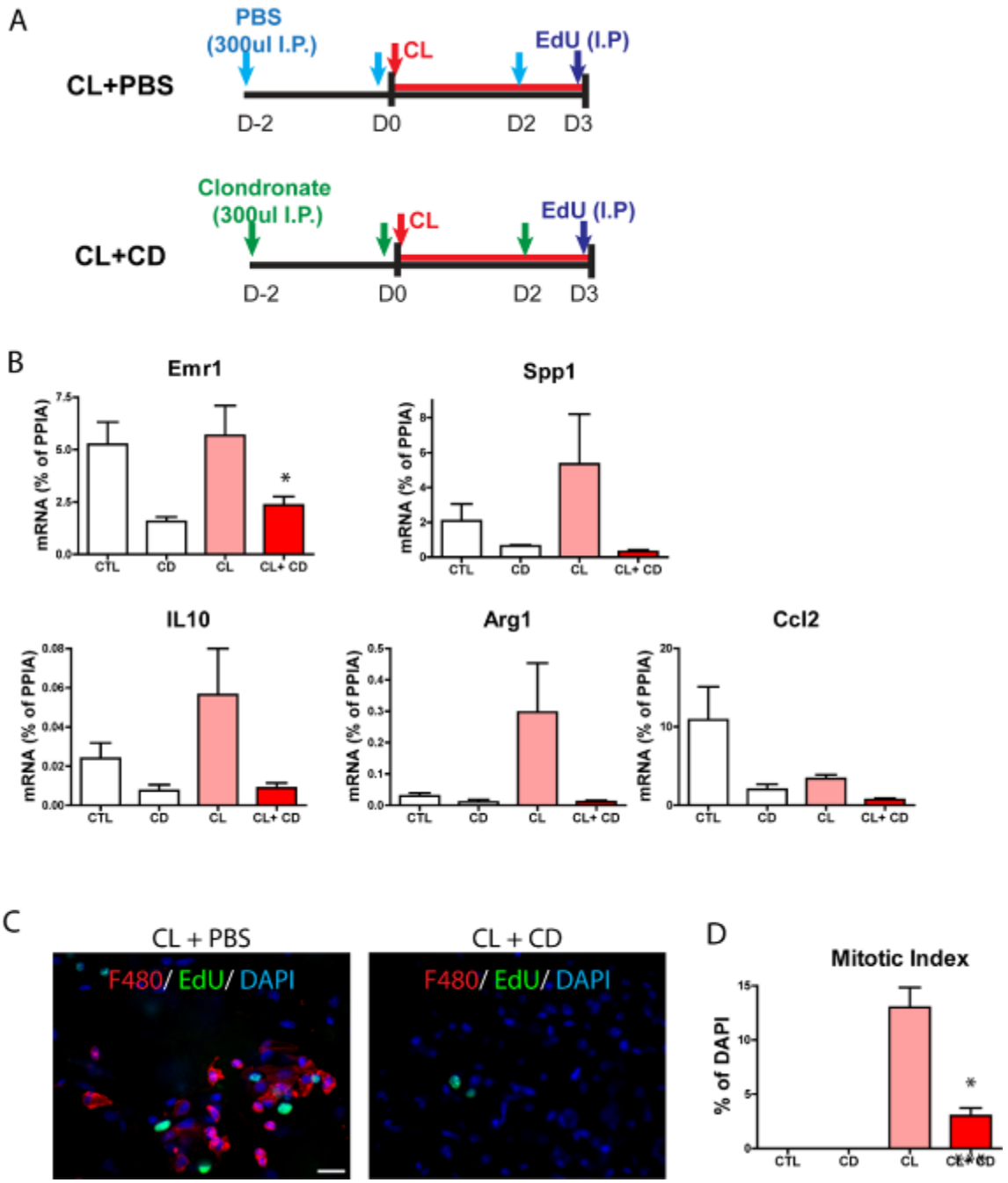

Figure 18. Macrophage depletion reduces mitogenic effect of CL in eWAT.

(A) qPCR analysis for macrophage specific gene expression. A pan-macrophage marker, Emr1 and alternatively activated macrophage markers, IL-10 and Arg1 were depleted to the same level of controls. (n=4-6, * $p<0.05$). Level of Spp1 expression, a cytokines known to be secreted from macrophages, was reduced in CD treated group. (B) Representative images of eWAT whole mount from 129S1 mice treated with CL for 3 days double-stained for F4/80 and EdU. Clodronate treatment depleted macrophages, and reduced cell proliferation in eWAT during CL treatment. Nuclei counterstained with DAPI. Bar=20um. (C) Quantification of mitotic index.

4.2 Identification of molecular niche factors that activate progenitors

4.2.1 OPN is highly expressed in CLS-associated macrophages.

As the trafficking of macrophages to adipose tissue critically depends on the chemo-attractants, such as TNF-α, CCL2, we examined expression levels of several chemokines by global gene expression profiling. Our microarray analysis demonstrated that SPP1, the gene for osteopontin (OPN), is the only chemoattractant upregulated during CL treatment. OPN is the primary phosphorylated glycoprotein of bone and is also expressed in a wide variety of other cells and tissues, including immune cells (98). OPN can be cleaved by both thrombin and MMPs, and full length and processed forms of OPN can engage a number of receptors, such as integrins and CD44 (99). While OPN has a central role in bone remodeling (100, 101), mounting evidence suggests that OPN also participates in immune responses (99), such as macrophage and neutrophil migration (98, 102) and wound healing (103). Thus, OPN is considered to be a chemotactic factor and a cytokine that possess pleiotropic functions.

We confirmed upregulation of OPN by western blot and qPCR, and found that OPN at protein and mRNA levels was significantly upregulated and peaked at D2, prior to D3 that showed maximal proliferation and macrophage recruitment (**Figure 19A and 19B**). This implies that OPN may function as a chemoattractant to induce infiltration of macrophages from

circulation. In addition to recruitment of macrophages from circulation, directional migration within the microenvironment can be achieved by a local gradient of chemoattractant. If OPN is a key niche factor that recruits and activates progenitors and niche components, it should be accumulated within CLS, the potential adipogenic niches. Therefore, to examin localization of OPN expression within tissue, histologic sections of eWAT from CL- treated mice were stained for OPN, and F4/80. Indeed, OPN expression was colocalized in macrophages that formed CLS (**Figure 19C)**, further supporting our hypothesis that OPN recruits macrophages and potentially progenitors to form adipogenic niches.

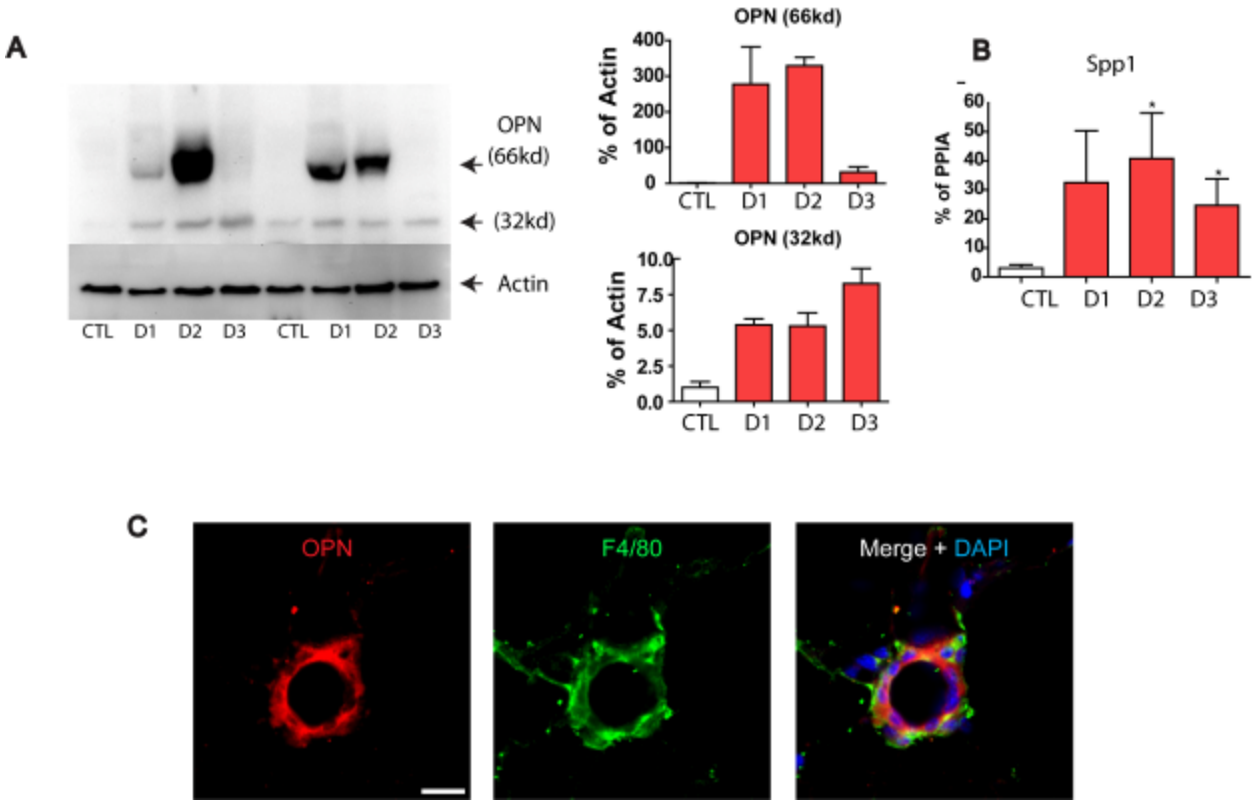

Figure 19. OPN are upregulated by ADRB3 stimulation, and are highly expressed in CLS-associated macrophages. (A) Immunoblot analysis of eWAT from 129S1 mice treated with CL at the indicated day. full-length and fragmented form of SPP1 were detected in CL treated group, indicating

increase in level of expression and cleavage-mediated activation of SPP1. (B) Quantification of immunoblot, (n=4-6, * $p<0.05$). (B) qPCR analysis on SPP1 expression. (C) Representative images of eWAT paraffin sections from 129S1 mice treated with CL for 3 days double-stained for F4/80 and SPP1. Nuclei counterstine with DAPI. Bar=20um.

4.2.2 PDGFC is highly expressed in CLS-associated macrophages.

To define candidate signaling factors expressed by macrophages that could mediate proliferation of PDGFRα+ progenitors, we analyzed mRNA expression for growth factors that have been implicated in cell mitosis. Although the migration and proliferation have been attributed to many factors, our particular interest was possible involvement of PDGF signaling, because PDGF receptor expression is one of the prominent characteristics of progenitor cells and PDGF is an important mitogenic/chemotactic regulator, known to be secreted from macrophages in many circumstances such as injury- repair, and regeneration (104-106)

We first examined gene expression levels of four PDGF isoforms and found no significant changes in mRNA and protein level during the course of CL treatment. It is highly likely that the heterogeneous nature of the tissue may confound molecular analysis because signals from small cell populations can be diluted in a given tissue lysate, even though the molecular changes are sufficient to direct cellular communication within microenvironment. Therefore, we detected PDGF on histologic sections by immunostainging that enables direct microscopic visualization of local distribution and found high concentration of PDGFC expression in

macrophages forming CLS. (**Figure 20B**). Interestingly, the level of processed active form was increased during the course of CL treatment, suggesting possible involvement of ECM remodeling enzymes (107) (**Figure 20A**). In a serial section, recruitment of PDGFRα+ cells in CLS was observed (**Figure 20C)**, indicating PDGFRα+ cells actively migrated toward CLS.

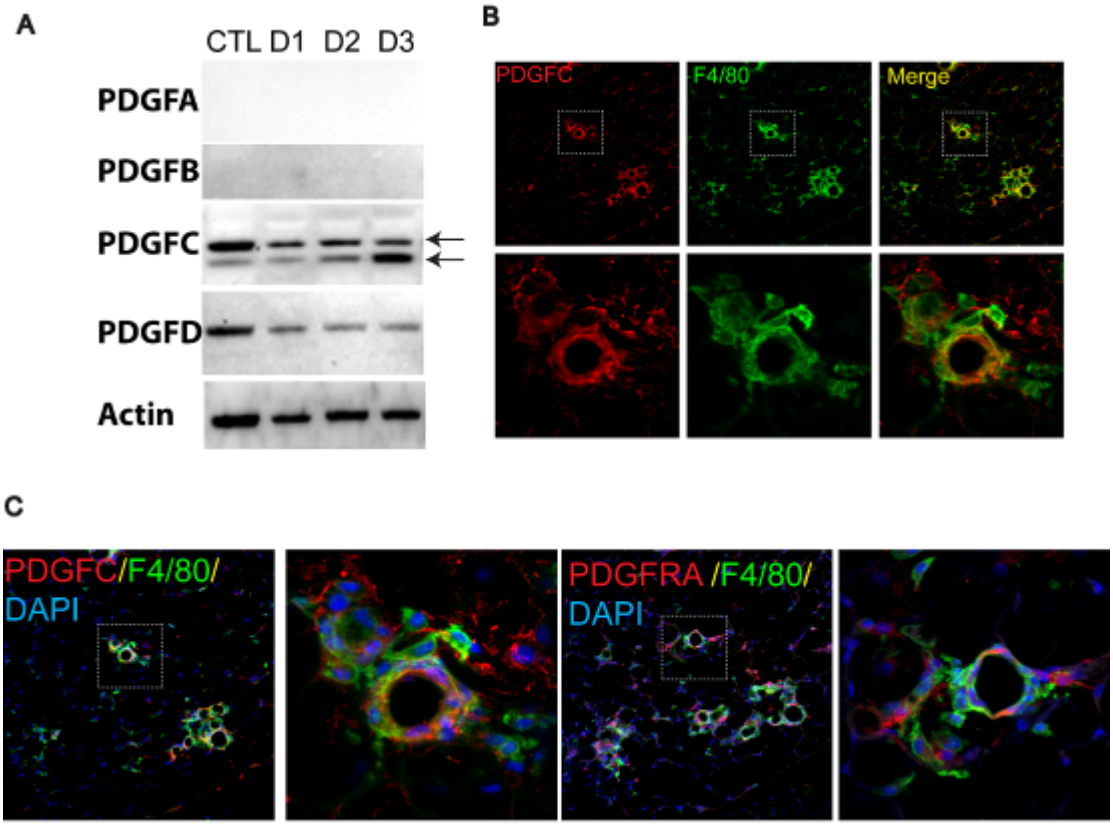

Figure 20. PDGFC are upregulated by ADRB3 stimulation, and are highly expressed in CLS-associated macrophages. (A) Immunoblot analysis of eWAT from 129S1 mice treated with CL at the indicated day. All known isoform of PDGF ligand were analyzed. Full-length and processed form of PDGFC were detected in CL treated group, indicating increase in cleavage mediated activation of PDGFC. (B) Representative images of eWAT paraffin sections from 129S1 mice treated with CL for 3 days double-stained for F4/80 and PDGFC. Nuclei counterstained with DAPI. (C) A serial section adjacent to (B) stained for PDGFRA and F480. Indicating recruitment of PDGFRA+ cells in close proximity to the region that had concentrated PDGFC expression. Bar=20um.

4.2.3. Proliferating PDGFRα cells contain elevated levels of tyrosine-phosphoproteins

Next, we sought to determine PDGFRα activation during CL treatment by immunostaining for phospho-tyrosine (p-Tyr). Data showed colocalization of concentrated p-Tyr staining with PDGFRα in eWAT from CL-treated mice. Especially, p-Tyr was detected in clusters of PDGFRα expressing cells that were presumably present within CLS (**Figure 21)**. p-Tyr was also detected in other cell types that do not expressed PDGFRα, implicating the activation of other tyrosine kinases during CL-induced remodeling processes.

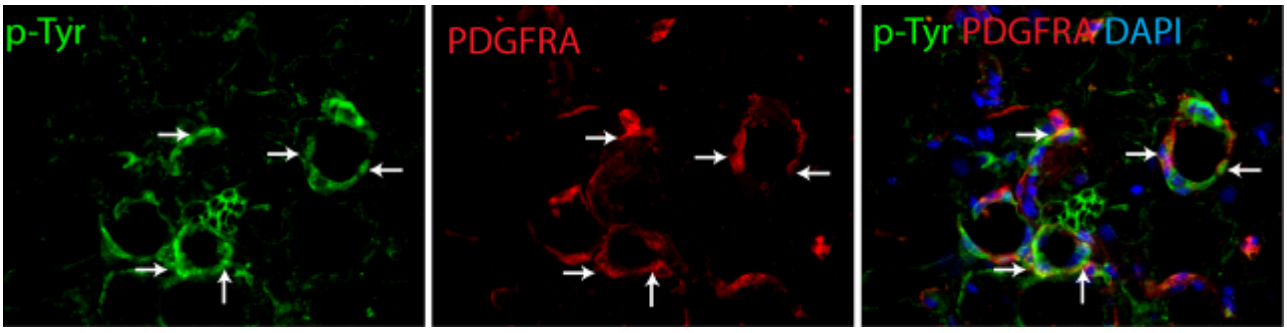

Figure 21. Detection of p-Tyrosin within CLS 3 days after CL treatment: potential involvement of RKT activation in PDGFRα+ progenitor migration and proliferation.
Representative images of eWAT paraffin sections from 129S1 mice treated with CL for 3 days double-stained for p-Tyr and PDGFRα. The merged image (right) shows that PDGFRα+ cells contained p-tyrosine, indicating possible PDGFRα activation. Nuclei were counterstained with DAPI. Arrows indicate double positive cells. Bar=20um.

4.2.4 PDGF and OPN are chemo-attractants for dissociated PDGFRα+ cells.

To test the specific role of PDGF ligands and SPP1 on progenitor migration, we tested migration of PDGFRα+ cells by a transwell migration assay. We used SVF of WAT from Pdgfra-

H2BeGFP mice to examine migration of PDGFRα+ cells and PDGFRα- cells at the same time. Data indicate that GFP+ cells preferentially migrated along with PDGF and OPN gradients toward lower chambers compared to control conditions (**Figure 23**). While PDGFAA had no effect on GFP- populations, OPN induced migration of GFP- cells, which can be explained by the ability of OPN to recruit other cell types, including macrophages.

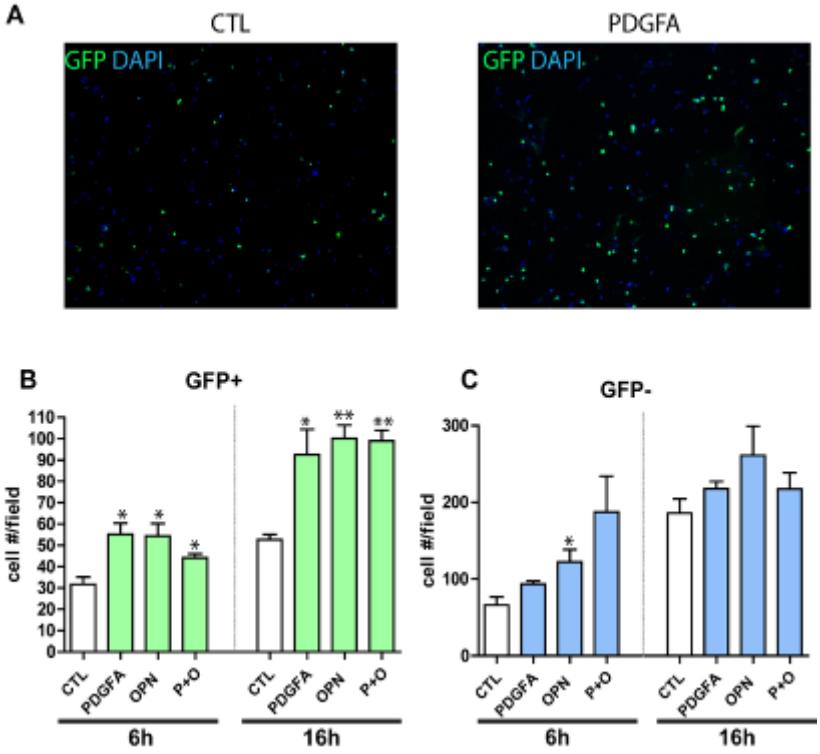

Figure 22. PDGF and OPN are chemo-attractants for dissociated PDGFRα+ cells. (A) Representative images of bottom of transwell stained with DAPI 16 hours after plating, showing higher level of migration of GFP+ cells. (B) qunatificcation of GFP+ cells and GFP- cells 6 h and 16h after plating. PDGFA and OPN treatment induce migration of GFP+ cells (n=3, $p<0.05$), CTL (control): 0.1% BSA DMEM, PDGFA (50ng/ml), OPN (200ng/ml), P+O: PDGFA (50ng/ml) + OPN (200ng/ml).

4.2.5. Inhibition of RTK reduced brown adipogenesis during CL treatment.

If PDGF signaling is a critical factor in the activation of progenitors, then brown adipognesis from proliferating cells should be diminished by blockade of PDGFR activation. To test this, we inhibited RTK auto-phosphorylation by a pharmacological agent, sunitinib (108, 109) and examined BA differentiation during CL treatment (**Figure 22A**). Analysis of the EdU/UCP1 double positive fraction demonstrated that 7 days of co-administration of sunitinib with CL reduced BA generation by 82% (76 ±3.9 % in CL v.s. 13 ± 1.1 % in CL+RTKX) (**Figure 22B and 22C**). Consistently, the expression level of UCP1 was downregulated by sunitinib treatment in the CL treated group; however, other catabolic gene expression was not affected by RTK inhibition (**Figure 22D)**. This could be explained by a UCP1-independent metabolism occurring mostly in existing WA in CL-treated WAT (13), and possible involvement of compensatory mechanisms. In our experimental conditions, macrophage recruitment during CL treatment is a transient phenomenon that peaks on day 3 and is gradually resolved by catabolic remodeling of adipose tissue and incorporation of newly generated BA from progenitor cells by day 7. Interestingly, pharmacological blockade of RTK activity in CL-treated mice led to an impaired resolution process and caused persistent stress, indicated by sustained Emr1 and Spp1 levels, pointing to a critical role of PDGFRα+ cell activity in this catabolic remodeling process. It is highly plausible that newly differentiated BA are a key for the timely resolution of

this macrophage-initiated process.

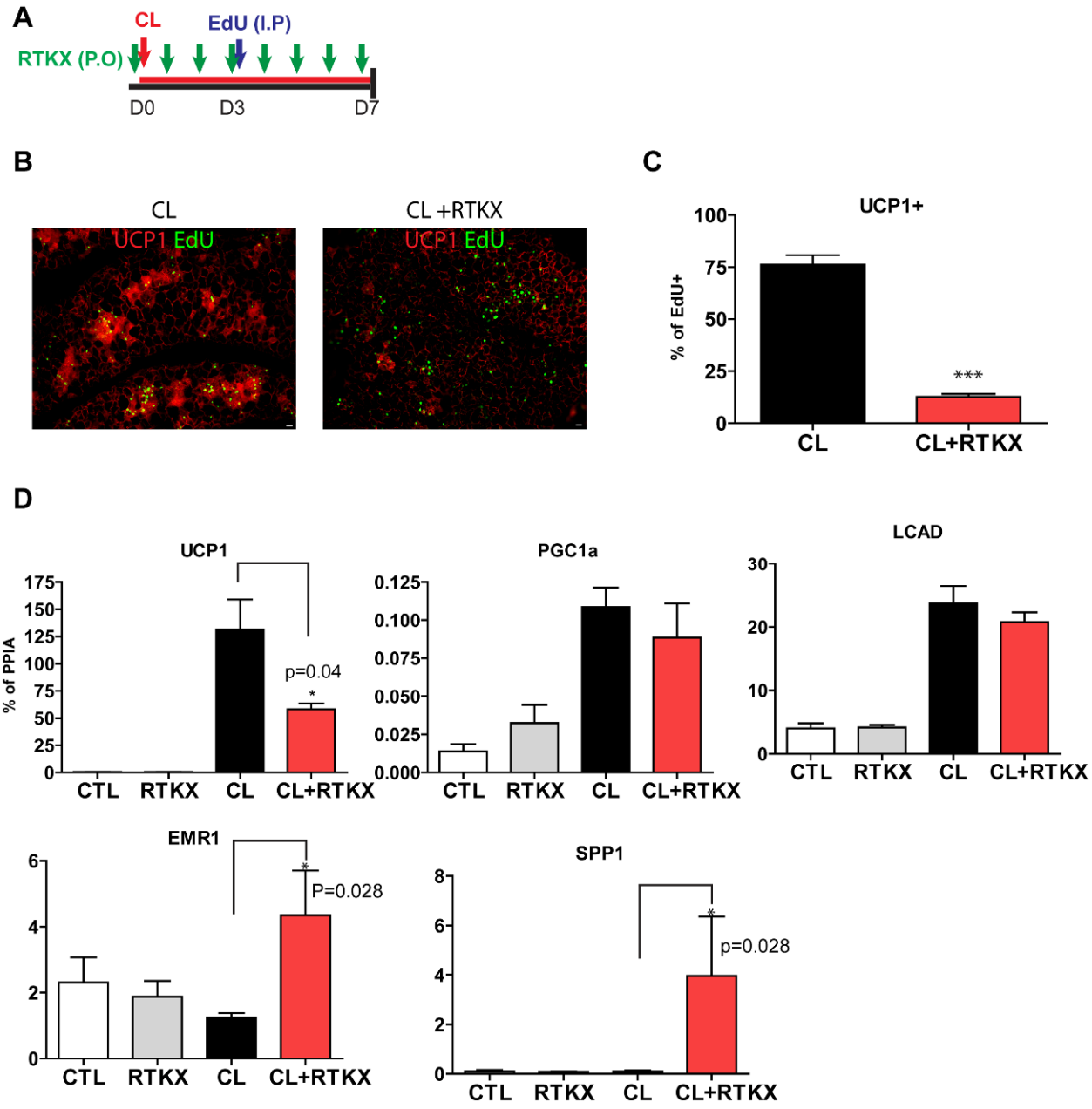

Figure 23. BA differentiation was reduced by sunitinib treatment. (A) Schematic diagram of CL and RTKX (sunitinib) treatment procedures. (B) Representative images of eWAT paraffin sections from 129S1 mice treated with CL with/without RTKX treatment, double stained for UCP1 and EdU. (C) Quantification of EdU+UCP1+ cells. (n=4, *** p<0.0001) (D) qPCR analysis for catabolic gene and macrophage marker expression. UCP1 expression was reduced by CL treatment (n=4, * p<0.05). Levels of EMR1 and Spp1 expression were sustained in RTKX treated group.

Chapter 5. *In vitro* brown/ white dual adipogenic potential of PDGFRα+ progenitors

5.1. PDGFRα+ cells are highly proliferative, migratory, and adipopgenic in organotypic cultures

We further investigated the characteristics of PDGFRα$^+$ cells in organotypic culture system of reporter-induced adipose tissues from Pdgfra-CreER^{T2}/R26-LSL-tdTomato mice (**Figure 24A**). Immediately after plating and during the first day of culture, tdTomato labeled cells were only observed within the tissue explants. By the second day of culture, tdTomato$^+$ cells began to migrate from tissue, rapidly replicated and reached full confluence as early as 5 days after plating. Confluent cells from explants were treated with insulin for 4 days and exposed to EdU 2 h before fixation. Immunofluorescence analysis of PPARγ expression (**Figure 24B**) and PLIN1 (**Figure 24D**) confirmed that tdTomato$^+$ cells have high capacity for spontaneous differentiation into adipocytes (15.3% of tdTomato$^+$ cells)**.** When treated for 24 hours with 8-bromo-cyclic AMP, >95% of differentiated adipocytes (those with lipid droplets > 2 μm) expressed UCP1, whereas newly differentiating cells with sparse droplets lacked UCP1

expression (**Figure 24C**). Flash labeling with EdU demonstrated active proliferation (4.7%) of tdTomato$^+$ cells. Interestingly, various mitotic figures were observed in tdTomato$^+$ cells that were EdU$^+$ and contained small PLIN1$^+$ lipid droplets **(Figure 24D**), further demonstrating that newly-differentiating adipocytes can divide. These findings indicate that PDGFRα+ cells are highly proliferative and migratory in organotypic cultures. Explant outgrowth culture models, such as muscle fiber cultures, have been utilized as a robust and reliable method for isolating proliferative cells from tissue as a source of stem cells (110). The adipose tissue explant culture developed in current study, can establish primary cultures for expansion and in vivo transplantation. In addition, it can be utilized as a model system where PDGFRα+ cell motility, proliferation, differentiation can be monitored to test effects of several candidate molecules on PDGFRα+ progenitors.

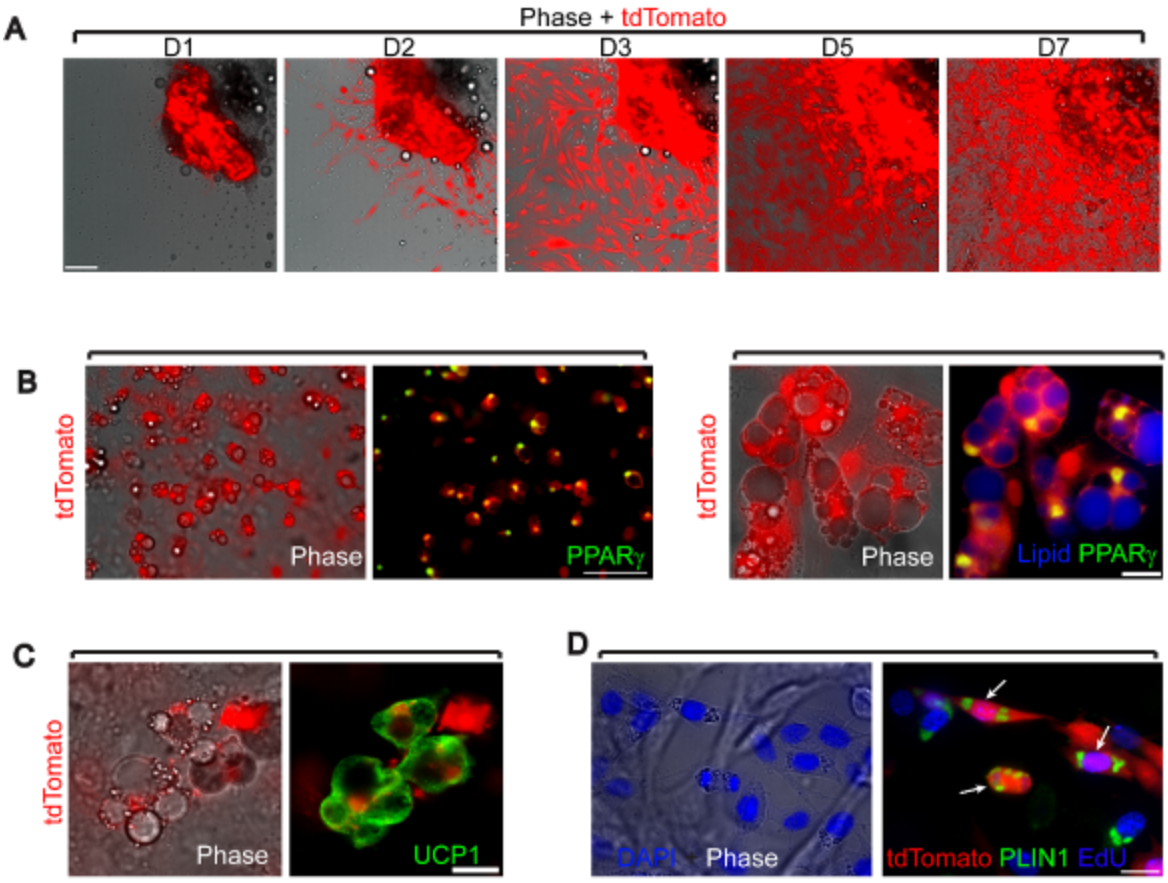

Figure 24. PDGFRα+ progenitors are highly mobile, proliferative and adipogenic *in vitro*.

(A) eWAT fragments from reporter-induced Pdgfra-CreERT2/R26-LSL-tdTomato mice were maintained in growth medium and examined over time. PDGFRα+ cells migrated from tissues and became confluent after 5-7 days in culture. Bar = 100 μm. (B) Confluent cells were induced to differentiate with insulin for 4 days stained for PPARγ and Lipid (B, left) A low magnification field of explant cultures showing expression of PPARγ in multilocular tdTomato+ cells. Bar = 100 μm (B, right) High magnification of triple-positive cells (tdTomato+, lipid, PPARγ) from explants. Bar = 20 μm. (C) UCP1 expression in tdTomato+ adipocytes treated with 8-bromo-cyclic AMP. Bar = 20 μm. (D) HIgh magnification image of proliferating (EdU+) tdTomato+ adipocytes (PLIN1+). Bar = 20 μm.

5.2. Clonal analysis demonstrates that PDGFRα+ cells have BA and WA potential.

PDGFRα$^+$ progenitors were isolated by single cell FACS, and individual colonies were expanded and subjected to adipocyte-differentiating conditions (57) used for establishing adipogenic potential in prospective analyses. While 5 % of FACS-isolated PDGFRα+ cells had clonogenicity, numerous adipocytes were found in approximately 75% of clones derived from single cells (**Figure 25A**). The potential of PDGFRα$^+$ to form colonies and differentiate into adipocytes was similar to that reported for muscle-derived PDGFRα$^+$ cells (57, 58). Interestingly, the adipogenic potential of clones derived from eWAT, iWAT and iBAT did not differ significantly (Fisher's exact test, $p > 0.95$). When differentiated by a cocktail of insulin, IBMX, and dexamethasone, all adipogenic clones contained cells expressing UCP1 to varying degrees (**Figure 25B**).

A

	eWAT	iWAT	BAT
Clonogenicity (% of total wells)	5.2% (40/768)	5.1% (39/768)	5.1% (39/768)
Adipogenic colonies (% of total colonies)	72.5% (29/40)	74.4% (29/39)	74.4% (29/39)

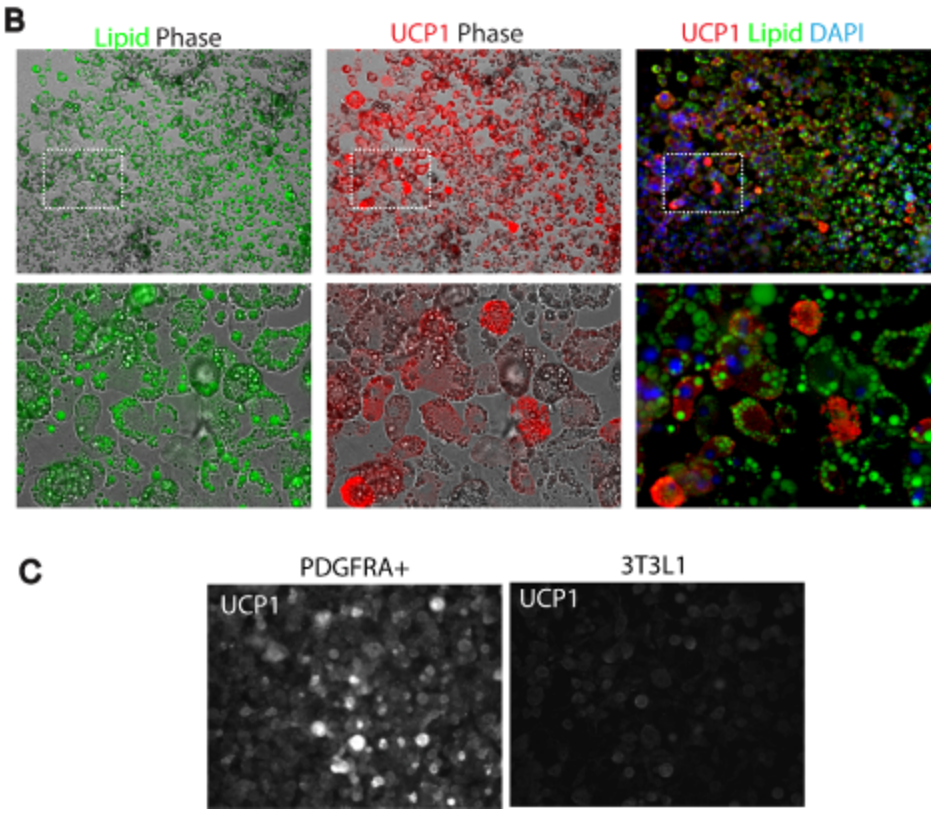

Figure 25. PDGFRα-expressing progenitors are white and brown adipogenic *in vitro*.

(A-B) Adipogenic potential of clones (n ≥ 39) derived from FACS-isolated PDGFRα+ single cells. (B) Representative images of adipogenic clones double-stained for UCP1 and Lipid (LipidTox). Lipid (left) and UCP1 (middle) fluorescent images were merged with phase contrast, and Lipid and UCP1 images were merged wth DAPI-counterstained images. Bottom row is a magnified view of the boxed regions from top row. All adipogenic clones contained UCP1+ and UCP1- adipocytes, demonstrating WA and BA bipotentiality of PDGFRα+ progenitors. Bar = 100 μm. (C) Adipogenesis of 3T3 L1 cells were induced with the same differentiation protocol used in this clonal analysis, and then stained for UCP1, confirming absence of UCP1 expression in WA cell line.

We also tested the *in vitro* differentiation potential of PDGFRα$^+$ cells that were isolated from WAT of Pdgfra-H2BeGFP mice by FACS (**Figure 26A**). Each fraction was expanded under growth conditions, and then exposed to insulin for 7 days to induce adipogenesis. Expanded PDGFRα$^+$ cells retained expression of *Pdgfra*, *Cd34, Sca1* (*Ly6a*) and *CD29 (Itgb1)*, but did not express *Pdgfrb* or *Cd24* (**Figure 26B**). Although both populations formed adipocytes after insulin treatment, the adipogenic potential of PDGFRα$^+$ population was much higher than that of PDGFRα$^-$ population based on the proportion of lipid-laden cells in culture (**Figure 26C**) and the expression of terminal adipocyte differentiation markers (**Figure 26D**). This adipogenic induction did not require isobutylmethylxanthine and dexamethasone, which are typically used to trigger preadipocyte differentiation. We also evaluated whether differentiated cultures could be induced to express BA markers in response to β-adrenergic stimulation. β-adrenergic stimulation strongly induced expression of peroxisome proliferator-activated receptor γ coactivator 1α (*PGC1α*) *Ucp1* and *Dio2* (**Figure 26E**), confirming brown adipogenic potential of PDGFRα$^+$ cells *in vitro.*

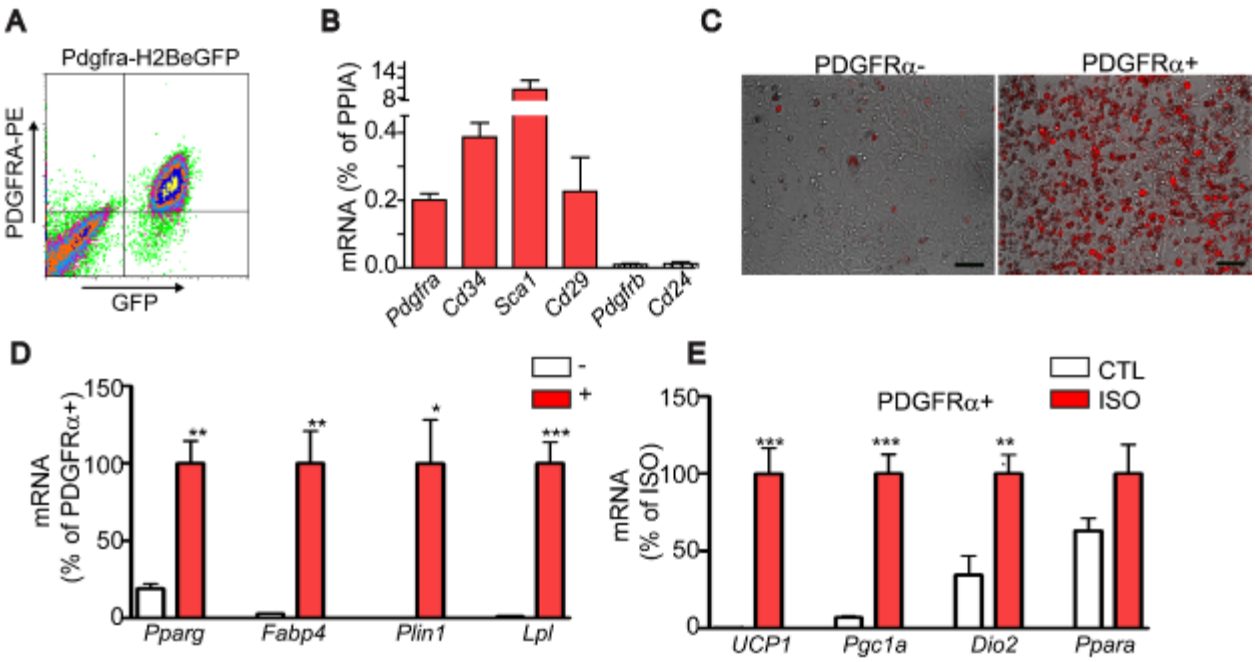

Figure 26. *In vitro* adipogenic potential of FACS-isolated PDGFRα+ cells. (A) FACS analysis of H2BeGFP+ (PDGFRα+) cells from WAT. (B) qRT-PCR analysis of surface marker expression after 5-7 days of culture in growth medium (means ± SEM, n=4). (C) Representative images of PDGFRα+ or PDGFRα- cells cultured in the presence of insulin (1μg/mL) for 7 days. Boron-dipyrromethene (BODIPY, red) staining indicates higher insulin-stimulated adipogenesis in PDGFRα$^+$ fractions. (H, I) qRT-PCR analysis on adipocyte gene expression. (D) Expression of adipocyte-specific markers, normalized to that of PDGFRa+ cells. PDGFRα+ cells were significantly more responsive to insulin-induced adipogenesis, compared to PDGFRα- cells (means ± SEM, n=4, *Pparg*: p=0.002, *Fabp4*: p=0.004, *Plin1*: p=0.012, and *lipoprotein lipase (Lpl*): p=0.0003). (E) Expression of brown adipocyte-specific markers, normalized to levels induced by ISO. Differentiated PDGFRα+ populations (cultured in the presence of Insulin for 7 days) were treated with vehicle (CTL) or isoproterenol (ISO, 10 μM) for 4 h before analysis. (means ± SEM, n=4, *Ucp1*: p=0.0009, *Pgc1*: p=0.0003, *Dio2:* p=0.0095, *Ppara*: p=0.120). Experiments were repeated 4 times.

5.3. Transplanted FACS-purified PDGFRα^+ cells from WAT form WA *in vivo.*

As a final demonstration of the white adipogenic potential of isolated PDGFRα+ progentiors, we transplanted PDGFRα^+ and PDGFRα^- cells, purified by FACS from WAT of GFP transgenic mice, into syngenic mice (C57B/6) and determined the efficiency of transplantation 4 weeks later (**Figure 27**). Matrigel transplants contain a mixture of donor and recipient-derived fat cells (111). The donor contribution, calculated as the fraction of GFP$^+$ adipocytes over total adipocytes in the Matrigel transplant, was 20-fold higher in transplants of PDGFRα^+ cells (**Figure 27F**). Although multilocular adipocytes were detected, none were UCP1$^+$ BA. Moreover, CL treatment 4 weeks after transplantation failed to induce UCP1 expression in transplants (data not shown), implying a crucial role of the endogenous microenvironment in progenitor fate determination. This result further substantiates that PDGFRα^+ cells are bipotential progenitors that can give rise to WA or BA.

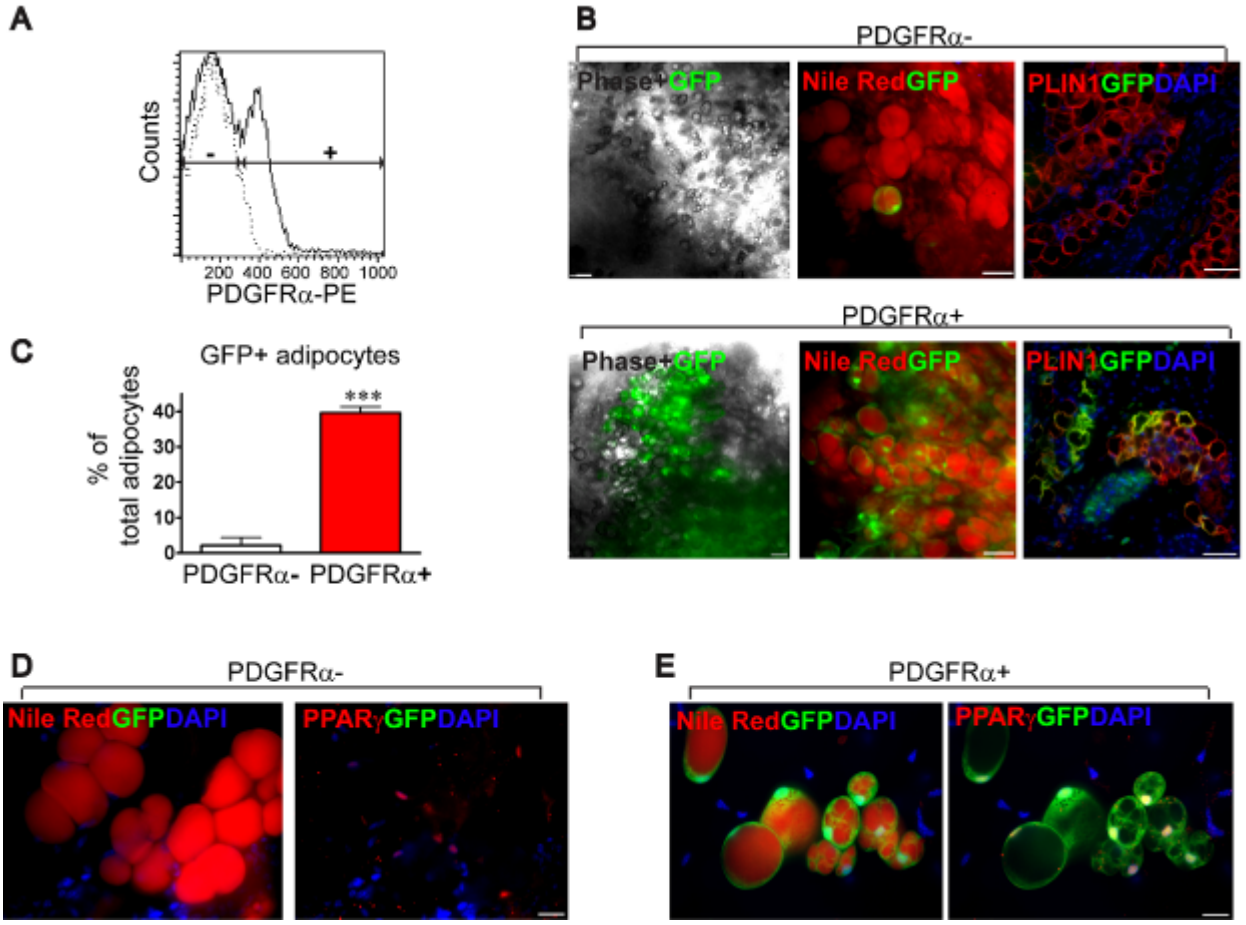

Figure 27. *In vivo* adipogenic potential of FACS-purified PDGFRα expressing progenitors.

(A) FACS analysis of PDGFRα+ cells from WAT of GFP transgenic mice. The X-axis indicates PE intensity (PDGFRα expression). Histogram with dashed line represents the negative control for PDGFRα staining. (B) Representative low magnification images of engrafted PDGFRα+ or PDGFRα- cells in Matrigel 4 weeks after transplantation. Bars = 50 μm. GFP (green) fluorescent images were merged with phase contrast (left), nile red fluorescence (middle, red) or Plin1 immunofluorescence (right, red). Images demonstrate abundance of GFP+ adipocytes in PDGFRα+ transplants by native fluorescence in whole mount tissue (left and middle) and by immunostaining on paraffin sections (right). Nuclei were counterstained with DAPI. (C) Quantitative analysis of GFP+ adipocytes. Donor contribution is the percentage of total adipocytes (nile red+, PPARγ+) from the transplant that were donor-derived (GFP+). Values are means ± range for 2 independent experiments ($p<0.0001$, Fisher's exact test). (D-E) High magnification images of nile red (left, red) and PPARγ (right, red) in whole mount tissues. Bars = 20 μm.

Chapter 6. *In vivo* white adipogenic potential of the PDGFRα+ progenitors

6.1. PDGFRα$^+$ progenitors contribute to adult white adipogenesis.

In vitro analysis indicated that PDGFRα cells may become BA or WA, depending on method of induction and level of adrenergic stimulation. To test whether PDGFRα$^+$ cells contribute to white adipogenesis *in vivo*, PDGFRα cells were tagged with tdTomato, and mice were maintained on chow or were fed high fat diet (HFD) for 8 weeks. tdTomato-labeled adipocytes were found in isolated small clusters throughout control eWAT pads (**Figure 28A**). HFD greatly increased the number tdTomato+ adipocytes, which were found in large, extensive clusters throughout eWAT pads (**Figure 28A**). Immunofluorescence analysis of paraffin sections confirmed extensive co-expression of PLIN1 in tdTomato+ adipocytes (**Figure 28B**). Furthermore, all tdTomato+ cells adipocytes of controls and HFD mice were unilocular and none expressed UCP1 (not shown). HFD greatly increased fat tissue mass, and sizing of adipocytes indicated the tissue expansion was mediated largely by adipocyte hypertrophy (**Figure 28C**). Although there was considerable overlap in adipocyte cellularity between groups (not shown, p = 0.22), there was no overlap between chow and HFD mice in the number or density of

adipocytes derived from PDGFRα+ cells (**Figure 28D**, p <.0002). Indeed, we estimate that up to 25% of total eWAT adipocytes were derived from PDGFRα^{+} cells after 8 weeks of HFD versus < 1.8% in controls.

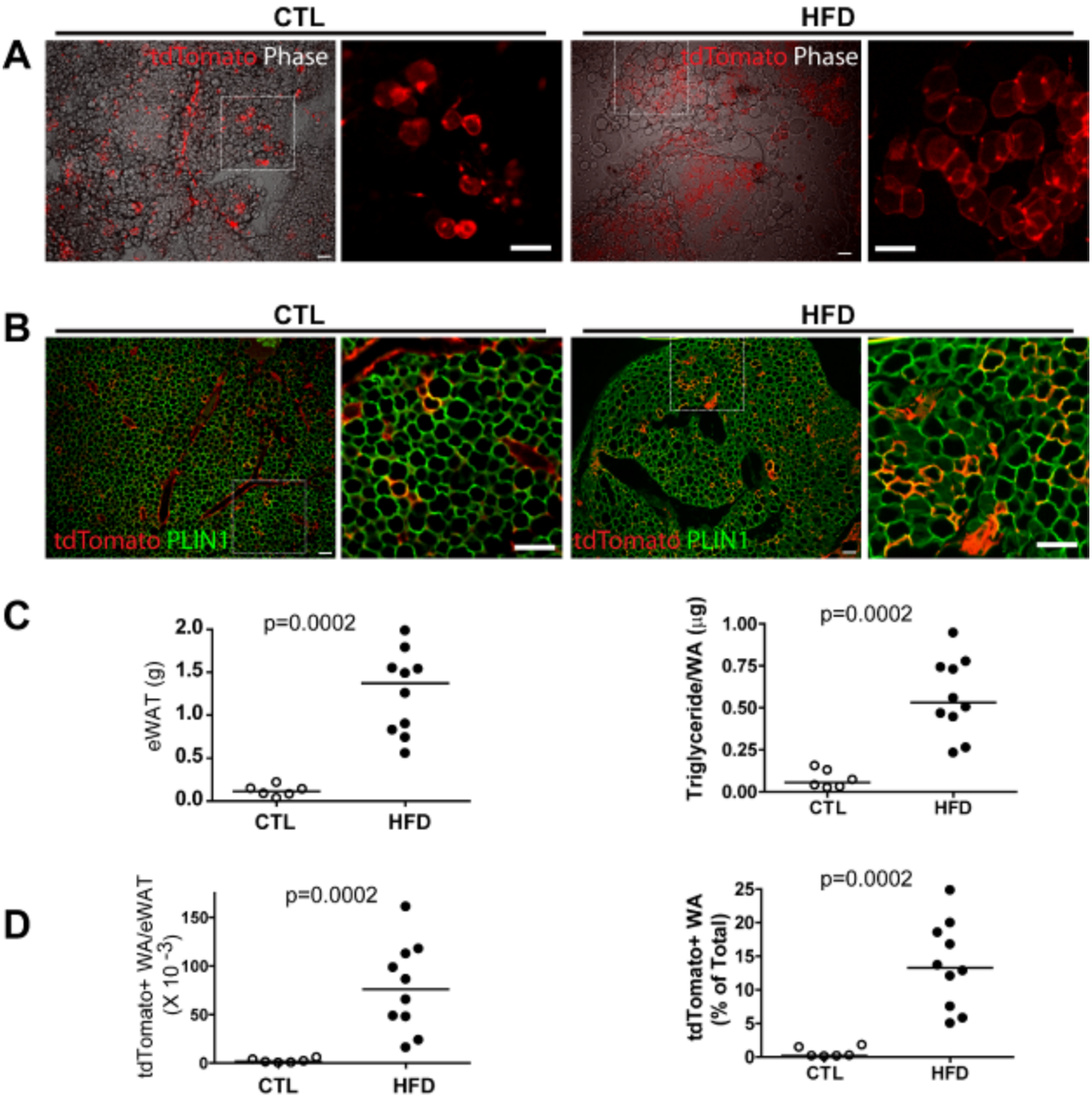

Figure 28. PDGFRα^{+} progenitors contribute to adult white adipogenesis under control conditions and during adipose tissue expansion induced by high fat feeding.

(A) Representative images of tdTomato+ cells in eWAT whole mount from control and HFD mice.

tdTomato fluorescent images are merged with phase contrast (left) along with a magnified region illustrating tdTomato+ adipocyte clusters (right). (B) Representative images of eWAT paraffin sections double-stained for tdTomato and PLIN1. Images demonstrate abundance of tdTomato+ adipocytes in eWAT from HFD mice. (C) Effect of HFD on the weight of eWAT pads (left) and adipocyte triglyceride content (right). (d) The density of tdTomato+ adipocytes in these pads of mice on chow and HFD. The number of tdTomato+ cells was estimated in eWAT pads and proportion of tdTomato+ adipocytes is expressed as percentage of the total adipocytes. Bar = 100 μm.

6.2 CLS form in hyperplastic WAT and recruit PDGFRα+ cells

Adipogenic niches in obesity model have been described as clusters of cells including CD68+ CD34+ macrophages and proliferating endothelial cells (112). We have identified adipogenic niches as M2-CLS, cell clusters of M2 macrophages and proliferating PDGFRα+ cells in eWAT during ADRB3 stimulation. Based on our observation and published data by others, we hypothesized CLS may have overlapping roles in white adiogenesis under high fat feeding conditions.

We examined CLS formation by immunostaining in WAT whole mounts from 8 week-HFD mice and found a significant number of CLS. Surprisingly, PDGFRα+ cells are closely associated with macrophages within CLS, forming the outermost layer of CLS. Macrophages surrounded hypertropic adipocytes and cleared lipid debris, indicated by penetrating macrophages inside of the lipid droplet (**Figure 29A**). Contrary to the overt changes by ADRB3 stimulation that induce synchronized cellular responses (proliferation and differentiation) in WAT,

the heterogeneous nature of adipose tissue expansion under high fat feeding limited quantitative analysis. However, these findings suggest CLS function as adipogenic niches that clear lipid debris from malfunational adipocytes and recruit PDGFRα+ progenitors to replace dying adipocytes.

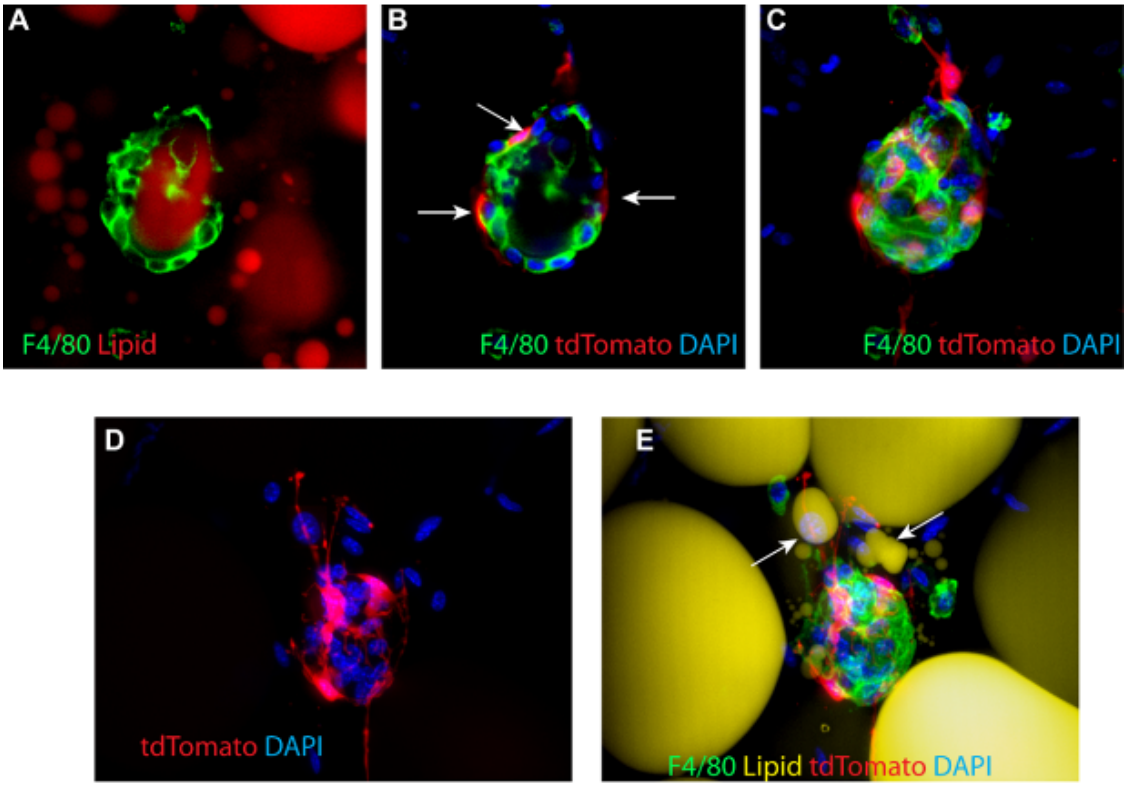

Figure 29. PDGFRα+ cells actively recruited to CLS that clear lipid droplets in HFD induced hyperplastic WAT. Representative images of CLS stained for F4/80, lipid and tdTomato, found in WAT whole mount from HFD mice. (A-C) Lipid clearing CLS. (A) A merge of LipdTox fluorescent (red) and F4/80 (green). (B) A merge of tdTomato fluorescent (red) and F4/80 (green). (C) z-stack projection images of B. Arrows indicate tdTomato+ progenitors that recruited to F4/80+ CLS (right). (D & E) Adipogenic CLS. No lipid detected the center of CLS, suggesting clearance by macrophages. PDGFRα+ cells and numerous other cell types were recruited to CLS. PDGFRα+ cells (red) formed outermost layer of CLS. Small adipocytes (arrow) appeared nearby the CLS.

Chapter 7. Discussion

In this study, we identified a novel population of adipocyte progenitors with *in vivo* dual adipogenic potential that respond to pharmacologic stimulation and nutritional modification (**7.1 & 7.3**), and investigated their phenotypic characteristics (**7.2**) and interaction with niche components (**7.4**).

7.1. PDGFRα+ cells are remodeling stem cells in adult WAT.

With the introduction of the stem cell concept, cellular plasticity of adipose tissue has been investigated to explain the mechanism for its unique capacity for expansion and regeneration (113). It is believed that adipocyte progenitors make an important contribution to these dynamic changes in cellular composition and function of adipose tissue (73): however, the identity and nature of the progenitors remained unknown. Identification of adipocyte progenitors according to *in vivo* differentiation potential is essential to understand how adipose tissue remodels in response to altered metabolic status.

Importantly, our lineage tracing studies using a PDGFRα genetic reporter system are the first demonstration of endogeneous progenitors with *in vivo* brown/white adipogenic potential. Major efforts have been made to identify progenitor markers that are specifically expressed in adipose progenitors. In search of progenitor markers, several FACS-based studies

characterized molecular signatures of the highly adipogenic progenitors and demonstrated *in vitro* adipogenic potential of the isolated cells (56, 57, 114, 115). Even though this approach has proven useful in defining adpogenic potential from heterogeneous SVF from WAT, it should be noted that differentiation potential of isolated progenitors that can be induced in certain experimental conditions, do not necessarily reflect what they will become in the course of normal development or in response to endogenous *in vivo* stimuli. Therefore, lineage tracing that enable labeling and tracking in intact tissue is an essential tool for studying *in vivo* progenitor behavior in adult tissues (116)

As summarized in **Figure 30**, the results of this current study clearly demonstrated that adult WAT possess white/brown bipotent progenitors: PDGFRα+ progenitors are responsible for BA generation induced by ADRB3 stimulation (**Chapter 3**), as well as WA generation during homeostatic turnover and hyperplastic expansion of WAT under HFD feeding (**Chapter 6**). Our clonal level analysis showed that a single cell-derived clone can differentiate into BA and WA under neutral adipogenic conditions (standard adipogenic cocktail), further supporting the dual potential of PDGFRα+ cells (**Chapter 5**). It seems that WA differentiation may be the default fate of PDGFRα+ cells in WAT, based on the observation that they become WA in normal development.

Together, this study provides evidence for existence of adipose progenitors that

contribute to tissue maintenance and plasticity, leading us to propose PDGFRα+ cells as remodeling stem cells in adult adipose tissue. Future steps include investigating their behavior under other adipogenic stimuli, such as injury or FFA overload. It would also be interesting to examine other potential fates of PDGFRα+ progenitors, including a potential contribution to fibrosis.

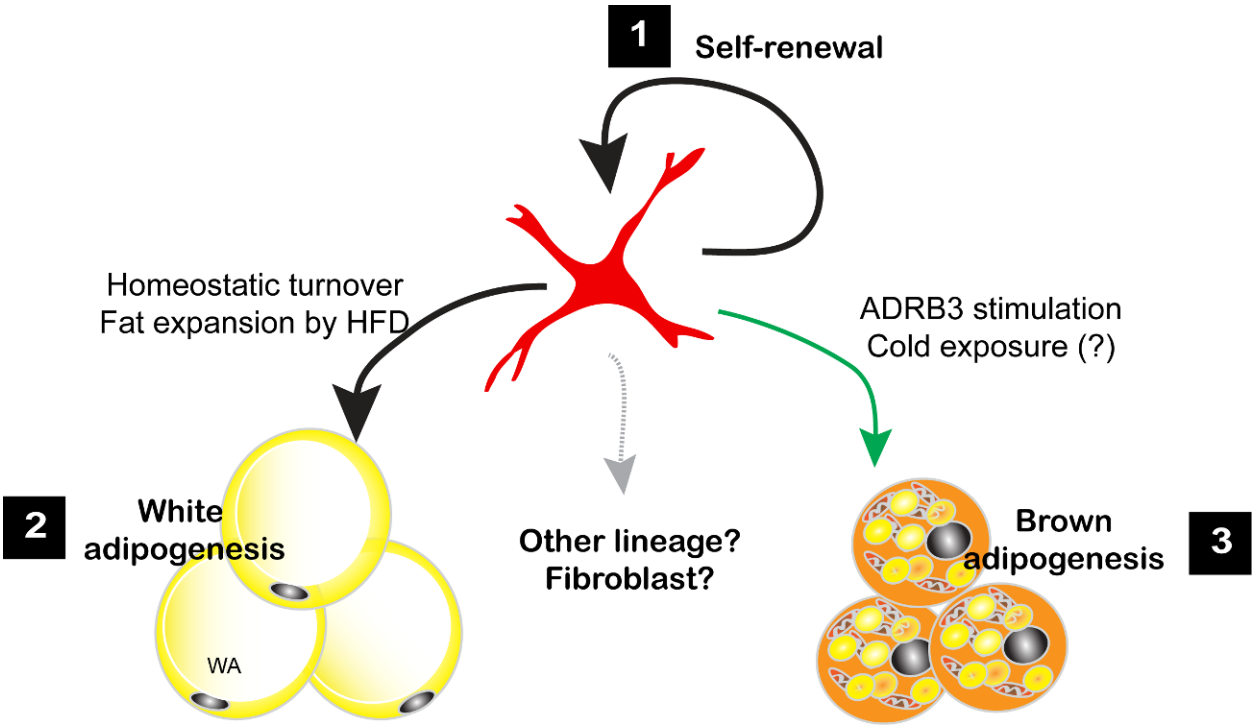

Figure 30. PDGFRα+ cells are remodeling stem cells in adult WAT.

Adult mouse WAT possess white/brown bipotent progenitors: (1) Stable distribution of PDGFRα+ cells throughout CL time course suggest that they repopulate themselves during remodeling process. Clonogenicity of FACS-isolated cells support self-renewal potential. (2) WA generation during homeostatic turnover and hyperplastic expansion of WAT under HFD feeding. (3) PDGFRα+ progenitors are responsible for BA generation induced by ADRB3 stimulation. Our clonal level analysis showed that single cell-derived clones can differentiate into BA and WA, further supporting dual potential of PDGFRα+ cells.

7.2. Characterization of PDGFRα expressing cells in WAT.

The PDGFRα+ progenitors identified in the present experiments can be distinguished from previously described progenitors of WA by several criteria. Tang, et.al. (49) identified direct precursors of WA in rapidly growing perinatal WAT as pericyte-like cells that express PPARγ and several pericyte markers. The PDGFRα+ cells were negative for PPARγ, SMA, and PDGFRβ. While often localized near blood vessels and capillaries, they are clearly outside of the mural compartment, having extended processes that contact other cell types. We believe that PDGFRα$^+$ progenitors described here can be distinguished from WA progenitors described by Rodeheffer et al (56) on the basis of tissue abundance and CD24 expression. It seems likely that PDGFRα$^+$ cells were a subpopulation of the isolated Sca1$^+$ cells that Schultz et al. (2011) showed were capable of brown adipogenesis. However, in contrast to our experiments, cells isolated by these investigators required *ex vivo* treatment with bone morphogen-7 for BA differentiation and these cells were absent in eWAT.

There is no report describing in detail the three dimensional morphology of adipocyte progenitors *in situ*. Imaging the fine morphology of PDGFRα+ progenitors demonstrated their unique stellate morphology, characterized by thin cytoplasmic processes that cover long distances and contact numerous cell types. These observations suggest that PDGFRα+ cells actively monitor the local microenvironment and might be recruited during metabolic stress or

damages.

PDGFRα$^+$ progenitors are found in numerous tissues where they appear to be involved in cellular repair and restoration (59, 61). For example, PDGFRα$^+$ cells may differentiate into fibroblasts or adipocytes in damaged muscle (57, 58), depending on the nature of the damage. PDGFRα$^+$ progenitors comprise 5% of cells in brain and contribute to oligodendrocyte formation in adults, and CNS remyelination following injury (117). Interestingly, the three dimensional morphology of brain and adipose PDGFRα$^+$ progenitors is strikingly similar: both extend multiple cellular processes that contact numerous cell types and give the impression of being capable of monitoring the microenvironment (Richardson et al. 2011). In the case of adipose tissue, we suggest that PDGFRα$^+$ cells are adult stem cells that sense metabolic stress or adipogenic signals, and contribute to tissue remodeling and restoration.

7.3. Brown adipogenic potential of PDGFRα + progenitors.

With the re-discovery of metabolically active BAT in humans, there has been intensive attention on iBA appearing in WAT as a potential cellular target to treat obesity and related metabolic diseases, but the origin of iBA has remained unknown. Although the contribution of proliferating cells to iBA formation differs among WAT depots, the fact that proliferation is the source of the new BA provided a strategy to identify and trace the origin and fate of iBA

progenitors *in vivo*. We established that cells marked with the proliferation marker EdU after one day of CL treatment expressed PDGFRα, but not previously identified markers of developmental WA progenitors. We then used two independent transgenic models to trace the fate of PDGFRα+ proliferating cells. The first model used tamoxifen-inducible cre-mediated recombination to permanently tag PDGFRα+ cells immediately prior to CL treatment. These experiments provided compelling data demonstrating that β3-AR stimulation triggers proliferation of PDGFRα+ cells and their differentiation into brown adipocytes In the second model, we examined the fate of cells that express H2BeGFP (Pdgfra promoter driven), a durable, but not indelible marker of PDGFRα expression and demonstrated that proliferating cells lose expression of PDGFRα as the cells differentiated into PPARγ+PLIN1+ UCP1+ multipocular adipocytes.

β3-AR stimulation triggered proliferation as early as the first day of CL treatment, generating a transiently amplifying population. Transiently amplifying populations contain small newly differentiated cells with PLIN1+ lipid droplets. Cell culture studies using the 3T3-L1 model system (118, 119) have proposed that clonal expansion precedes expression of adipocyte genes that lead accumulation of lipid. However, our study demonstrated that newly-generated adipocytes contain PLIN1-coated lipid droplets and can divide multiple times. This expansion appears to be the major reason why iBA are formed as clusters in eWAT.

7.4. Macrophages: a crucial niche component in adipose tissue remodeling.

Our in situ analysis demonstrated that PDGFRα+ cells reside in a complex three-dimensional network, which comprises a plethora of other cell types such as, adipocytes, endothelial cells, interstitial stromal cells, and immune cells. Often, tissue remodeling processes involve alterations in cell-cell contact and signaling that lead to activation and differentiation of progenitors and parallel integration of newly-differentiated progenies (120). We report here that CLS formed during adrenergic activation are adipogenic niches that are essential for iBA recruitment and catabolic remodeling of WAT. CLS contained alternatively-activated (M2) macrophages and PDGFRα+ progenitors are recruited specifically to these structures. Importantly, depletion of tissue macrophages with clodronate liposomes prevented migration and proliferation of BA progenitors during adrenergic stimulation. M2 macrophages that form CLS expressed high levels of PDGFC and osteopontin (OPN), the potential niche factors that recruit PDGFRα+ cells. Supporting our *in vivo* observation, PDGFRα+ progenitors were highly mobile in organotypic culture, and exogenous PDGF ligands and OPN trigger migration of PDGFRα+ cells *in vitro* migration assay. PDGFC and OPN acquire their activities after proteolytic processing (107). One of intriguing finding is that the processed form of PDGFC and OPN were highly enriched in WAT by CL treatment, implying potential involvement of proteases

that are responsible for the conversion of inactive proforms.

Together, we have defined macropahges as a niche component that secrete cytokines (PDGFC and SPP1) to activate progenitors. Those signals seem to facilitate progenitor proliferation and migration at the initial step of activation, since differentiating newly-born adipocytes (small immature adipocytes) no longer contact with macrophages. What is unclear is the mechanisms by which those soluble factors regulate the fate decision of progenitor cells. Even though we demonstrated multiple divisions during differentiation, it is not clear whether proliferation of immature adipocytes also requires same mitogenic signals. Further study on the interplay of these niche factors at various stages is important to fully understand mechanisms that mediate progenitor activation and differentiation.

We are proposing a model system where macrophages and progenitors play a crucial role in the adipose tissue remodeling process, as summarized in **Figure 31.** In our model, sudden lipolysis by ADRB3 stimulation causes acute FFA overload, and generates a stress condition (e.g. local damage). Macrophages sense this stress, secrete mediators to further recruit macrophages/progenitors and activate progenitor proliferation and differentiation. Macrophages remove lipid debris from malfunctioning or damaged adipocytes, and progenitors replace damaged adipocytes by differentiation to form new adipocytes. Thus, macrophages and progenitors function as essential effectors in this remodeling process. In contrast, other adipose

depots, such as subcutaneous WAT or BAT, which have higher oxidative capacity to utilize FFA, can handle increase lipolysis, maintaining tissue homeostasis, without causing macrophage recruitment or progenitor activation.

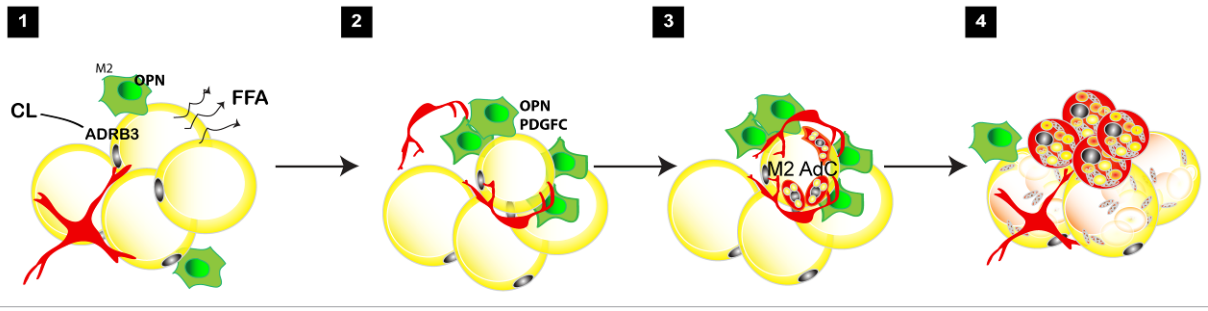

Adipose tissue	ADRB3 stimulation Lipolysis	Formation of M2 CLS	Formation of brown adipogenic clusters	Catabolic remodeling
M2 Macrophage	Stress sensing & recruitment	Mediator production Mitogen & Chemokine (OPN, PDGFC)	Clearance of lipid	Resoultion Homeostasis
PDGFRα+ progenitors		Migration & proliferation	Differentiation	New iBA incorporation

Figure 31. Interplay between macrophages and PDGFRα+ cells during WAT remodeling by ADRB3 stimulation. In our model, sudden lipolysis by ADRB3 stimulation causes acute FFA overload, and generate a stress condition (e.g. local damage). Macrophages sense this stress, secrete mediators to further recruit macrophages/ progenitors and activate progenitor proliferation and differentiation. Macrophages remove lipid debris from malfunctioning or damaged adipocytes, and progenitors replace damaged adipocytes by differentiation to form new adipocytes. Thus, macrophages and progenitors function as essential effectors in this remodeling process.

7.5. Molecular mechanisms that regulate the fate decision of PDGFRα+ cells.

The regulatory pathway that controls the progenitor fate and behavior remains to be elucidated. Lipolysis may play a key role in providing a permissive environment for BA differentiation. FFA liberated from adipocytes has been known to function as signaling molecules in many circumstances. For instance, FFA can function as ligands for PPARs that are critical transcription factors mediating adipogenesis and BA differentiation (121, 122). Also, FFA-derived molecules, such as prostaglandin, can induce BA recruitment in WAT (123-125). In addition to soluble factors, physical and mechanical factors may be involved in controlling fate specification of the progenitors (126). Extensive lipolysis that reduces adipocyte mass may disturb tissue organization and architecture, and trigger cellular responses essential for progenitor activation. Evidence from the literature is that the recruitment of iBA in WAT by β–adrenergic stimulation is regulated by genetic components. Consistent with published data showing higher levels of iBA emergence in the obesity-resistant strain of mice, we have found that proliferation of PDGFRα+ cells is 3-fold greater in 129S1 versus C57BL6. Taken together, these data lead us to the hypothesis for future study that intrinsic and extrinsic factors will determine the behavior of PDGFRα+ progenitors in WAT during ADRB3 stimulation.

Chapter 8. Future directions

8.1. To identify BA/WA switches in PDGFRα+ progenitors

Identification of common progenitors for BA/ WA may offer a great opportunity to address the long-sought question how these progenitors switch their fate. Interplay of transcriptional regulation and epigenetic modification may be involved in this fate determination processes (127-130). Analysis of gene expression and epigenetic modification by global profiling is a very important future project that can enable us to discover molecular switches that regulate the fate decision of these cells

8.2. To characterize adipose tissue macrophages during adipose tissue remodeling.

We proposed that ADRB3 stimulation recruits M2 macrophages or induce macrophage polarization towards the M2 state, which seems to activate PDGFRα+ progenitors by releasing mitogens and tissue remodeling factors. Depletion of macrophges in WAT resulted in decreased BA progenitor proliferation, suggestive of an essential role of macrophages in BA recruitment in WAT. Interestingly, M2 CLS were also observed in the white adipogenic condition of HFD fed mice, even though it is premature to conclude that M2 macrophages are required for WA differentiation. Therefore, future work needs to be conducted to further establish the phenotype of macrophages in WA adipogenic conditions. In addition, detailed analysis on signaling

molecules generated by macrophages (such as growth factors, cytokines, ECM remodeling enzymes (e.g. MMPs) in various adipogenic conditions will be required. Data generated from this approach will help us to determine whether adipose tissue macrophages have a crucial role as mediators of progenitor activation in WAT.

REFERENCES

1. Haslam, D.W., and James, W.P. 2005. Obesity. *Lancet* 366:1197-1209.

2. Jia, H., and Lubetkin, E.I. 2010. Trends in Quality-Adjusted Life-Years Lost Contributed by Smoking and Obesity. *American journal of preventive medicine* 38:138-144.

3. Whittle, A.J., López, M., and Vidal-Puig, A. 2011. Using brown adipose tissue to treat obesity – the central issue. *Trends in Molecular Medicine* 17:405-411.

4. Galic, S., Oakhill, J.S., and Steinberg, G.R. 2010. Adipose tissue as an endocrine organ. *Molecular and Cellular Endocrinology* 316:129-139.

5. Stommel, M., and Schoenborn, C.A. 2010. Variations in BMI and Prevalence of Health Risks in Diverse Racial and Ethnic Populations. *Obesity* 18:1821-1826.

6. Ruderman, N., Chisholm, D., Pi-Sunyer, X., and Schneider, S. 1998. The metabolically obese, normal-weight individual revisited. *Diabetes* 47:699-713.

7. Unger, R.H., and Scherer, P.E. 2010. Gluttony, sloth and the metabolic syndrome: a roadmap to lipotoxicity. *Trends in Endocrinology & Metabolism* 21:345-352.

8. Samuel, V.T., Petersen, K.F., and Shulman, G.I. 2010. Lipid-induced insulin resistance: unravelling the mechanism. *The Lancet* 375:2267-2277.

9. Waki, H., and Tontonoz, P. 2007. Endocrine Functions of Adipose Tissue. *Annual Review of Pathology: Mechanisms of Disease* 2:31-56.

10. Gray, S.L., and Vidal-Puig, A.J. 2007. Adipose tissue expandability in the maintenance of metabolic homeostasis. *Nutrition reviews* 65:S7-12.

11. Tontonoz, P., and Spiegelman, B.M. 2008. Fat and Beyond: The Diverse Biology of PPARg. *Annual Review of Biochemistry* 77:289-312.

12. Crowley, V.E.F., Yeo, G.S.H., and O'Rahilly, S. 2002. Obesity therapy: altering the energy intake-and-expenditure balance sheet. *Nat Rev Drug Discov* 1:276-286.

13. Granneman, J.G., Burnazi, M., Zhu, Z., and Schwamb, L.A. 2003. White adipose tissue contributes to UCP1-independent thermogenesis. *Am J Physiol Endocrinol Metab* 285:E1230-1236.

14. Ghorbani, M., Claus, T.H., and Himms-Hagen, J. 1997. Hypertrophy of brown adipocytes in brown and white adipose tissues and reversal of diet-induced obesity in rats treated with a beta3-adrenoceptor agonist. *Biochem. Pharmacol.* 54:121-131.

15. Tseng, Y.-H., Cypess, A.M., and Kahn, C.R. 2010. Cellular bioenergetics as a target for obesity therapy. *Nat Rev Drug Discov* 9:465-482.

16. Gunawardana, S.C., and Piston, D.W. 2012. Reversal of Type 1 Diabetes in Mice by Brown Adipose Tissue Transplant. *Diabetes*.

17. Hamann, A., Flier, J.S., and Lowell, B.B. 1996. Decreased brown fat markedly enhances susceptibility to diet-induced obesity, diabetes, and hyperlipidemia. *Endocrinology* 137:21-29.

18. Lidell, M.E., and Enerback, S. 2010. Brown adipose tissue - a new role in humans? *Nat Rev Endocrinol* 6:319-325.

19. Bartelt, A., Bruns, O.T., Reimer, R., Hohenberg, H., Ittrich, H., Peldschus, K., Kaul, M.G., Tromsdorf, U.I., Weller, H., Waurisch, C., et al. 2011. Brown adipose tissue activity controls triglyceride clearance. *Nat Med* 17:200-205.

20. Arch, J.R.S. 2002. [beta]3-Adrenoceptor agonists: potential, pitfalls and progress. *European Journal of Pharmacology* 440:99-107.

21. Zeve, D., Tang, W., and Graff, J. 2009. Fighting Fat with Fat: The Expanding Field of Adipose Stem Cells. *Cell Stem Cell* 5:472-481.

22. Cannon, B., and Nedergaard, J. 2004. Brown adipose tissue: function and physiological significance. *Physiol. Rev.* 84:277-359.

23. Gesta, S., Tseng, Y.H., and Kahn, C.R. 2007. Developmental origin of fat: tracking obesity to its source. *Cell* 131:242-256.

24. Frontini, A., and Cinti, S. 2010. Distribution and Development of Brown Adipocytes in the Murine and Human Adipose Organ. *Cell Metabolism* 11:253-256.

25. Saito, M., Okamatsu-Ogura, Y., Matsushita, M., Watanabe, K., Yoneshiro, T., Nio-Kobayashi, J., Iwanaga, T., Miyagawa, M., Kameya, T., Nakada, K., et al. 2009. High incidence of metabolically active brown adipose tissue in healthy adult humans: effects of cold exposure and adiposity.(ORIGINAL ARTICLE)(Report). *Diabetes* 58:1526(1526).

26. Ouellet, V., Routhier-Labadie, A., Bellemare, W., Lakhal-Chaieb, L., Turcotte, E., Carpentier, A.C., and Richard, D. 2011. Outdoor Temperature, Age, Sex, Body Mass Index, and Diabetic Status Determine the Prevalence, Mass, and Glucose-Uptake Activity of 18F-FDG-Detected BAT in Humans. *Journal of Clinical Endocrinology & Metabolism* 96:192-199.

27. Vijgen, G.H.E.J., Bouvy, N.D., Teule, G.J.J., Brans, B., Schrauwen, P., and van Marken Lichtenbelt, W.D. 2011. Brown Adipose Tissue in Morbidly Obese Subjects. *PLoS ONE* 6:e17247.

28. Ouellet, V., Labbé, S.M., Blondin, D.P., Phoenix, S., Guérin, B., Haman, F., Turcotte, E.E., Richard, D., and Carpentier, A.C. 2012. Brown adipose tissue oxidative metabolism

contributes to energy expenditure during acute cold exposure in humans. *The Journal of Clinical Investigation* 0:0-0.

29. Nedergaard, J., and Cannon, B. 2010. The Changed Metabolic World with Human Brown Adipose Tissue: Therapeutic Visions. *Cell Metabolism* 11:268-272.

30. Prins, J.B., and O'Rahilly, S. 1997. Regulation of adipose cell number in man. *Clin Sci (Lond)* 92:3-11.

31. Joe, A.W.B., Yi, L., Even, Y., Vogl, A.W., and Rossi, F.M.V. 2009. Depot-Specific Differences in Adipogenic Progenitor Abundance and Proliferative Response to High-Fat Diet. *Stem Cells* 27:2563-2570.

32. Xaymardan, M., Gibbins, J.R., and Zoellner, H. 2002. Adipogenic healing in adult mice by implantation of hollow devices in muscle. *The Anatomical Record* 267:28-36.

33. Koh, Y.J., Kang, S., Lee, H.J., Choi, T.-S., Lee, H.S., Cho, C.-H., and Koh, G.Y. 2007. Bone marrow–derived circulating progenitor cells fail to transdifferentiate into adipocytes in adult adipose tissues in mice. *The Journal of Clinical Investigation* 117:3684-3695.

34. Crossno, J.T., Majka, S.M., Grazia, T., Gill, R.G., and Klemm, D.J. 2006. Rosiglitazone promotes development of a novel adipocyte population from bone marrow–derived circulating

progenitor cells. *The Journal of Clinical Investigation* 116:3220-3228.

35. Adams, M., Montague, C.T., and Prins, J.B. 1997. Activators of peroxisome proliferator-activated receptor gamma have depot-specific effects on human preadipocyte differentiation. *J Clin Invest* 100:3149-3153.

36. Cousin, B., Cinti, S., Morroni, M., Raimbault, S., Ricquier, D., Penicaud, L., and Casteilla, L. 1992. Occurrence of brown adipocytes in rat white adipose tissue: molecular and morphological characterization. *J. Cell Sci.* 103:931-942.

37. Young, P., Arch, J.R.S., and Ashwell, M. 1984. Brown adipose tissue in the parametrial fat pad of the mouse. *FEBS Letters* 167:10-14.

38. Ghorbani, M., and Himms-Hagen, J. 1997. Appearance of brown adipocytes in white adipose tissue during CL 316,243-induced reversal of obesity and diabetes in Zucker fa/fa rats. *International journal of obesity and related metabolic disorders* 21:465-475.

39. Guerra, C., Koza, R.A., Yamashita, H., Walsh, K., and Kozak, L.P. 1998. Emergence of brown adipocytes in white fat in mice is under genetic control. Effects on body weight and adiposity. *J. Clin. Invest.* 102:412-420.

40. Himms-Hagen, J., Melnyk, A., Zingaretti, M.C., Ceresi, E., Barbatelli, G., and Cinti, S.

2000. Multilocular fat cells in WAT of CL-316243-treated rats derive directly from white adipocytes. *Am J Physiol Cell Physiol* 279:C670-681.

41. Xue, B. 2007. Genetic variability affects the development of brown adipocytes in white fat but not in interscapular brown fat. *J. Lipid Res.* 48:41-51.

42. Xue, B., Rim, J.-S., Hogan, J.C., Coulter, A.A., Koza, R.A., and Kozak, L.P. 2007. Genetic variability affects the development of brown adipocytes in white fat but not in interscapular brown fat. *Journal of Lipid Research* 48:41-51.

43. Granneman, J.G., Li, P., Zhu, Z., and Lu, Y. 2005. Metabolic and cellular plasticity in white adipose tissue I: effects of {beta}3-adrenergic receptor activation. *Am J Physiol Endocrinol Metab* 289:E608-616.

44. Cinti, S. 2009. Transdifferentiation properties of adipocytes in the adipose organ. *Am. J. Physiol. Endocrinol. Metab.* 297:E977-E986.

45. Jopling, C., Boue, S., and Belmonte, J.C.I. 2011. Dedifferentiation, transdifferentiation and reprogramming: three routes to regeneration. *Nat Rev Mol Cell Biol* 12:79-89.

46. Barbatelli, G., Murano, I., Madsen, L., Hao, Q., Jimenez, M., Kristiansen, K., Giacobino, J.P., De Matteis, R., and Cinti, S. 2010. The emergence of cold-induced brown adipocytes in

mouse white fat depots is determined predominantly by white to brown adipocyte transdifferentiation. *Am J Physiol Endocrinol Metab* 298:E1244-1253.

47. Seale, P., Bjork, B., Yang, W., Kajimura, S., Chin, S., Kuang, S., Scime, A., Devarakonda, S., Conroe, H.M., Erdjument-Bromage, H., et al. 2008. PRDM16 controls a brown fat/skeletal muscle switch. *Nature* 454:961-967.

48. Timmons, J.A., Wennmalm, K., Larsson, O., Walden, T.B., Lassmann, T., Petrovic, N., Hamilton, D.L., Gimeno, R.E., Wahlestedt, C., Baar, K., et al. 2007. Myogenic gene expression signature establishes that brown and white adipocytes originate from distinct cell lineages. *Proc. Natl Acad. Sci. USA* 104:4401-4406.

49. Tang, W., Zeve, D., Suh, J.M., Bosnakovski, D., Kyba, M., Hammer, R.E., Tallquist, M.D., and Graff, J.M. 2008. White Fat Progenitor Cells Reside in the Adipose Vasculature. *Science* 322:583-586.

50. Tang, W., Zeve, D., Seo, J., Jo, A.Y., and Graff, Jonathan M. 2011. Thiazolidinediones Regulate Adipose Lineage Dynamics. *Cell Metabolism* 14:116-122.

51. Cinti, S. 2005. The adipose organ. *Prostaglandins, Leukotrienes and Essential Fatty Acids* 73:9-15.

52. Won Park, K., Halperin, D.S., and Tontonoz, P. 2008. Before They Were Fat: Adipocyte Progenitors. *Cell Metabolism* 8:454-457.

53. Lin, G., Garcia, M., Ning, H., Banie, L., Guo, Y.L., Lue, T.F., and Lin, C.S. 2008. Defining stem and progenitor cells within adipose tissue. *Stem Cells Dev* 17:1053-1063.

54. Bianco, P., Robey, P.G., and Simmons, P.J. 2008. Mesenchymal Stem Cells: Revisiting History, Concepts, and Assays. *Cell Stem Cell* 2:313-319.

55. da Silva Meirelles, L., Caplan, A.I., and Nardi, N.B. 2008. In Search of the In Vivo Identity of Mesenchymal Stem Cells. *Stem Cells* 26:2287-2299.

56. Rodeheffer, M.S., Birsoy, K., and Friedman, J.M. 2008. Identification of White Adipocyte Progenitor Cells In Vivo. *Cell* 135:240-249.

57. Uezumi, A., Fukada, S.-i., Yamamoto, N., Takeda, S.i., and Tsuchida, K. 2010. Mesenchymal progenitors distinct from satellite cells contribute to ectopic fat cell formation in skeletal muscle. *Nat Cell Biol* 12:143-152.

58. Joe, A.W.B., Yi, L., Natarajan, A., Le Grand, F., So, L., Wang, J., Rudnicki, M.A., and Rossi, F.M.V. 2010. Muscle injury activates resident fibro/adipogenic progenitors that facilitate myogenesis. *Nat Cell Biol* 12:153-163.

59. Andrae, J., Gallini, R., and Betsholtz, C. 2008. Role of platelet-derived growth factors in physiology and medicine. *Genes Dev* 22:1276-1312.

60. Fredriksson, L., Li, H., and Eriksson, U. 2004. The PDGF family: four gene products form five dimeric isoforms. *Cytokine & Growth Factor Reviews* 15:197-204.

61. Hoch, R.V., and Soriano, P. 2003. Roles of PDGF in animal development. *Development* 130:4769-4784.

62. Zawadzka, M., Rivers, L.E., Fancy, S.P., Zhao, C., Tripathi, R., Jamen, F., Young, K., Goncharevich, A., Pohl, H., Rizzi, M., et al. 2010. CNS-resident glial progenitor/stem cells produce Schwann cells as well as oligodendrocytes during repair of CNS demyelination. *Cell Stem Cell* 6:578-590.

63. Pringle, N.P., Mudhar, H.S., Collarini, E.J., and Richardson, W.D. 1992. PDGF receptors in the rat CNS: during late neurogenesis, PDGF alpha receptor expression appears to be restricted to glial cells of the oligodendrocyte lineage. *Development* 115:535-551.

64. Rivers, L.E., Young, K.M., Rizzi, M., Jamen, F., Psachoulia, K., Wade, A., Kessaris, N., and Richardson, W.D. 2008. PDGFRA/NG2 glia generate myelinating oligodendrocytes and piriform projection neurons in adult mice. *Nat Neurosci* 11:1392-1401.

65. Uezumi, A., Ito, T., Morikawa, D., Shimizu, N., Yoneda, T., Segawa, M., Yamaguchi, M., Ogawa, R., Matev, M.M., Miyagoe-Suzuki, Y., et al. 2011. Fibrosis and adipogenesis originate from a common mesenchymal progenitor in skeletal muscle. *Journal of Cell Science* 124:3654-3664.

66. Artemenko, Y., Gagnon, A., Aubin, D., and Sorisky, A. 2005. Anti-adipogenic effect of PDGF is reversed by PKC inhibition. *Journal of Cellular Physiology* 204:646-653.

67. Hayashi, I., Nixon, T., Morikawa, M., and Green, H. 1981. Adipogenic and anti-adipogenic factors in the pituitary and other organs. *Proceedings of the National Academy of Sciences of the United States of America* 78:3969-3972.

68. Schofield, R. 1978. The relationship between the spleen colony-forming cell and the haemopoietic stem cell. *Blood Cells* 4:7-25.

69. Greco, V., and Guo, S. 2010. Compartmentalized organization: a common and required feature of stem cell niches? *Development* 137:1586-1594.

70. Moore, K.A., and Lemischka, I.R. 2006. Stem Cells and Their Niches. *Science* 311:1880-1885.

71. Gordon, S., and Taylor, P.R. 2005. Monocyte and macrophage heterogeneity. *Nat Rev*

Immunol 5:953-964.

72. Kosteli, A., Sugaru, E., Haemmerle, G., Martin, J.F., Lei, J., Zechner, R., and Ferrante, A.W. 2010. Weight loss and lipolysis promote a dynamic immune response in murine adipose tissue. *The Journal of Clinical Investigation* 120:3466-3479.

73. Sun, K., Kusminski, C.M., and Scherer, P.E. 2011. Adipose tissue remodeling and obesity. *The Journal of Clinical Investigation* 121:2094-2101.

74. Lumeng, C.N., and Saltiel, A.R. 2011. Inflammatory links between obesity and metabolic disease. *The Journal of Clinical Investigation* 121:2111-2117.

75. Martinez, F.O., Helming, L., and Gordon, S. 2009. Alternative Activation of Macrophages: An Immunologic Functional Perspective. *Annual Review of Immunology* 27:451-483.

76. Medzhitov, R., and Horng, T. 2009. Transcriptional control of the inflammatory response. *Nat Rev Immunol* 9:692-703.

77. Gordon, S., and Martinez, F.O. 2010. Alternative Activation of Macrophages: Mechanism and Functions. *Immunity* 32:593-604.

78. Medzhitov, R. 2008. Origin and physiological roles of inflammation. *Nature* 454:428-435.

79. Odegaard, J.I., and Chawla, A. 2011. Alternative Macrophage Activation and Metabolism. *Annual Review of Pathology: Mechanisms of Disease* 6:275-297.

80. Lumeng, C.N., DelProposto, J.B., Westcott, D.J., and Saltiel, A.R. 2008. Phenotypic switching of adipose tissue macrophages with obesity is generated by spatiotemporal differences in macrophage subtypes.(ORIGINAL ARTICLE)(Clinical report). *Diabetes* 57:3239(3238).

81. Odegaard, J.I., Ricardo-Gonzalez, R.R., Goforth, M.H., Morel, C.R., Subramanian, V., Mukundan, L., Eagle, A.R., Vats, D., Brombacher, F., Ferrante, A.W., et al. 2007. Macrophage-specific PPAR[g] controls alternative activation and improves insulin resistance. *Nature* 447:1116-1120.

82. Nguyen, K.D., Qiu, Y., Cui, X., Goh, Y.P.S., Mwangi, J., David, T., Mukundan, L., Brombacher, F., Locksley, R.M., and Chawla, A. 2011. Alternatively activated macrophages produce catecholamines to sustain adaptive thermogenesis. *Nature* 480:104-108.

83. Molgat, A.S., Gagnon, A., and Sorisky, A. 2009. Preadipocyte apoptosis is prevented by macrophage-conditioned medium in a PDGF-dependent manner. *American Journal of Physiology - Cell Physiology* 296:C757-C765.

84. Molgat, A.S.D., Gagnon, A., and Sorisky, A. 2011. Macrophage-induced preadipocyte

survival depends on signaling through Akt, ERK1/2, and reactive oxygen species. *Experimental Cell Research* 317:521-530.

85. Madisen, L., Zwingman, T.A., Sunkin, S.M., Oh, S.W., Zariwala, H.A., Gu, H., Ng, L.L., Palmiter, R.D., Hawrylycz, M.J., Jones, A.R., et al. 2010. A robust and high-throughput Cre reporting and characterization system for the whole mouse brain. *Nat Neurosci* 13:133-140.

86. Moore, H.-P.H., Silver, R.B., Mottillo, E.P., Bernlohr, D.A., and Granneman, J.G. 2005. Perilipin Targets a Novel Pool of Lipid Droplets for Lipolytic Attack by Hormone-sensitive Lipase. *Journal of Biological Chemistry* 280:43109-43120.

87. Hirsch, J., and Gallian, E. 1968. Methods for the determination of adipose cell size in man and animals. *Journal of Lipid Research* 9:110-119.

88. Granneman, J.G., Moore, H.-P.H., Mottillo, E.P., and Zhu, Z. 2009. Functional Interactions between Mldp (LSDP5) and Abhd5 in the Control of Intracellular Lipid Accumulation. *Journal of Biological Chemistry* 284:3049-3057.

89. Mottillo, E.P., Shen, X.J., and Granneman, J.G. 2007. Role of hormone-sensitive lipase in beta-adrenergic remodeling of white adipose tissue. *Am J Physiol Endocrinol Metab* 293:E1188-1197.

90. Li, P., Zhu, Z., Lu, Y., and Granneman, J.G. 2005. Metabolic and cellular plasticity in white adipose tissue II: role of peroxisome proliferator-activated receptor-α. *American Journal of Physiology - Endocrinology And Metabolism* 289:E617-E626.

91. Fischer-Posovszky, P., Wang, Q.A., Asterholm, I.W., Rutkowski, J.M., and Scherer, P.E. 2011. Targeted Deletion of Adipocytes by Apoptosis Leads to Adipose Tissue Recruitment of Alternatively Activated M2 Macrophages. *Endocrinology* 152:3074-3081.

92. Pilgrim, C. 1971. DNA synthesis and differentiation in developing white adipose tissue. *Developmental Biology* 26:69-76.

93. Voog, J., and Jones, D.L. 2010. Stem Cells and the Niche: A Dynamic Duo. *Cell Stem Cell* 6:103-115.

94. Hachiya, R., Itoh, M., Ogawa, Y., and Suganami, T. 2011. Adipose tissue remodeling as homeostatic inflammation. *International Journal of Inflammation*.

95. Cinti, S., Mitchell, G., Barbatelli, G., Murano, I., Ceresi, E., Faloia, E., Wang, S., Fortier, M., Greenberg, A.S., and Obin, M.S. 2005. Adipocyte death defines macrophage localization and function in adipose tissue of obese mice and humans. *Journal of Lipid Research* 46:2347-2355.

96. Strissel, K.J., Stancheva, Z., Miyoshi, H., Perfield, J.W., II, DeFuria, J., Jick, Z., Greenberg, A.S., and Obin, M.S. 2007. Adipocyte death, adipose tissue remodeling, and obesity complications. *Diabetes* 56:2910(2919).

97. Van Rooijen, N., and Sanders, A. 1994. Liposome mediated depletion of macrophages: mechanism of action, preparation of liposomes and applications. *Journal of immunological methods* 174:83-93.

98. Rittling, S.R. 2011. Osteopontin in macrophage function. *Expert Reviews in Molecular Medicine* 13:1-21.

99. Denhardt, D.T., Noda, M., O'Regan, A.W., Pavlin, D., and Berman, J.S. 2001. Osteopontin as a means to cope with environmental insults: regulation of inflammation, tissue remodeling, and cell survival. *The Journal of Clinical Investigation* 107:1055-1061.

100. Nagao, M., Feinstein, T.N., Ezura, Y., Hayata, T., Notomi, T., Saita, Y., Hanyu, R., Hemmi, H., Izu, Y., Takeda, S., et al. 2011. Sympathetic control of bone mass regulated by osteopontin. *Proceedings of the National Academy of Sciences* 108:17767-17772.

101. Gravallese, E.M. 2003. Osteopontin: a bridge between bone and the immune system. *The Journal of Clinical Investigation* 112:147-149.

102. O'Regan, A., and Berman, J.S. 2000. Osteopontin: a key cytokine in cell-mediated and granulomatous inflammation. *International Journal of Experimental Pathology* 81:373-390.

103. Liaw, L., Birk, D.E., Ballas, C.B., Whitsitt, J.S., Davidson, J.M., and Hogan, B.L. 1998. Altered wound healing in mice lacking a functional osteopontin gene (spp1). *The Journal of Clinical Investigation* 101:1468-1478.

104. Barrientos, S., Stojadinovic, O., Golinko, M.S., Brem, H., and Tomic-Canic, M. 2008. Growth factors and cytokines in wound healing. *Wound Repair & Regeneration* 16:585-601.

105. Triantafyllopoulou, A., Franzke, C.-W., Seshan, S.V., Perino, G., Kalliolias, G.D., Ramanujam, M., van Rooijen, N., Davidson, A., and Ivashkiv, L.B. 2010. Proliferative lesions and metalloproteinase activity in murine lupus nephritis mediated by type I interferons and macrophages. *Proceedings of the National Academy of Sciences* 107:3012-3017.

106. De Donatis, A., Comito, G., Buricchi, F., Vinci, M.C., Parenti, A., Caselli, A., Camici, G., Manao, G., Ramponi, G., and Cirri, P. 2008. Proliferation Versus Migration in Platelet-derived Growth Factor Signaling. *Journal of Biological Chemistry* 283:19948-19956.

107. Li, X., and Eriksson, U. 2003. Novel PDGF family members: PDGF-C and PDGF-D. *Cytokine & Growth Factor Reviews* 14:91-98.

108. Faivre, S., Demetri, G., Sargent, W., and Raymond, E. 2007. Molecular basis for sunitinib efficacy and future clinical development. *Nat Rev Drug Discov* 6:734-745.

109. imatinib Chen, H., Gu, X., Liu, Y., Wang, J., Wirt, S.E., Bottino, R., Schorle, H., Sage, J., and Kim, S.K. 2011. PDGF signalling controls age-dependent proliferation in pancreatic [bgr]-cells. *Nature* 478:349-355.

110. Rudnicki, M.A., and Wang, Y.X. 2012. Satellite cells, the engines of muscle repair. *Nature Reviews Molecular Cell Biology* 13:127+.

111. Kawaguchi, N., Toriyama, K., Nicodemou-Lena, E., Inou, K., Torii, S., and Kitagawa, Y. 1998. De novo adipogenesis in mice at the site of injection of basement membrane and basic fibroblast growth factor. *Proceedings of the National Academy of Sciences* 95:1062-1066.

112. Nishimura, S., Manabe, I., Nagasaki, M., Hosoya, Y., Yamashita, H., Fujita, H., Ohsugi, M., Tobe, K., Kadowaki, T., Nagai, R., et al. 2007. Adipogenesis in Obesity Requires Close Interplay Between Differentiating Adipocytes, Stromal Cells, and Blood Vessels. *Diabetes* 56:1517-1526.

113. Cawthorn, W.P., Scheller, E.L., and MacDougald, O.A. 2012. Adipose tissue stem cells meet preadipocyte commitment: going back to the future. *Journal of Lipid Research* 53:227-246.

114. Schulz, T.J., Huang, T.L., Tran, T.T., Zhang, H., Townsend, K.L., Shadrach, J.L., Cerletti, M., McDougall, L.E., Giorgadze, N., Tchkonia, T., et al. 2011. Identification of inducible brown adipocyte progenitors residing in skeletal muscle and white fat. *Proceedings of the National Academy of Sciences* 108:143-148.

115. Petrovic, N., Walden, T.B., Shabalina, I.G., Timmons, J.A., Cannon, B., and Nedergaard, J. 2010. Chronic Peroxisome Proliferator-activated Receptor γ (PPARγ) Activation of Epididymally Derived White Adipocyte Cultures Reveals a Population of Thermogenically Competent, UCP1-containing Adipocytes Molecularly Distinct from Classic Brown Adipocytes. *Journal of Biological Chemistry* 285:7153-7164.

116. Kretzschmar, K., and Watt, Fiona M. 2012. Lineage Tracing. *Cell* 148:33-45.

117. Zawadzka, M., Rivers, L.E., Fancy, S.P.J., Zhao, C., Tripathi, R., Jamen, F., Young, K., Goncharevich, A., Pohl, H., Rizzi, M., et al. 2010. CNS-Resident Glial Progenitor/Stem Cells Produce Schwann Cells as well as Oligodendrocytes during Repair of CNS Demyelination. *Cell Stem Cell* 6:578-590.

118. Rosen, E.D., and Spiegelman, B.M. 2000. Molecular regulation of adipogenesis. *Annu. Rev. Cell Dev. Biol.* 16:145-171.

119. Tang, Q.-Q., Otto, T.C., and Lane, M.D. 2003. Mitotic clonal expansion: A synchronous

process required for adipogenesis. *Proceedings of the National Academy of Sciences* 100:44-49.

120. Koh, T.J., and DiPietro, L.A. 2011. Inflammation and wound healing: the role of the macrophage. *Expert Reviews in Molecular Medicine* 13:null-null.

121. Lefterova, M.I., and Lazar, M.A. 2009. New developments in adipogenesis. *Trends in Endocrinology & Metabolism* 20:107-114.

122. Spiegelman, B.M., and Flier, J.S. 1996. Adipogenesis and Obesity: Rounding Out the Big Picture. *Cell* 87:377-389.

123. Vegiopoulos, A., Muller-Decker, K., Strzoda, D., Schmitt, I., Chichelnitskiy, E., Ostertag, A., Diaz, M.B., Rozman, J., Hrabe de Angelis, M., Nusing, R.M., et al. 2010. Cyclooxygenase-2 Controls Energy Homeostasis in Mice by de Novo Recruitment of Brown Adipocytes. *Science* 328:1158-1161.

124. Madsen, L., Pedersen, L.M., Lillefosse, H.H., Fjre, E., Bronstad, I., Hao, Q., Petersen, R.K., Hallenborg, P., Ma, T., De Matteis, R., et al. 2010. UCP1 Induction during Recruitment of Brown Adipocytes in White Adipose Tissue Is Dependent on Cyclooxygenase Activity. *PLoS ONE* 5:e11391.

125. Ghoshal, S., Trivedi, D.B., Graf, G.A., and Loftin, C.D. 2011. Cyclooxygenase-2

Deficiency Attenuates Adipose Tissue Differentiation and Inflammation in Mice. *Journal of Biological Chemistry* 286:889-898.

126. Li, D., Zhou, J., Chowdhury, F., Cheng, J., Wang, N., and Wang, F. 2011. Role of mechanical factors in fate decisions of stem cells. *Regenerative Medicine* 6:229-240.

127. Meissner, A. 2010. Epigenetic modifications in pluripotent and differentiated cells. *Nat Biotech* 28:1079-1088.

128. Gupta, Rana K., Rosen, Evan D., and Spiegelman, Bruce M. 2011. Identifying Novel Transcriptional Components Controlling Energy Metabolism. *Cell Metabolism* 14:739-745.

129. Surani, M.A., Hayashi, K., and Hajkova, P. 2007. Genetic and epigenetic regulators of pluripotency. *Cell* 128:747-762.

130. Hemberger, M., Dean, W., and Reik, W. 2009. Epigenetic dynamics of stem cells and cell lineage commitment: digging Waddington's canal. *Nat Rev Mol Cell Biol* 10:526-537.

ABSTRACT

CELLULAR PLASTICITY IN WHITE ADIPOSE TISSUE: IN VIVO IDENTIFICATION OF BIPOTENTIAL ADIPOCYTE PROGENITOR IN ADULT WHITE ADIPOSE TISSUE

by

YUN-HEE LEE

May 2012

Advisor: Dr. James G. Granneman

Major: Pathology

Degree: Doctor of Philosophy

Nutritional and pharmacological stimuli can dramatically alter the cellular composition and phenotype of white adipose tissue (WAT). Nonetheless, the identity of progenitors that contribute to this cellular plasticity *in vivo* remains poorly understood. Utilizing genetic lineage tracing techniques in combination with in situ immunohistochemical analysis, we demonstrate that brown adipocytes (BA) that are induced by β3-adrenergic receptor activation (ADRB3) in WAT arise from the proliferation and differentiation of cells that express platelet-derived growth factor receptor alpha (PDGFRα), CD34 and Sca1 (PDGFRα+ cells). PDGFRα+ cells have a unique morphology in which extended processes contact multiple cells in the tissue microenvironment. Surprisingly, these cells also give rise to white adipocytes (WA) that can

comprise up to 25% of total fat cells in abdominal fat pads following 8 weeks of high fat feeding. PDGFRα+ cells isolated by fluorescence-activated cell sorting differentiated into both BA and white adipocytes (WA) *in vitro,* and generated WA after transplantation *in vivo*, confirming dual potential. Studies on the interplay of progenitors with niche components demonstrated that ADRB3 activation recruited alternatively activated (M2) macrophage to form crown-like structures (CLS) in epididymal WAT. M2 macrophages in CLS released OPN and PDGFC to induce progenitor migration and proliferation. Progenitor activation was dependent on PDGF signaling and attenuated by pharmacologic inhibition of receptor tyrosine kinases. Together, we identified a novel population of adipocyte progenitors with *in vivo* dual adipogenic potential and their interaction with adipose tissue macrophages. These finding provides new information on adipose lineage specification and have clinical implication for diabetes therapy and restorative medicine.

AUTOBIOGRAPHICAL STATEMENT

YUN-HEE LEE

EDUCATION

2007-20012 Wayne State University Detroit, MI
PhD Candidate in Patholgy; Grade point 4.0/4.0

2001-2003 Seoul National University. South Korea
M.S. in Pharmacology & Toxicology; Grade point 3.8/4.0

1996-2001 Seoul National University, South Korea
B.S. in Pharmacy Grade point 3.6/4.0

AWARDS

2001 An honor prize for academic achievement in Collage of Pharmacy, Seoul National University
2011 3rd place poster presentation, Wayne State University School of Medicine Graduate Student Research Day

PUBLICATIONS

1. Yun JS, Na HK, Park KS, **Lee YH**, Kim EY, Lee SY, Kim JI, Kang JH, Kim DS, Choi KH: Protective effect of vitamine E on endocrine disruptors, PCB-induced dopaminergic neurotoxicity. *Toxicology* 216: 140-146 (2005)
2. Choi KH, Park KS, **Lee YH**, Na HK, Yun JS, Kim DS, Kim JI: Studies for the guidance of safety pharmacology studies in compliance with Good Laboratory Practice. *J Toxicol Pub Health* 22: 109-116 (2006)
3. **Lee YH**, Na HK, Yun JS, Chung SY, Kim JI, Choi KH: Effects of antihistamins on the cardiovascular system in telemetered conscious dogs. *Yakhak Hoeji* 50: 129-135 (2006)
4. Kim YO, Park IS, Wang SY, Lim HK, Kim SH, Lee JH, Kim MJ, Youn KE, **Lee YH**, Lee SJ, Kim DS, Kim IK, Choi BK: Development and establishment of Good Review Practice for drug products in Korea. *Drug Information Journal* 42: 487–491 (2008)
5. **Lee YH**, Petkova AP, Mottillo EP, Granneman JG: In vivo identification of bipotential adipocyte progenitors recruited by β3-adrenoceptor activation and high fat feeding *Cell metabolism* (manuscript accepted)